Department of Biomedical Sciences
University of Veterinary Medicine, Vienna

Institute of Physiology, Pathophysiology and Biophysics
Head: Univ.-Prof. Dr.med. Dr.med.vet. Reinhold Erben

Enhancer regulation in kidney epithelial cells

PhD thesis submitted in fulfilment of the requirements for the degree of Doctor of Philosophy (PhD)

Submitted by
Jakub Jankowski

Vienna, October 2022

Table of contents

Declaration

I, Jakub Jankowski, declare that this thesis, entitled “Enhancer regulation in kidney epithelial cells”, is based on my original work. I attest that the research was conducted with complete adherence to the Good Scientific Practice as outlined by the University of Veterinary Medicine, Vienna and the National Institutes of Health of the United States of America.

PhD Committee

1st Advisor

Dr.rer.nat Julia Wilflingseder

Department of Physiology and Pathophysiology, University of Veterinary Medicine,

Veterinärplatz 1, 1210 Vienna, Austria

2nd Advisor

Dr. Lothar Hennighausen

Laboratory of Genetics and Physiology, NIDDK, NIH

8 Center Dr, Bethesda, MD 20814, USA

3rd Advisor

Univ.-Prof. Dr.med. Dr.med.vet. Reinhold Erben

Department of Physiology and Pathophysiology, University of Veterinary Medicine,

Veterinärplatz 1, 1210 Vienna, Austria

Acknowledgements

This work would not be possible without the help of many people who were able to share their talent and time with me. Please know, that if we crossed paths, I remember your help and will forever be grateful.

I would like to thank my mentors, Dr. Wilflingseder and Dr. Hennighausen, for their patience and persistent belief in my abilities. It was only thanks to your guidance that I made it to the goal.

I would like to thank my family, especially my parents, for their continued love and support. I know you wished I was closer to home, but you cheered me on from across the ocean regardless.

Last but not least, thank you, Kinga, for keeping me sane during the times of isolation and self-doubt. Your friendship was truly invaluable.

Publications included in the PhD thesis

1. **JAK inhibitors dampen activation of interferon-activated transcriptomes and the SARS-CoV-2 receptor ACE2 in human renal proximal tubules.**
Jakub Jankowski, Hye Kyung Lee, Julia Wilflingseder, Lothar Hennighausen; iScience 2021, 24:102928

Detailed contributions:
Conceptualization and methodology, Formal analysis and validation, Data curation and visualization, Investigation, Writing

2. **Enhancer and super-enhancer dynamics in repair after ischemic acute kidney injury.**
Julia Wilflingseder, Michaela Willi, Hye Kyung Lee, Hannes Olauson, Jakub Jankowski, Takaharu Ichimura, Reinhold Erben, M. Todd Valerius, Lothar Hennighausen, Joseph V. Bonventre; Nature Communications 2020, 11:3383

Detailed contributions:
Formal analysis and validation, Data curation and visualization, Investigation, Writing

Publications not included in PhD thesis

1. **Novel Genetic Melanoma Vaccines Based on Induced Pluripotent Stem Cells or Melanosphere-Derived Stem-Like Cells Display High Efficacy in a Murine Tumor Rejection Model.**

Agnieszka Gąbka-Buszek, Eliza Kwiatkowska-Borowczyk, Jakub Jankowski, Anna Karolina Kozłowska, Andrzej Mackiewicz; Vaccines (Basel) 2020, 8(2):147

Detailed contributions:
Conceptualization and methodology, Formal analysis and validation, Data curation and visualization, Investigation, Writing

2. **Identification and characterization of the enhancers of kidney injury regulator *Klotho***

Jakub Jankowski, Hye Kyung Lee, Julia Wilflingseder, Lothar Hennighausen; In preparation

Detailed contributions:
Conceptualization and methodology, Formal analysis and validation, Data curation and visualization, Investigation, Writing

3. **TF-Prioritizer: a java pipeline to prioritize condition-specific transcription factors**

Markus Hoffmann, Nico Trummer, Jakub Jankowski, Hye Kyung Lee, Lina-Liv Willruth, Olga Lazareva, Kevin Yuan, Nina Baumgarten, Florian Schmidt, Jan Baumbach, Marcel H. Schulz, David B. Blumenthal, Lothar Hennighausen, and Markus List; In preparation

Detailed contributions:
Data curation and visualization, Writing

List of awards and presentations

2020 – 2024 Graduate Partnership Program NIH Fellowship Award

2023 NIH Fellows Award for Research Excellence

Identification of enhancers and their impact on the kidney injury regulator Klotho

American Society of Nephrology's Kidney Week 2022 (Poster presentation)
Identification of enhancers and their impact on the kidney injury regulator Klotho

American Society of Nephrology's Kidney Week 2021 (Poster presentation)
Interferon-activated genetic programs and a novel short isoform of the SARS-CoV-2 receptor ACE2 in the kidney

Abbreviations

ACE2 – angiotensin converting enzyme 2

AKI – acute kidney injury

ATAC-seq - Assay for Transposase-Accessible Chromatin and Sequencing

BET – Bromodomain and Extraterminal protein

ChIP-seq – Chromatin Immunoprecipitation and Sequencing

CKD – chronic kidney disease

COVID-19 – coronavirus disease 19

DAMP – damage-associated molecular pattern

DHS - DNase Hypersensitive Site

DNMT – DNA methyltransferase

EMA – European Medicines Agency

ESRD – end-stage renal disease

FDA – Food and Drug Administration

FRA – Fos-related antigen

GEO – Gene Expression Omnibus

GFR – glomerular filtration rate

GR – glucocorticoid receptor

HDAC – histone deacetylase

HERV – human endogenous retrovirus

HNF4a – hepatic nuclear factor 4a

Ifnα – interferon alpha

Ifnβ – interferon beta

Ifnγ – interferon gamma

Il-6 – interleukin 6

ISH – in-situ hybridization

IRI – ischemia-reperfusion injury

KDIGO – Kidney Disease: Improving Global Outcomes

KLF-4 – Krüppel-Like Transcription Factor-4

MERS – Middle East Respiratory Syndrome

ncRNA – non-coding RNA

NGS – Next Generation Sequencing

PRRs – Pattern Recognition Receptors

RAAS – renin-angiotensin-aldosterone system

ROS – reactive oxygen species

RTEC – renal tubular epithelial cells

SARS – Severe Acute Respiratory Syndrome

SCr – serum creatinine

SNP – single-nucleotide polymorphism

STAT – Signal Transducer and Activator of Transcription

TAD – topologically-associated domains

TEM – transmission electron microscopy

TGFβ – transforming growth factor beta

TNFα – tumor necrosis factor alpha

WHO – World Health Organization

Summary

Epigenetics drive an often underestimated set of mechanisms governing the fundamental regulation of gene expression. Selective availability of chromatin not only dictates cell differentiation and identity, but can drastically change, as pathological conditions are a potent catalyst for shifts in epigenetic landscape. Our studies show how renal injury is not an exception and aim to investigate how the transcription patterns of the kidney epithelium change in response to an insult.

First, we analyzed renal epithelial response to cytokine stimulation to help elucidate the potential effects of SARS-CoV-2 on the kidney. Our work was the first to show that interferons induce expression of an alternative *ACE2* isoform, *dACE2*, in renal epithelium, but not the canonical protein, showing bias of earlier reports and indicating the need of careful study of the genetic loci of known disease-related genes. We also generated and compared a wide range of the next-generation sequencing datasets pertaining to tubular response to proinflammatory stimuli. We show that distinct transcription programs are enabled in response to interferons and injury models, and that they differ between stimulated tissues. Our results clearly show how non-homogenous the term renal inflammation is and indicate how much its attenuation may need to be adjusted based on the injury's origin.

Second, we used an ischemic acute kidney injury model to investigate the dynamic changes in the entire epigenetic landscape of mouse kidney. We showed hundreds of promoter and candidate enhancer elements gaining or losing their activity in the early repair phase following renal insult, as well as identified transcription factors driving this process. We used compounds disrupting RNA transcription and observed that they can partly inhibit the repair of the epithelial cells, but also attenuate fibrosis. This study provides first insight into the robustness of the epigenetic changes renal cells undergo to initiate repair mechanisms, as well as indicate that timing is a key factor for therapeutic strategies aiming adjust them.

These discoveries further our understanding of the extent, variability and regulation of epigenetic landscape of the kidney. They will aid in development of novel therapeutic strategies aiming to combat diseases and adverse physiological processes in the kidney.

Introduction

1. Epigenetics

The term epigenetics covers a wide range of mechanisms regulating changes in chromatin states and gene expression, which are independent of DNA sequence and can persist after cell division. Regulation of gene transcription by this molecular machinery is one of the most fundamental levels governing cellular function. The term itself was coined in 1942 (Deichmann, 2016) and referred to all mechanisms causing changes in gene expression. Only relatively recently the definition was narrowed, in tandem with development of next generation sequencing (NGS) methods allowing for detailed investigation in this field.

1.1. Role of epigenetic modifications

There are two basic functions of epigenetic homeostasis. The first one is maintaining chromosomal stability. Chromatin must conform to an optimized, three-dimensional format to be able to perform its role (Gollin, 2004; Weyemi & Galluzzi, 2021). This requires proper organization of centromeres and telomeres and maintenance of functional DNA repair systems. Large structural changes in chromosomal architecture may be fatal, either as congenital defects or as an immense contributor to cancer development. The second function of the epigenetic control is regulation of gene expression, either by silencing or enhancing gene transcription. This allows the cell populations to grow into specialized tissues and for the dying cells to be replaced by ones with the same transcriptional programming. This process is relatively plastic, as pathological conditions impacting the homeostasis can cause transient or permanent changes to the epigenetic landscape.

1.2. Mechanisms of epigenetic control

There are three major ways the epigenetic programming is maintained. DNA methylation is one of the most well-known mechanisms of gene suppression. Addition of methyl group to DNA cytosine bases leads to recruitment of gene silencing proteins and to inhibition of transcription factor binding (Moore et al., 2013). Significant portions of mammalian genomes are silenced by

methylation, including the 45% of human genome encoding retrotransposons such as inactivated human endogenous retroviruses (HERVs). This process is governed by DNA methyltransferases (DNMTs). Cancer is known to cause aberrant methylation, which can be combated with DNMT inhibitors (Giri & Aittokallio, 2019). At lower doses, DNA silencing caused by cancer can be reversed, but higher amounts of the drug might be cytotoxic due to DNA hypomethylation and increased chromosomal instability (Hoffmann & Schulz, 2005). Further, epigenetic control can be elicited through histone modification. Short fragments of DNA, approximately 150 base pair in length, are spooled over histone protein octamers (Luger et al., 2012). Biochemical changes, such as acetylation, methylation or phosphorylation, regulate the histones' function and dictate how permissible the associated DNA fragment is to binding other proteins such as transcription factors. With the development of ChIP-seq and anti-histone antibodies, it was possible to isolate distinct histone modifications and their roles. For example, monomethylation of the lysine 4 of the H3 histone (H3K4me1), combined with acetylation of lysine 27 of the H3 histone (H3K427ac) indicates presence of a putative gene enhancer (Heintzman et al., 2007). Similarly to the methylation, histone modification can be pharmaceutically altered. Histone deacetylase (HDAC) inhibitors are a line of mostly anti-cancer agents more cytotoxic for the tumor than for the healthy tissue (Sanaei & Kavoosi, 2019). The third of the key epigenetic mechanisms is regulation through non-coding RNAs (ncRNAs). Those RNAs are not translated, instead work together with the other two mechanisms to elicit transcriptional control. ncRNAs were reported to affect both histone modification and DNA methylation (Khraiwesh et al., 2010; Tuddenham et al., 2006), and their function is multimodal. For example, they can serve as intracellular molecular decoys, attracting proteins regulating transcription (Li et al., 2021) or as extracellular modulators of immune response (Sharma et al., 2021).

1.3. Gene expression enhancers

The gene bodies are not the only DNA elements undergoing epigenetic modifications. Genes are surrounded by untranslated cis-regulatory elements, such as enhancers. As the name suggests, enhancer elements can positively influence gene transcription. Enhancers are very variable in respect to their length and distance to their target gene. They can span anywhere between 50 and 1000 bp and be located even 1 Mbp away from the gene promoter they interact with (Krivega & Dean, 2012). Hypothetically, the enhancers could interact with promoters on other chromosomes, like the enhancer of the odorant receptor gene was proposed to do (Lomvardas et al., 2006). This

would require investigating additional mechanisms of coordinated chromosomal interaction within the nucleus. In most cases, it is accepted that enhancers and their targets are located within linear topologically associated domains (TADs) on the same chromosome. TADs are surrounded by CTCF binding sites. CTCF forms chromatin loops and helps establish the hierarchical three-dimensional topology of the DNA (Rowley & Corces, 2018). Surprisingly, TAD borders can often remain intact despite deletion of the CTCF sites, though in some cases the enhancer activity can extend outside the original TAD in an unpredictable fashion (Barutcu et al., 2018; Lee et al., 2017). Activation of an enhancer starts by transcription factors and regulators attaching to open chromatin of the enhancer. This allows for histone remodeling at the target promoter and recruitment of the Mediator complex to the enhancer (Soutourina, 2018). Mediator consists of several subunits that bridge the enhancer and the polymerase II complex at the promoter and enable transcription.

Single enhancers can have several target genes, further complicating the directionality and predictability of enhancer interactions. Despite the detection of chromatin modifications by ChIP-seq and visualization of promoter-enhancer interplay through chromatin conformation capture techniques, the only way to confirm putative enhancer's activity is to delete it in an *in vitro* or *in vivo* model. To make things worse, it is possible that only select detected histone modification peaks or predicted transcription factor binding sites within are responsible for the enhancer's function. In case of super-enhancers, finding the key sequence is even more difficult as they can span over 10 kbp. At first, those massive enhancers were proposed to play a key role in development of cellular lineages and in regulation of tissue-specific genes (Shin et al., 2016; Whyte et al., 2013), but they can regulate other processes as well, such as cardiovascular health and cancer progression (Ounzain & Pedrazzini, 2016; Sengupta & George, 2017).

1.4. Diseases impacted by enhancer biology

Studying enhancer biology is vital, as aberrant enhancer activation or silencing is a common factor fueling a wide variety of pathological conditions. It can be caused by deregulation of epigenetic mechanisms or disruption of the enhancer DNA sequence. The simplest way to disable an enhancer is to introduce a mutation or delete a part of it. This is a basis of several disorders such as Pierre Robin sequence or heart arrhythmia (Galang et al., 2020; Long et al., 2020). Further, single-nucleotide polymorphisms (SNPs) in enhancer regions can contribute to development of, among others, osteoporosis or schizophrenia (Tuo et al., 2020; Zhang et al., 2022). Wilson disease and Alzheimer's disease can be caused by hypermethylation of relevant enhancer regions

(Qazi et al., 2018; Sarode et al., 2021). Disruption of the aforementioned TADs can cause fragile X syndrome (Lanni et al., 2013). Finally, all of the processes above contribute to cancer development, as progressive genomic instability is one of its hallmarks.

1.5. Renal epigenetics

Compared to other tissues, especially cancerous, there are not enough high quality NGS datasets available to the public to paint a clear picture of the epigenetic landscape of the kidney, which is why our research is of high significance. However, there is ample evidence for the impact of epigenetic processes on renal health. Probably the most impressive dissection of renal development was performed using combination of single-cell ATAC-seq and RNA-seq (Miao et al., 2021). The authors present a map of open chromatin loci and separate cell populations to indicate distinct differences in gene expression.

What we are the most interested in, however, is not the developmental aspect, but rather the foundation of renal pathological processes - persistent reprogramming of gene expression patterns. For example, a streptozotocin-induced diabetes model revealed that the renal repair programs are impaired even after streptozotocin withdrawal (Sarras et al., 2013). Diabetic disease's development is also sped up by aberrant methylation driven by Krüppel-Like Transcription Factor-4 (KLF4) (Coskun et al., 2019). HDAC proteins, responsible for histone modifications, were reported to be a part of renal repair system as well (Hyndman et al., 2019). Their activity changes after insult, acutely aiding in epithelial proliferation, but promoting fibrosis in the long-term. Similarly, fibrosis is enhanced through increased TGFβ signaling interacting with DNMT proteins and causing excessive DNA methylation, as well as altering ncRNA activity (Yin et al., 2017). ncRNA, especially miRNA, are still a relatively new and rapidly developing topic in renal research. Several species are upregulated in AKI models, working both as proinflammatory agents and regenerative factors (Godwin et al., 2010; Lorenzen et al., 2014).

It is not surprising, that the kidney health is heavily dependent on epigenetic mechanisms both during normal development, physiology and disease. The complexity of the interplay of all the epigenetic factors, not only molecular, but also behavioral, like nutrition and hygiene, still eludes us. The next important step is to generate and compile genomic datasets of the kidney in various pathophysiological states to elucidate common factors and unique regulators driving renal gene expression.

2. Kidney disease

Diseases of the kidney are a silent epidemic, affecting millions of people worldwide. One in four patients admitted to an intensive care unit may experience a temporary or permanent decrease in kidney function (Sovik et al., 2019). Estimates show that one in seven adults in developed countries suffers from chronic kidney disease (CKD) (Chu et al., 2021) and the global prevalence of diabetes, a major cause of CKD, nears ten percent of the population (Saeedi et al., 2019).

2.1. Kidney disease – treatment and etiology

Despite the prevalence, therapeutic options available for those with decreased renal function are limited. Approaches like high blood pressure adjustment (Kalaitzidis & Elisaf, 2018), anemia prevention (Atkinson & Warady, 2018), dietary recommendations (Ikizler et al., 2020), vitamin D and calcium supplementation (Jean et al., 2017) and lifelong dialysis (Cullis et al., 2021) are focused on alleviating the symptoms rather than treating the cause. In severe cases, such as end-stage renal disease (ESRD), renal replacement therapy can be utilized, but has its own risks, including high mortality, even in the pediatric population, usually suffering from less extra-renal comorbidities (Chesnaye et al., 2018; Hod & Goldfarb-Rumyantzev, 2015).

There are several reasons why renal therapies are lacking. The main cause is that the kidney disease is not a monolithic condition, and its development and progression is dependent on multiple factors, often uncertain due to late detection. They include common variables like age, race and sex and comorbidities, but also the disease's etiology, a category which includes, but is not limited to viral, congenital, hereditary, traumatic, or drug-induced insults (Hoste et al., 2018). Unfortunately, the immediate cause of renal dysfunction is often hard to establish, as the disease can manifest a long time after its induction. While the origin of the kidney injury might dictate the therapeutic approach, damage ultimately happens within the cells of the kidney itself, undergoing transformation at the transcriptional level. If the mechanisms governing those changes were to be understood, more effective therapies could be developed, aiming at the source of kidney injury and repair.

2.2. Acute kidney injury

In our work, we use ischemia-reperfusion injury (IRI) as a model of acute kidney injury (AKI). This model reflects a significant portion of patient cases (Sharfuddin & Molitoris, 2011). Further, ischemia itself has been widely discussed as a common element in AKI development, not only following physical trauma, but also in renal transplantation and other surgical interventions (Mannon, 2018; Yokoyama et al., 2020). Since AKI has many manifestations and accompanying symptoms, there were numerous attempts to classify and diagnose its occurrences (Kwong & Liu, 2017). Currently, the majority of the scientific literature uses guidelines established by the Kidney Disease: Improving Global Outcomes (KDIGO) conference (Ostermann et al., 2020). To qualify as an undergoing AKI event, a patient must exhibit one of the following markers: increase in serum creatinine (SCr) by x0.3 mg/dl (x26.5 mol/l) within 48 hours; 1.5 times increase in SCr compared to baseline, known or presumed to have occurred within the prior 7 days; or maintaining 0.5 ml/kg/h urine volume for 6 hours. Depending on the patient's SCr levels and urine volume, AKI can be further classified in stages, I to III, narrowing down the optimal therapeutic approach. It is worth noting that decrease in renal function might seem only temporary, however, every incident increases the risk of developing CKD later in life (Kurzhagen et al., 2020).

2.2.1. AKI mechanisms

Another one of the causes for the diminished efficacy of renal therapies are the mechanisms of AKI development and resolution. They are still relatively unknown and while we can identify several elements common or unique to the various AKI subtypes, the key to understanding those processes lies in deciphering the epigenetic machinery that puts them into motion (Xu et al., 2017). The core target of renal injury and repair are renal tubular epithelial cells (RTEC), mainly the proximal tubule. They form the bulk of the organ (Hommos et al., 2017), and are the key to maintaining homeostasis by reabsorbing majority of the water and salts in the pre-urine, as well as being a source of cytokines, hormones and mediators. They are also the most vulnerable to injury (El-Achkar & Dagher, 2015), including ischemia.

Proximal tubules contain dense mitochondrial networks used to satisfy their high metabolic needs (Neufeld et al., 1980). One of the mechanisms through which the kidney epithelium is disrupted, is by induction of mitochondrial dysfunction, for example during hypoxia and rapid reoxygenation. After injury, abundance of the reactive oxygen species (ROS) generated by mitochondria can

easily push the cell towards cell death pathways, such as apoptosis or necrosis (Himmelfarb et al., 2004; Martin et al., 2019). Dying cells, in turn, can release damage-associated molecular patterns (DAMPs). These are often simply molecules found inside the cell, which after release can bind to Pattern Recognition Receptors (PRRs) on immune cells and trigger the development of kidney inflammation. Renal milieu already possesses a number of resident macrophages and dendritic cells (Munro & Hughes, 2017; Summers et al., 2020), but in AKI, large quantities of neutrophils start infiltrating the tissue as well (Bolisetty & Agarwal, 2009). What follows is an inflammatory response, fueled by cytokines and chemokines released by the cells of both renal epithelium and innate immune response (Rabb et al., 2016). Evidence of altered epigenetic landscape contributing to AKI development has been established as well. For example, the complement system C5a protein can cause aberrant DNA methylation and senescence as it alters the WNT4/β-catenin signaling (Castellano et al., 2019) in renal epithelium. Despite us having established the basic mechanisms of the injury process, the underlying changes in gene regulation driving them are largely unknown.

2.3. Chronic kidney disease

Chronic kidney disease often develops as a comorbidity caused by other serious medical conditions, such as impairment of the cardiovascular system (Schefold et al., 2016) or diabetes (Anders et al., 2018). Altered blood pressure or osmolality of serum can slowly cripple the kidney until pathophysiological signs can be seen and reported by the patient. Unfortunately, unless monitored, those suffering from CKD can easily overlook those signs until serious damage is done. Additionally, it is now accepted knowledge that AKI incidents, even if resolved, contribute to increased risk of kidney disease later in life, suggesting pervasive gene reprogramming. Similarly to AKI, KDIGO established a set of diagnostic and prognostic markers which can assist in CKD identification, based on the patient's glomerular filtration rate (GFR) and albuminuria.

2.3.1. CKD progression mechanisms

CKD is a progressive condition, where several mechanisms work together to wear down the kidney function finally resulting in ESRD and organ failure. It is well established that hypertension is a significant CKD contributor (Ku et al., 2019). Increased blood pressure can lead to hyperperfusion and hypertrophy exerting mechanical stress on the organ (Chagnac et al., 2019). Kidney itself is largely responsible for maintaining the blood pressure, as it's a vital part of the renin-angiotensin-aldosterone system (RAAS), disrupted in CKD. Renal epithelium produces renin, a rate-limiting hormone of the system (Danser et al., 1994). Downstream, renin is responsible for adjusting blood pressure, water intake and serum sodium concentration, on a complex, multi-organ level.

Regardless of the cause of CKD, during the development, a continuous low-grade inflammatory response to the cellular stress is always present. Proinflammatory cytokines, such as TNFα and IL-6 and cells of the innate immune system contribute to the destruction of healthy renal architecture (Ebert et al., 2020; Kipari & Hughes, 2002). Further, cells which underwent apoptosis are replaced by progressive fibrosis, with collagen fibers diminishing nephron area and renal function. Most commonly, TGFβ is identified as the main culprit behind the pro-fibrotic processes (Meng et al., 2016). Each of the mechanisms above and several others, such as podocyte loss and proteinuria, can exacerbate the other mechanisms of CKD progression and work as multiple positive feedback loops to gradually increase the damage over time.

Considering the above, it is not surprising that CKD rarely develops with no comorbidities. Perhaps the most publicly recognized danger to kidney health are diabetes. Inseparably linked to hypertension, diabetes is responsible for development of approximately 25% of CKD cases, and an enormous contributor to its death toll (Cheng et al., 2021). Another common ailment aiding in development of nephropathies is cancer (Stengel, 2010). It doesn't need to originate within the kidney itself to throw the bodily homeostasis off balance. Additionally, agents used in cancer treatment like radiation or cisplatin, are often damaging and nephrotoxic, fueling the inflammation and remodeling (Miller et al., 2010).

2.3.2. AKI to CKD transition

As it was mentioned before, AKI can be a cause or a contributor to the development of CKD. As the kidney fails to recover entirely from the initial insult, gene expression programs are permanently altered, and the recovery and remodeling of the kidney can take on pathophysiological characteristics. For example, the mechanism of autophagy is a physiological way for a cell to degrade accumulated misfolded proteins or faulty organelles (Glick et al., 2010). After AKI, not all epithelial cells retain this ability, leading to increased cell death and necrosis (Lin et al., 2014), impairing potential for self-repair and fueling inflammation. Additionally, AKI can trigger several pathways, such as Wnt, Notch or Hedgehog, increasing senescence and diminishing tubular regeneration post-injury (Edeling et al., 2016). This, in tandem with prolonged TGFβ activation, which might be beneficial during the AKI period itself (Guan et al., 2010), contributes to progressive fibrosis and development of CKD. There are several other mechanisms briefly described earlier as driving the AKI damage, such as the reactive oxygen species aggregation and factors contributing to the prevalence of tubular apoptosis and necrosis, which contribute to AKI-CKD transition as well. The common denominator between all of them is that they require aberrant cellular reprogramming at the transcriptional level.

3. SARS-CoV-2 and the kidney

Since early 2020, the SARS-CoV-2 pandemic has become yet another contributor to the global decline of renal health. The prevalent theory indicates that the virus originated in the Wuhan province of China (Phelan et al., 2020) in the last quarter of the year 2019. It was able to spread rapidly throughout the world, prompting the World Health Organization (WHO) to declare a state of pandemic in March 2020.

3.1. SARS-CoV-2 – an overview

SARS-CoV-2 belongs to the *Coronaviridae* family. Coronaviruses are single-stranded RNA viruses, ubiquitous in the environment and able to cause gastrointestinal and pulmonary diseases of varying severity. In most patients COVID-19 symptoms resemble flu, with high fever, cough and fatigue. Acutely, this develops into severe pneumonia and respiratory system collapse. Patients with resolved SARS-CoV-2 infection often suffer from post-acute COVID syndrome (or long COVID). It is an umbrella term for multi-organ changes caused by the virus, which can also affect kidney health, including increase in susceptibility to AKI incidents (Bowe et al., 2021). The host repertoire of coronaviruses is wide, ranging from poultry and bats to primates (Peck et al., 2015). They are zoonotic viruses, able to switch between host species or change their preference as they evolve, as evidenced by the MERS-CoV, which spread from dromedary camels and caused an epidemic originating in Saudi Arabia in 2012 (Corman et al., 2018). Host specificity is largely regulated by the viral spike protein, which in the case of SARS-CoV-2 functions as a receptor binding cellular angiotensin converting enzyme 2 (ACE2) and facilitating infiltration into the cells (Piplani et al., 2021).

3.2. ACE2 biology

The affinity of coronaviruses for ACE2 binding has been known for a long time, as it played a key role in SARS-CoV outbreak in the year 2002 (Li et al., 2003). However, ACE2 also plays several roles in regular homeostasis. Its basic function as a dipeptidyl carboxypeptidase is to cleave angiotensins I and II, parts of the RAAS system regulating blood pressure and body fluid volume. Angiotensin I's cleavage produces anti-inflammatory angiotensin 1-9 (Donoghue et al., 2000; Flores-Munoz et al., 2011), while angiotensin II's makes angiotensin 1-7, which counters high

blood pressure and hypertensive cardiac remodeling (Gironacci, 2015; Mercure et al., 2008). *ACE2* gene expression is ubiquitous. It is present in multiple organs and the average level of expression in the pulmonary system, the main target of SARS-CoV-2, is exceeded by elements of the gastrointestinal tract and the kidneys (Li et al., 2020). In fact, the kidney boasts one of the highest levels of *ACE2* expression, indicating them as a good potential target for viral infection.

3.3. Direct renal infection with SARS-CoV-2

The abundance of ACE2 on the surface of renal epithelium notwithstanding, the validation of the direct viral infection of the kidney proved difficult. ACE2 on the surface of the cell is localized to its apical membrane, that is the ciliated side facing the lumen of the pulmonary tract segment or a renal nephron (Sims et al., 2005). While this is not an issue for a respiratory tract infection, in the case of the kidney, the viral particle would need to cross the glomerular membrane to efficiently attach to ACE2 receptors. Coronaviruses are relatively large, and SARS-CoV-2 is approximately 100 nm in diameter (Bar-On et al., 2020), while the pores of the glomerular filtering membrane are much smaller (Kawachi & Fukusumi, 2020), seemingly prohibiting viral entry. Several alternative hypotheses were formed, including the infection disseminating through endothelium (Cantuti-Castelvetri et al., 2020) or neurons (Fenrich et al., 2020). In airway epithelia, a lower efficiency of infection through a basal membrane was observed as well (Jia et al., 2005).

Those hypotheses of alternative tropism were necessary, as despite the filtration barrier, SARS-CoV-2 has been detected in patient kidney samples. Using Transmission Electron Microscopy (TEM), viral particles were identified in post-mortem renal samples (Abbate et al., 2020; Su et al., 2020). Those findings, however, need to be evaluated carefully, as a vesicle-like structures can be easily misinterpreted (Cassol et al., 2020). That being said, immunohistochemistry, in-situ hybridization (ISH) and reverse transcription polymerase chain reaction (RT-PCR) confirm the TEM findings. For any publication that found viral RNA or protein in a kidney biopsy sample (Bouquegneau et al., 2021; Diao et al., 2021; Puelles et al., 2020), there is one refuting such findings in a similar setting (Best Rocha et al., 2020; Massoth et al., 2021; Sharma et al., 2020). However, the combined evidence and the alternative tropism hypotheses strongly indicate that SARS-CoV-2 can indeed directly impact kidney cells.

3.4. SARS-CoV-2 and the impact on kidney health

Difficulty in establishing the original cause of the kidney injury is also a factor in the discussion about direct infection. It is almost never certain whether a viral disease caused the kidney injury, or if a preexisting condition allowed for it. Whichever comes first, the association between COVID-19 and kidney disease has become clear as the pandemic progressed. Initial reports from single-center studies were optimistic and indicated no correlation between the viral infection and AKI (Wang et al., 2020). Several months later, however, similar studies started to show a strong link between the two (Rubin et al., 2020). The difference can be explained by small sample sizes, but also by differential demographics of the cohorts in the studies. With time, the term of COVID-19-associated AKI has been accepted by the research community, regardless of the fact if the virus itself causes kidney injury, or if it's a result of the inflammation and cytokine storms incited by SARS-CoV-2 (Ahmadian et al., 2021).

4. Impact of our research on the understanding of renal injury

Our research, presented in this thesis, aims to broaden the current understanding of kidney injury. First, we focus on *ACE2*, a gene key in COVID-19 infection, but also deeply involved in regulation of water and mineral balance. We analyze the *ACE2* locus in human renal epithelial cells to elucidate its regulatory landscape. We describe new putative promoter and enhancer elements governing the expression of *dACE2*, a shorter, interferon-inducible isoform. We showed that it is one of many genes transcribed in response to cytokine stimulation, as we generated ChIP-seq and RNA-seq data allowing for the first time for in-detail comparisons of renal epithelial reaction to interferon stimulation to other similar datasets. We show that despite having a similar core response, IFNα, IFNβ and IFNγ induce distinctly different genes in RTEC. Renal IFNβ stimulation results in activation of genes different than in lung and liver epithelium. Finally, we show the grave need for generation of more renal sequencing datasets, as COVID-19, AKI and interferon response have very little transcriptional overlap.

Next, we investigated in detail the changes in mouse epigenetic landscape after renal IRI. We visualized the kidney losing and gaining thousands of epigenetic markers, including promoters and enhancers. We used bioinformatics' tools to propose a set of transcription factors governing those changes and showed promoter and enhancer activity shift in *loci* of several genes affiliated with renal ischemia-reperfusion. Further, we treated the mice with JQ1, a BET inhibitor. If administered at the time of injury, JQ1 caused increase in mortality after surgery, which can be contributed to disruption of early repair programs. BET-dependent transcriptional activation changes four days after injury, when BET inhibition starts to have an anti-fibrotic effect instead of a detrimental effect on survival. This adds new insight into temporal changes in renal epithelial repair programs and can help narrow down optimal therapeutic windows for preventing permanent organ damage.

Our data allows for a wider overlook of the physiological and pathophysiological response to proinflammatory stimuli, injury and transcription-regulating therapeutics. It can be used as a basis for further research, both concerning established injury models like IRI and emergencies like the SARS-CoV-2 pandemic.

Publication 1

JAK inhibitors dampen activation of interferon-activated transcriptomes and the SARS-CoV-2 receptor ACE2 in human renal proximal tubules.

Jakub Jankowski, Hye Kyung Lee, Julia Wilflingseder, Lothar Hennighausen

iScience 2021, 24:102928

iScience

CellPress
OPEN ACCESS

Article

JAK inhibitors dampen activation of interferon-activated transcriptomes and the SARS-CoV-2 receptor ACE2 in human renal proximal tubules

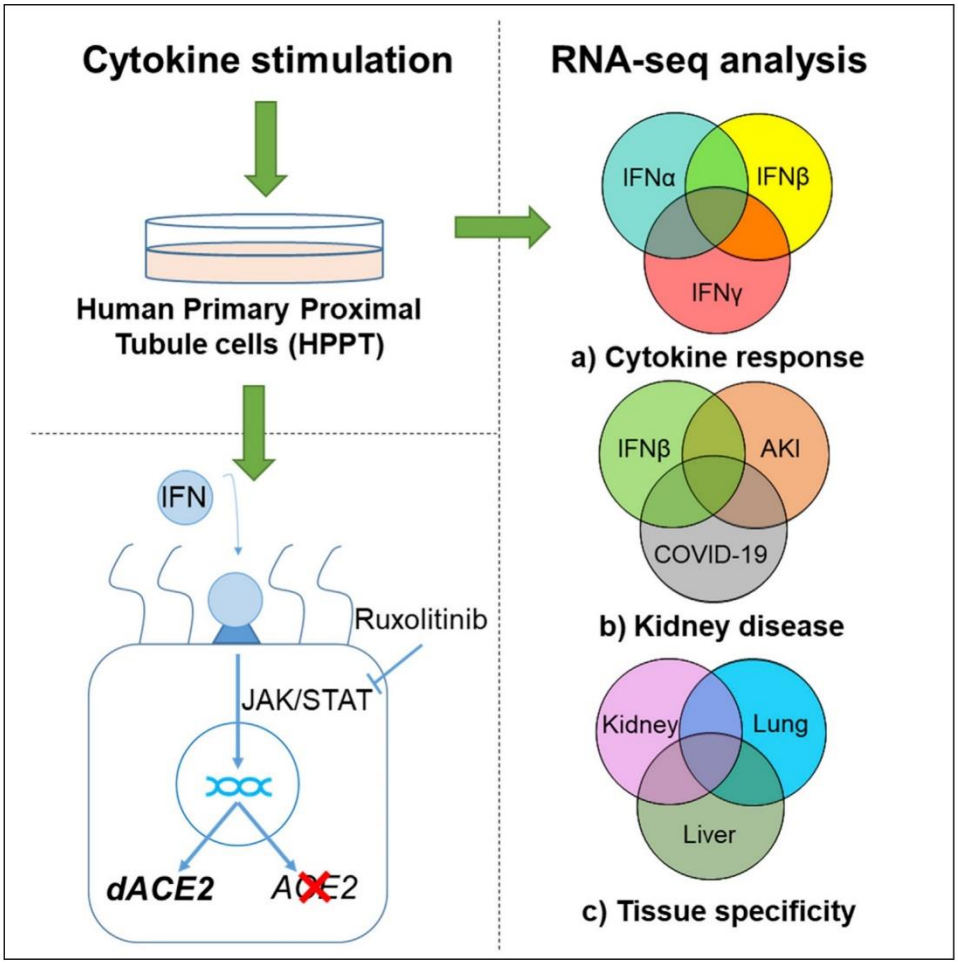

Jakub Jankowski, Hye Kyung Lee, Julia Wilflingseder, Lothar Hennighausen

jakub.jankowski@nih.gov (J.J.)
lotharh@nih.gov (L.H.)

Highlights

We provide transcriptomic and epigenetic data sets for human renal proximal tubules

Cytokine stimulation induces distinct genetic pathways in the kidney

Short isoform of *ACE2*, *dACE2*, is expressed in renal proximal tubules

Type I interferons increase *dACE2*, but not full *ACE2* expression

Jankowski et al., iScience *24*, 102928
August 20, 2021
https://doi.org/10.1016/j.isci.2021.102928

iScience

CellPress
OPEN ACCESS

Article

JAK inhibitors dampen activation of interferon-activated transcriptomes and the SARS-CoV-2 receptor ACE2 in human renal proximal tubules

Jakub Jankowski,[1,2,*] Hye Kyung Lee,[1] Julia Wilflingseder,[2] and Lothar Hennighausen[1,3,*]

SUMMARY

SARS-CoV-2 infections initiate cytokine storms and activate genetic programs leading to progressive hyperinflammation in multiple organs of patients with COVID-19. While it is known that COVID-19 impacts kidney function, leading to increased mortality, cytokine response of renal epithelium has not been studied in detail. Here, we report on the genetic programs activated in human primary proximal tubule (HPPT) cells by interferons and their suppression by ruxolitinib, a Janus kinase (JAK) inhibitor used in COVID-19 treatment. Integration of our data with those from patients with acute kidney injury and COVID-19, as well as other tissues, permitted the identification of kidney-specific interferon responses. Additionally, we investigated the regulation of the recently discovered isoform (dACE2) of the angiotensin-converting enzyme 2 (ACE2), the SARS-CoV-2 receptor. Using ChIP-seq, we identified candidate interferon-activated enhancers controlling the *ACE2* locus, including the intronic *dACE2* promoter. Taken together, our study provides an in-depth understanding of genetic programs activated in kidney cells.

INTRODUCTION

A form of acute respiratory distress syndrome (ARDS) caused by SARS-CoV-2 is a major contributor to the death toll of COVID-19 (Gibson et al., 2020). ARDS is closely linked to cytokine storm, an unrestrained release of proinflammatory cytokines and chemokines (Kim et al., 2021). This, in turn, may result in multi-organ failure (Mokhtari et al., 2020) and coagulopathies (Vinayagam and Sattu, 2020), affecting, amongst others, the kidney (Ahmadian et al., 2021). Acute kidney injury (AKI), potentially resulting from cytokine storm (Chong and Saha, 2021), is a known complication of COVID-19, and it has also been proposed that decline in renal function in hospitalized patients is caused by the virus itself (Lynch and Tang, 2020). Even before the SARS-CoV-2 pandemic, AKI was a significant medical and socioeconomic burden, with estimated one in three intensive care patients suffering from decline in kidney function (Hoste et al., 2018).

In addition to other mechanisms, SARS-CoV-2 was shown to able to infect kidney epithelium, directly contributing to organ damage (Braun et al., 2020; Peng et al., 2020; Su et al., 2020; Sun et al., 2020). It is known that its infectivity depends on the receptor, angiotensin-converting enzyme 2 (ACE2) (Hoffmann et al., 2020). Physiologically, ACE2 serves as an element of renin-angiotensin-aldosterone system and bradykinin system (Donoghue et al., 2000; Tipnis et al., 2000). In SARS-CoV-2 infection, the viral spike protein binds ACE2 and facilitates viral entry into cells. ACE2 expression has been detected in the kidney (Sungnak et al., 2020) and proximal tubules via single-cell transcriptome analysis (Chen et al., 2020; He et al., 2020). However, transcriptional regulation of *ACE2* and its expression pattern in the kidney are poorly understood. Human studies indicate that changes in *ACE2* expression are linked to type 2 diabetic nephropathy (Mizuiri et al., 2008), IgA nephropathy (Mizuiri et al., 2011), hypertension (Koka et al., 2008), and nephrosclerosis (Wang et al., 2010). Usually, decrease in ACE2 is associated with disease, which may dysregulate ACE/ACE2 ratio; however, both ACE and ACE2 may be regulated by independent pathways (Mizuiri and Ohashi, 2015).

Recently, a new isoform of *ACE2*, *deltaACE2* (*dACE2*), was identified in several cell types (Blume et al., 2020; Fignani et al., 2020; Lee et al., 2021; Ng et al., 2020; Onabajo et al., 2020). Contrary to earlier reports (Ziegler et al., 2020), where *ACE2* was suggested to be an interferon-stimulated gene (ISG), its new isoform *dACE2*

[1]Laboratory of Genetics and Physiology, National Institute of Diabetes and Digestive and Kidney Diseases, U.S. National Institutes of Health, Building 8, Room 101, 8 Center Dr, Bethesda, MD 20892, USA

[2]Department of Physiology and Pathophysiology, University of Veterinary Medicine, Veterinärplatz 1, 1210 Vienna, Austria

[3]Lead contact

*Correspondence: jakub.jankowski@nih.gov (J.J.), lotharh@nih.gov (L.H.)

https://doi.org/10.1016/j.isci.2021.102928

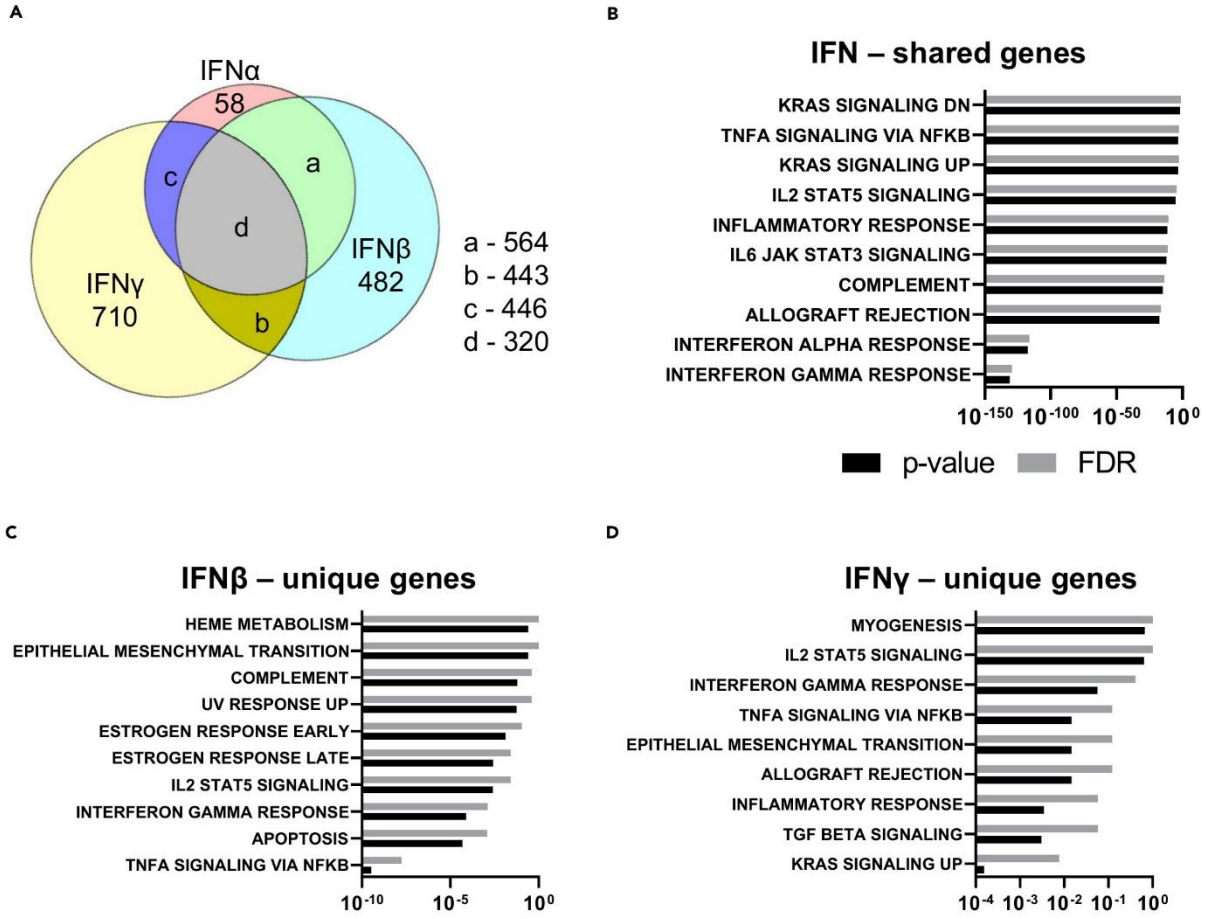

Figure 1. Comparison of signaling pathways induced by IFNα, IFNβ, and IFNγ stimulation of HPPT cells

(A) Venn diagram of unique and common genes induced by each cytokine.

(B–D) GSEA results of p values and FDR in top 10 significantly represented pathways in gene groups shared by all three conditions and unique for IFNβ and IFNγ. See also Tables S1–S3.

expression appears to be significantly regulated by cytokine or viral stimulation. In fact, in some cells, such as pancreatic β-cells, *dACE2* may be the prevalent isoform even at the baseline (Fignani et al., 2020). Usually, decrease in *ACE2* expression is linked with disease progression; however, it is unknown whether *dACE2* has an impact on these readouts, as methods used to this date assessed *ACE2* without discerning between isoforms. Additionally, increased *ACE2* levels were found in several animal models of kidney disease, and contribution of *dACE2* to these changes remains to be assessed (Moon et al., 2008).

Here, for the first time, we show global transcriptional regulation in cytokine-stimulated human primary proximal tubule (HPPT) cells. We assess overlaps between responses to IFNα, IFNβ, and IFNγ, and we compare IFNβ-stimulated genetic programs to available AKI and COVID-19 data sets to investigate shared pathways in renal response to injury. We show interferon-inducible genetic pathways unique for the kidney and shared with other human tissues. We assess interferon stimulated gene downregulation by JAK inhibitor ruxolitinib and, finally, describe in detail the regulatory landscape of the *ACE2* locus in renal proximal tubule cells.

These findings provide in-depth understanding of interferon-mediated immune responses in the kidney, especially in the context of *ACE2* activation observed in SARS-CoV-2 infection, and may serve as a basis for better understanding of the commonalities and differences between cytokine stimulation of various tissues.

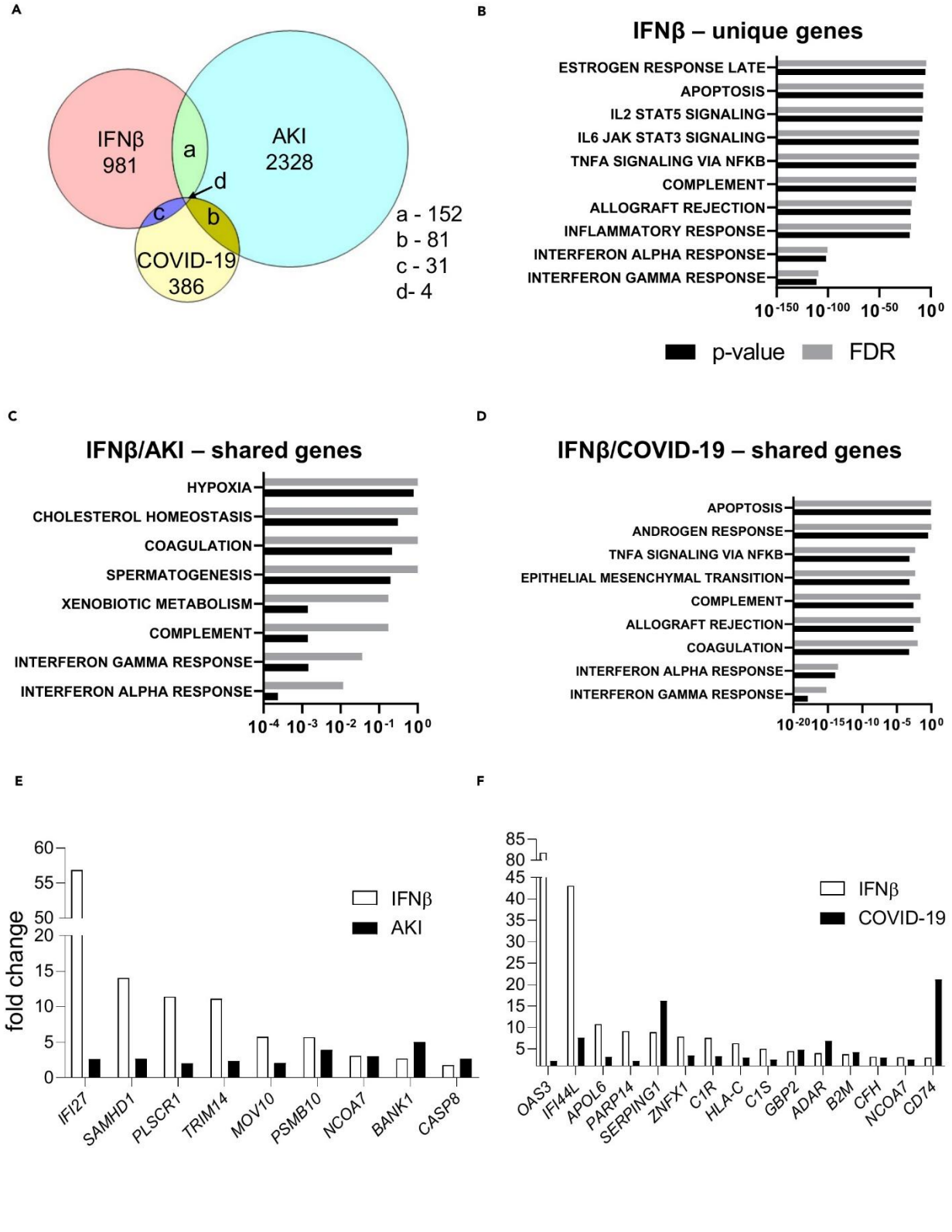
A
IFNβ
981
AKI
2328
COVID-19
386
a
b
c
d
a - 152
b - 81
c - 31
d- 4
B
IFNβ – unique genes
ESTROGEN RESPONSE LATE
APOPTOSIS
IL2 STAT5 SIGNALING
IL6 JAK STAT3 SIGNALING
TNFA SIGNALING VIA NFKB
COMPLEMENT
ALLOGRAFT REJECTION
INFLAMMATORY RESPONSE
INTERFERON ALPHA RESPONSE
INTERFERON GAMMA RESPONSE
10-150 10-100 10-50 100
p-value
FDR
C
IFNβ/AKI – shared genes
HYPOXIA
CHOLESTEROL HOMEOSTASIS
COAGULATION
SPERMATOGENESIS
XENOBIOTIC METABOLISM
COMPLEMENT
INTERFERON GAMMA RESPONSE
INTERFERON ALPHA RESPONSE
10-4 10-3 10-2 10-1 100
D
IFNβ/COVID-19 – shared genes
APOPTOSIS
ANDROGEN RESPONSE
TNFA SIGNALING VIA NFKB
EPITHELIAL MESENCHYMAL TRANSITION
COMPLEMENT
ALLOGRAFT REJECTION
COAGULATION
INTERFERON ALPHA RESPONSE
INTERFERON GAMMA RESPONSE
10-20 10-15 10-10 10-5 100
E
fold change
60
55
50
20
15
10
5
0
IFNβ
AKI
IFI27
SAMHD1
PLSCR1
TRIM14
MOV10
PSMB10
NCOA7
BANK1
CASP8
F
85
80
45
40
35
30
25
20
15
10
5
IFNβ
COVID-19
OAS3
IFI44L
APOL6
PARP14
SERPING1
ZNFX1
C1R
HLA-C
C1S
GBP2
ADAR
B2M
CFH
NCOA7
CD74

Figure 2. Comparison of signaling pathways induced by IFNβ stimulation of HPPT cells, and human kidneys during AKI and COVID-19 infection

(A) Venn diagram of unique and common genes induced by IFNβ, AKI, and COVID-19.

(B–D) GSEA results of p values and FDR in top 10 significantly represented pathways in gene groups unique for HPPT and shared between HPPT and COVID-19 or AKI.

(E and F) Comparison of fold increase in expression of shared genes involved in IFN signaling in HPPT vs AKI and COVID-19 (in relation to untreated, healthy, and mild COVID-19 samples, respectively). See also Tables S1–S3.

RESULTS

To investigate renal cytokine-induced genetic programs, we conducted unbiased RNA-seq analyses on HPPT cells treated for 12 hr with IFNα, IFNβ, IFNγ, or IL-1β. A total of 746 genes were significantly induced by IFNα, 1169 by IFNβ, 1280 by IFNγ, and 2190 by IL-1β (Tables S1 and S2). Next, we investigated the degree of interferon response overlap. IFNα induced expression of 58 unique genes, while IFNβ and IFNγ induced 482 and 710 genes, respectively (Figure 1A). The overlap between all three interferons (320 genes) was enriched for interferon response genes (Figure 1B and Table S3), while gene sets unique for IFNβ and IFNγ were more diverse (Figures 1C and 1D). Next, we focused on IFNβ. It statistically significantly altered the most diverse signaling pathways as identified by Gene Set Enrichment Analysis (GSEA) (Table S3); it is also a known antiviral used against COVID-19. Additionally, several public transcriptomic data sets from cells treated with IFNβ are available to help elucidate interferon-regulated genetic programs specific for renal epithelium.

First, we compared whether expression patterns in patients with AKI (Park et al., 2020) and patients with severe COVID-19 (Desai et al., 2020) bear resemblance to those stimulated in HPPT cells by IFNβ. To our knowledge, only one RNA-seq data set with human ischemia-reperfusion AKI data is publicly available (Park et al., 2020). Similarly, only one renal data set from patients with COVID-19 could be found for our comparison, differentiating between severe and nonsevere disease (Desai et al., 2020). IFNβ stimulation of HPPT cells resulted in upregulation of 981 unique genes compared with other conditions (Figures 2A and 2B). AKI resulted in increased expression of 2566 genes including 156 shared with IFNβ-stimulated HPPT cells (Figures 2A and 2C; Table S3). Expression of 35 genes was induced in both severe COVID-19 and IFNβ-treated HPPT cells (Figures 2A and 2D; Table S3). Although more genes were shared between IFNβ-HTTP and AKI than between IFNβ-HPPT and COVID-19, genes involved in the interferon signaling pathways were preferentially activated in IFNβ-HPPT cells and COVID-19 compared to IFNβ-HPPT cells and AKI (Figures 2C and 2D). We also visualized the genes identified as involved in interferon signaling pathway and overlapping between conditions to see whether similar fold increases in expression can be observed (Figures 2E and 2F). The degree of gene induction varied between data sets, possibly reflecting differences in sample type and technical preparation.

Next, to elucidate cell-specific and common genes induced by IFNβ in primary cells and cell lines, we compared our HPPT data (12-hr *in vitro* IFNβ treatment) with similarly treated human primary lung epithelium (Lee et al., 2021) and the PH5CH8 hepatocyte cell line (Forero et al., 2019) (Figure 3). A total of 685 genes were uniquely activated in HPPT cells, 203 in the lung cells, and 198 in the liver, showing tissue-specific gene induction by cytokine stimulation (Figures 3A and 3B). IFNβ-stimulated renal cells shared 444 genes with the lung and 195 with the liver, and 154 genes were common for all three tissues. They are enriched in various immune hallmarks in GSEA analysis (Figures 3C and 3D), and average fold read increase of genes most upregulated in HPPT cells did not correlate with other tissues (Figures 3E and 3F).

To gauge the extent of IFNβ response through the JAK/STAT pathway, we compared gene expression of cells stimulated by IFNβ to cells cultured additionally with the JAK inhibitor ruxolitinib (Figure 4, Table S3). Immune response genes were significantly enriched in the gene set upregulated by IFNβ, and their expression was dampened by ruxolitinib in RNA-seq analysis. We identified interleukins (*IL4I1*, *IL15*), toll-like receptors (*TLR2*, *TLR4*), interferon regulatory factors (*IRF1*, *IRF7*, *IRF9*), interferon-induced proteins (*IFIT1*, *IFIT2*, *IFIT3*, *IFI44*), and chemoattractants (*CXCL10*, *CXCL11*) as significantly upregulated by type I interferons (Figure 4, Table S2). Extended GSEA analyses for all data presented here can be found in Table S3.

Recent research (Blume et al., 2020; Lee et al., 2021; Ng et al., 2020; Onabajo et al., 2020) revealed the presence of an alternative promoter expressing *deltaACE2* (*dACE2*), a short isoform of *ACE2*, within intron 9 of the *ACE2* gene. Although some studies found the presence of *dACE2* RNA in healthy kidney tissue and tumors (Ng et al., 2020; Onabajo et al., 2020), its structure, function, and the presence of regulatory

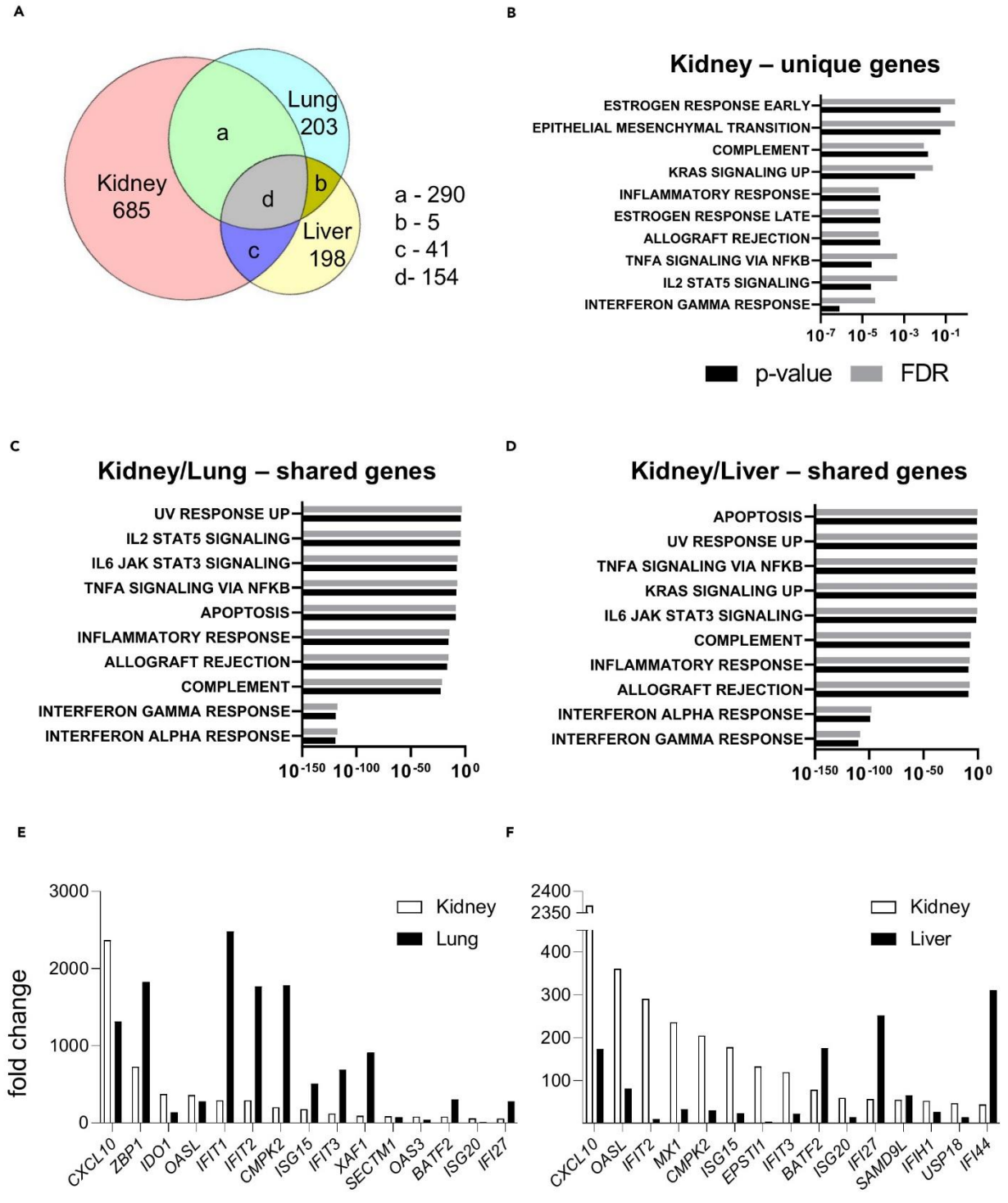
A
Kidney
685
Lung
203
Liver
198
a
b
c
d
a - 290
b - 5
c - 41
d- 154
B
Kidney – unique genes
ESTROGEN RESPONSE EARLY
EPITHELIAL MESENCHYMAL TRANSITION
COMPLEMENT
KRAS SIGNALING UP
INFLAMMATORY RESPONSE
ESTROGEN RESPONSE LATE
ALLOGRAFT REJECTION
TNFA SIGNALING VIA NFKB
IL2 STAT5 SIGNALING
INTERFERON GAMMA RESPONSE
10-7 10-5 10-3 10-1
p-value
FDR
C
Kidney/Lung – shared genes
UV RESPONSE UP
IL2 STAT5 SIGNALING
IL6 JAK STAT3 SIGNALING
TNFA SIGNALING VIA NFKB
APOPTOSIS
INFLAMMATORY RESPONSE
ALLOGRAFT REJECTION
COMPLEMENT
INTERFERON GAMMA RESPONSE
INTERFERON ALPHA RESPONSE
10-150 10-100 10-50 100
D
Kidney/Liver – shared genes
APOPTOSIS
UV RESPONSE UP
TNFA SIGNALING VIA NFKB
KRAS SIGNALING UP
IL6 JAK STAT3 SIGNALING
COMPLEMENT
INFLAMMATORY RESPONSE
ALLOGRAFT REJECTION
INTERFERON ALPHA RESPONSE
INTERFERON GAMMA RESPONSE
10-150 10-100 10-50 100
E
fold change
3000
2000
1000
0
Kidney
Lung
CXCL10 ZBP1 IDO1 OASL IFIT1 IFIT2 CMPK2 ISG15 IFIT3 XAF1 SECTM1 OAS3 BATF2 ISG20 IFI27
F
2400
2350
400
300
200
100
Kidney
Liver
CXCL10 OASL IFIT2 MX1 CMPK2 ISG15 EPSTI1 IFIT3 BATF2 ISG20 IFI27 SAMD9L IFIH1 USP18 IFI44

Figure 3. Comparison of signaling pathways induced by IFNβ stimulation of HPPT, lung, and liver epithelial cells

(A) Venn diagram of unique and common genes induced by IFNβ in the kidney, lung, or liver epithelial cells.

(B–D) GSEA results of p values and FDR in top 10 significantly represented pathways in gene groups unique for HPPT and shared between HPPT and the lung or liver.

(E and F) Comparison of fold increase in expression of top 15 genes involved in IFN signaling in HPPT vs lung and liver tissue (in relation to untreated cells).

See also Tables S1–S3.

elements, as well as cytokine inducibility in kidney cells, have not been investigated. First, we assessed the levels of *ACE2* and *dACE2* mRNA after cytokine treatment using quantitative real-time polymerase chain reaction (qRT-PCR) (Figure 5 and S1). We analyzed the expression of total *ACE2*, serine protease *TMPRSS2* (which primes viral S protein), and the transcription factor *STAT1* to investigate JAK/STAT pathway activation (Figures 5A–5C and S1). While *ACE2* mRNA was increased 6- and 13-fold by IFNα and IFNβ, respectively, expression of the serine protease *TMPRSS2* was not affected by them, but rather was elevated by IL-1β, indicating its regulation by an independent pathway. Expression of *STAT1* was strongly upregulated after interferon treatment. To examine the expression changes of full-length *ACE2* (*flACE2*) and *dACE2* by IFNs, we performed qRT-PCR with isoform-specific primers (Figures 5D and 5E). While *flACE2* was elevated 3-fold, a 300-, 590-, and 27-fold upregulation of *dACE2* was detected upon IFNα, IFNβ, and IFNγ treatments, respectively. Similar increase in gene expression was observed in the studies cited earlier (Table S4).

To investigate whether *flACE2* and *dACE2* are regulated through the JAK/STAT pathway by interferon signaling, we used the JAK inhibitor ruxolitinib (Figures 5F, 5G, and S1). *dACE2* and *STAT1* levels elevated by IFNβ were ablated by ruxolitinib treatment, while no significant changes to full-length *ACE2* expression were observed.

To understand the regulation of the *ACE2* locus by IFNβ and to identify putative genetic control elements of *dACE2* in HPPT cells, we conducted ChIP-seq (Figures 6A–6E) for H3K27ac (active chromatin), H3K4me1 (enhancers), H3K4me3 (promoter marks), and RNA polymerase II loading (Pol II), as well as used available DNase hypersensitive sites (DHS) data set (Thurman et al., 2012).

Candidate regulatory elements were identified at upstream and intronic regions of the *ACE2* locus (Figures 6A–6C). H3K27ac marks and Pol II loading were enriched in the alternative exon 1c in intron 9, the first coding exon of *dACE2*. An increase in RNA-seq reads was detected after treatment, supporting the potential for the presence of a regulatory element (Figures 6C, 6F, and S2). In contrast, full-length *ACE2* promoter marks, which seem to be more pronounced in the kidney than in the lung (Lee et al., 2021), were reduced by IFNβ stimulation. The *STAT1* locus served as a control for the ChIP-seq and after interferon treatment increased H3K4me3 promoter marks and polymerase II binding can be seen, reflecting gene activation (Figure 6D). To confirm the presence of *dACE2*, we amplified and sequenced the novel *dACE2* transcript and confirmed that exon 1c is spliced to exon 10 of *ACE2* (Ng et al., 2020; Onabajo et al., 2020) (Figure S2A). Two TATA-box-like sequences were identified, suggesting the presence of more than one transcription start site (TSS) associated with the intronic promoter (Figure S2B). Additionally, strong H3K27ac marks induced by IFNβ were detected around exon 11 of *ACE2*. These marks are less pronounced in lung cells (Lee et al., 2021). In turn, two putative enhancer elements reported at the site corresponding to 3′ end of *ACE2* gene in lung cells seem to be weaker in the kidney. RNA-seq analyses demonstrated 5-fold IFN-β-induced expression of exon 1c, compared with exon 1a, which harbors the first methionine of the full-length *ACE2* (Figures 6F and S2C). Finally, in addition to the *ACE2* and *TMEM27* promoters, a candidate enhancer element can be seen between the two genes, as indicated by H3K4me1 marks. Additionally, an analysis of the extended *ACE2* locus revealed that *ACE2* and *TMEM27* are under similar interferon regulation and are bordered by CTCF chromatin boundaries, suggesting that they are part of a regulatory unit (Figure S3). The *TMEM27* locus displayed increased H3K27ac and H3K4me3 promoter marks, indicating gene activation after IFNβ treatment (Figure 6E).

DISCUSSION

Our study presents a broad overview of genetic programs stimulated by interferons in renal proximal tubules and compares them with other transcriptomic data. We show robust cytokine response with 1169 genes significantly induced by IFNβ and efficient quenching of gene expression by JAK inhibitor ruxolitinib. Some of those genes are known regulators of renal injury, belonging to divergent pathways, either driving inflammation similar to IRF1 or TLR4 (Wang et al., 2009; Wu et al., 2007) or attenuating it similar to IL4 and IL15 signaling

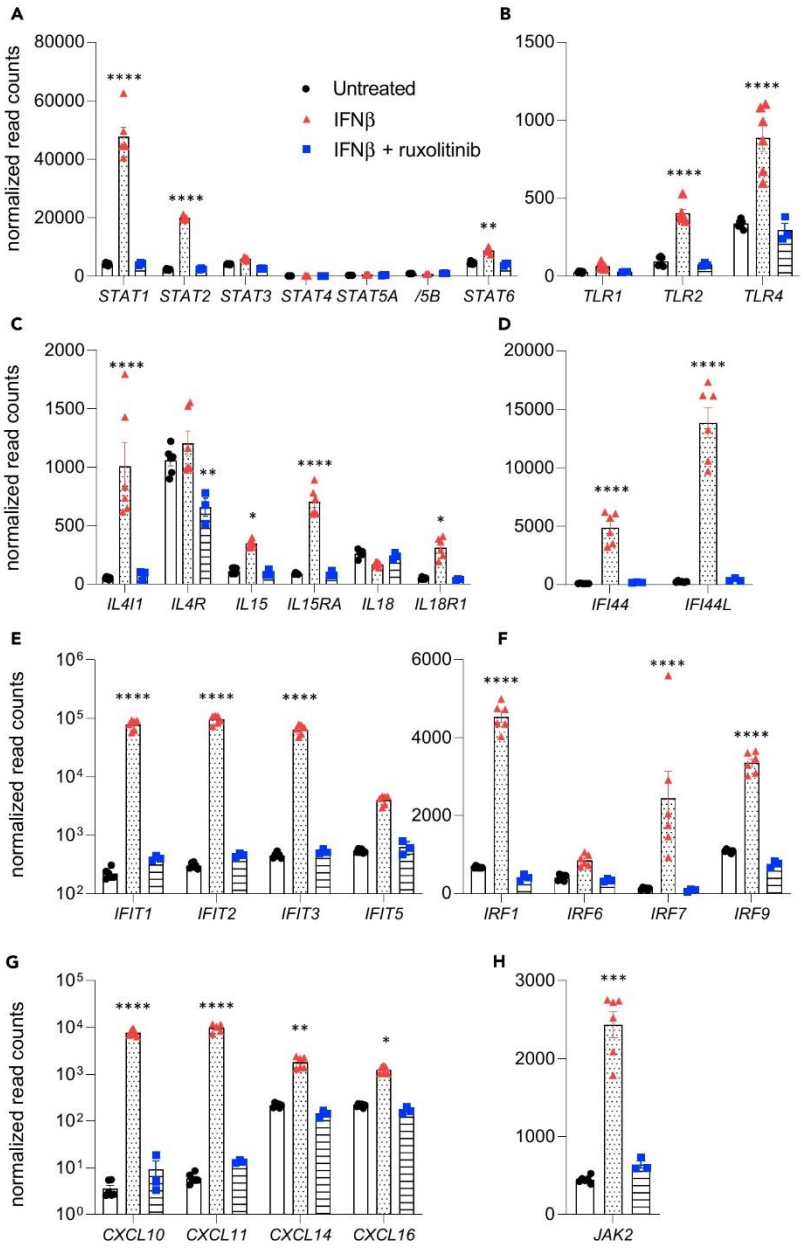

Figure 4. IFNβ-induced immune response genes and their downregulation by ruxolitinib

(A–H) Relative mRNA expression levels of multiple immune genes: (A) STAT gene family, (B) Toll-like receptors, (C) interleukins, (D and E) interferon-induced genes, (F) interferon-regulated factors, (G) CXCL chemokine family, and (H) Janus kinase 2 measured by RNA-seq. Individual data points as well as mean ± SEM of independent biological replicates (n = 3–6) are shown. Significance was analyzed with one-way ANOVA followed by Tukey's multiple comparisons test. *p < 0.05, **p < 0.01, ***p < 0.001, ****p < 0.0001. See also Tables S1–S3.

(Eini et al., 2010; Zhang et al., 2017). There is evidence that type I interferons may contribute to renal damage after ischemic AKI, suggesting that common pathways between IFNβ-treated HPPT cells and AKI could be found (Freitas et al., 2011). Conversely, we expected only a small overlap with SARS-CoV-2-induced genes, as IFNβ has antiviral activity. While we indeed found that interferon stimulation and AKI shared more upregulated genes, interferon-treated cells and COVID-19 samples shared more genes identified as interferon signaling related

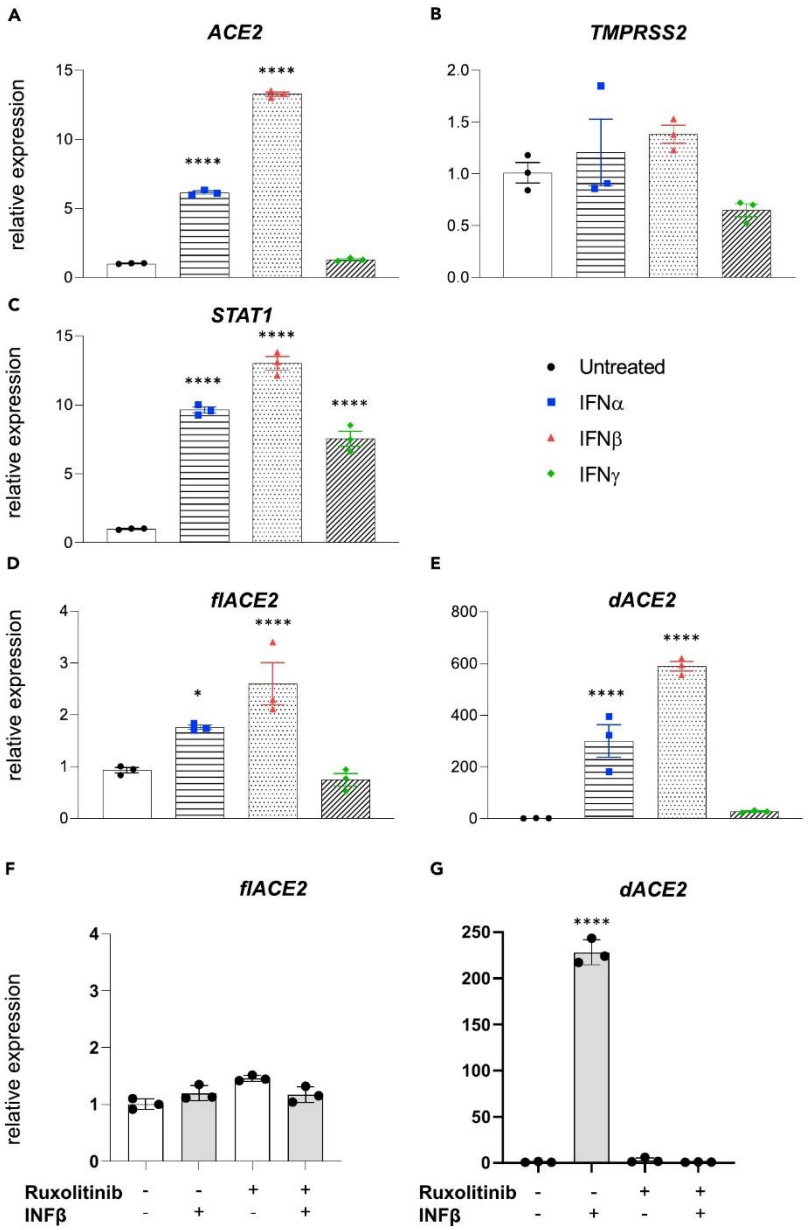

Figure 5. Differences in induction of total ACE2, full-length ACE2, and dACE2 after cytokine treatment

(A) *ACE2*, *TMPRSS2*, and *STAT1* mRNA levels from control and experimental cells were measured by qRT-PCR and normalized to *GAPDH* levels. Relative mRNA levels of (D) full-length *ACE2* (*flACE2*), (E) *dACE2*, after cytokine treatment. (F) *flACE2*, (G) *dACE2* in cells treated with JAK inhibitor ruxolitinib or vehicle, alone or together with IFNβ. Individual data points as well as mean ± SEM of independent biological replicates ($n = 3$) are shown. One- or two-way ANOVA followed by Tukey's multiple comparisons test were used to evaluate the statistical significance of differences relative to untreated cells. ****$p < 0.0001$. See also Figures S1 and S2.

by GSEA analysis. This may not reflect overall trend owing to diversity of AKI and only suggest the degree of similarity with ischemia-reperfusion. We also show uniqueness of renal response when compared with the lung and liver, with over half of the genes upregulated in the kidney being tissue specific. We did not observe significant regulation of *TMPRSS2*, protease involved in SARS-CoV-2 infection, by interferons. Instead, we saw upregulation of *TMPRSS2* expression after IL-1β treatment. Both *IL-1β* and *TMPRSS2* were reported to be

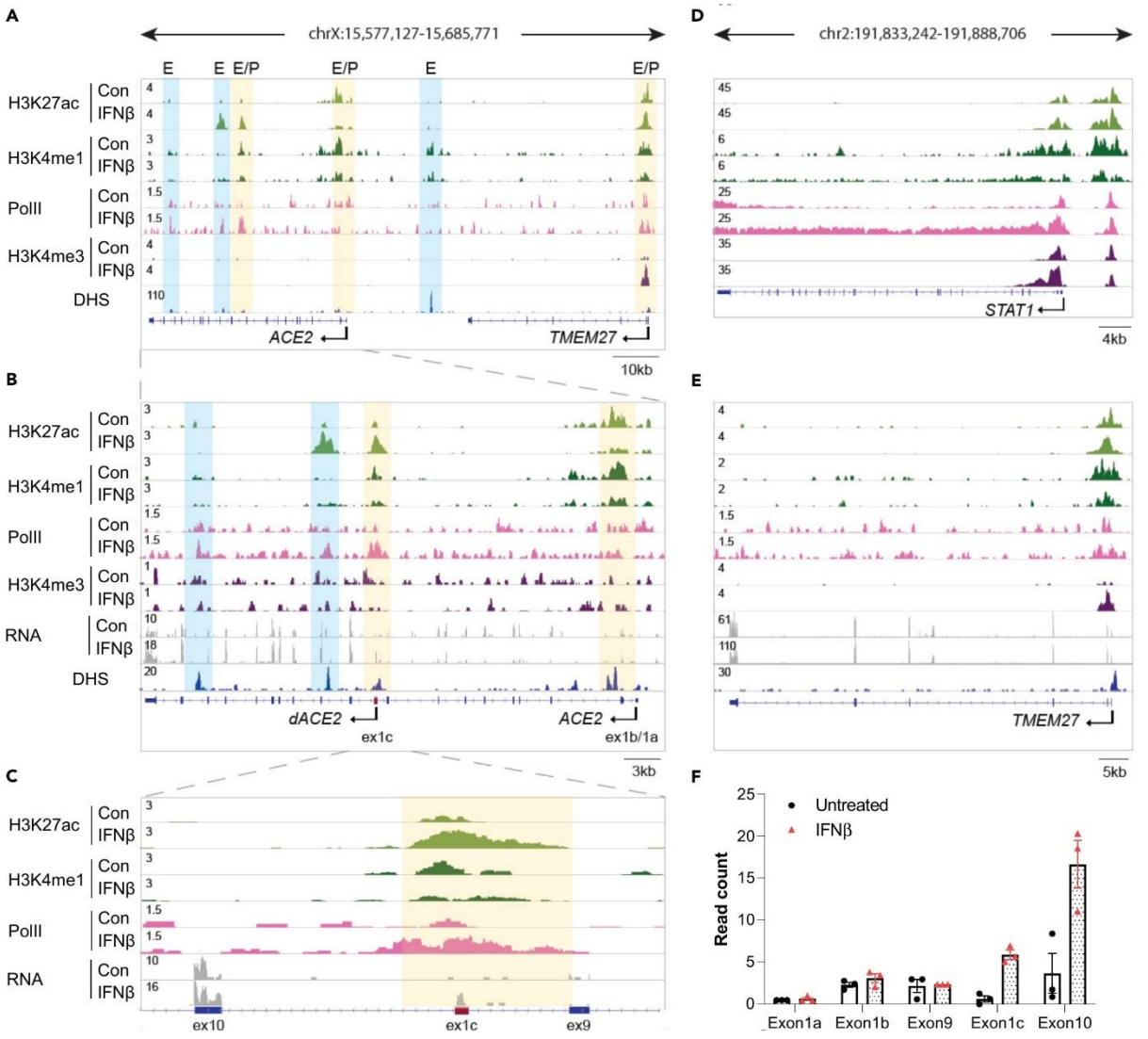

Figure 6. Activation of the novel intronic *ACE2* promoter by IFNβ

(A–E) ChIP-seq data for Pol II and histone markers H3K27ac, H3K4me1, and H3K4me3, DNase hypersensitivity sites and RNA-seq reads at the *ACE2*, *TMEM27*, and *STAT1* locus in human primary proximal tubule (HTTP) cells with and without IFNβ. Solid arrows indicate the orientation of genes. The blue and orange shades indicate regulatory elements, labeled as putative enhancers (E) or promoters (P), respectively.

(F) Number of RNA-seq reads at the exons 1a and 1b, and the new exon 1c. HTTP cells were grown in the absence or the presence of IFNβ. Individual data points as well as mean ± SEM of independent biological replicates (n = 3) are shown. See also Figure S3.

downregulated in nasal basal epithelium after azithromycin treatment (Renteria et al., 2020), reinforcing potential for the link between them. Our study of *ACE2* locus revealed coregulation of *ACE2* and *TMEM27*, which may have additional significance for the kidney, as *TMEM27* gene encodes collectrin, ACE2 homolog, primarily expressed in renal proximal tubule, and collecting duct (Mount, 2007). Collectrin, similarly to ACE2, regulates blood pressure (Chu and Le, 2014) and amino acid transport (Malakauskas et al., 2007). Overall, those results may serve as an important stepping-stone toward further elucidation of kidney-specific genetic programs.

Although our study demonstrates that *dACE2* expression is activated by interferon treatment, further work is needed to identify whether viral infection enhances *dACE2* expression in the kidney. Although several studies have identified *dACE2* after SARS-CoV-2 infection *in vitro*, its biological role remains

unknown. Based on lung epithelium cell data, it is proposed that its extracellular enzymatic and viral spike protein-binding domains are truncated, resulting in partial loss of its carboxypeptidase function. The *dACE2* promoter may be a remnant of a retroviral ISG (Ng et al., 2020). Blume (Blume et al., 2020) reports lack of increase of *ACE2* or *dACE2* after SARS-CoV-2 stimulated BCi-NS1.1 lung cells. Onabajo (Onabajo et al., 2020) similarly shows lack of their upregulation in lung Calu3 cell line, but colon cancer Caco-2 and T84 lines exhibited slightly increased *dACE2* expression after SARS-CoV-2 exposure. This may in part be due to tissue-specific cytokine regulation of *ACE2* and *dACE2*. A standardized and validated detection method of both ACE2 isoforms, as well as understanding of regulatory elements present in *ACE2* locus, is necessary to forward this topic. This is especially true for studies at the protein level, as detection methods such as Western blot are contradictory between reports (Blume et al., 2020; Ng et al., 2020). In our attempts to investigate protein levels of dACE2 using Western blot, we were able to observe a 50-kDa band; however, its presence and intensity were not consistent between various anti-ACE2 antibodies (data not shown). We summarized current knowledge on factors causing dACE2 upregulation in Table S4.

In our study, we present an in-depth analysis and comparison of interferon-stimulated human proximal tubule cells and other experimental data sets, providing insight into genetic pathways driving response to stimuli affecting renal health. In addition, by comparing our data sets with other similarly treated cells, we show unique renal regulation of interferon response. We also identified several putative regulatory elements controlling *ACE2*, as well as confirmed the presence of *dACE2* in renal epithelium. We describe reliance of *dACE2* expression on the JAK/STAT pathway, which may be of clinical importance, as JAK inhibitors are currently used to treat COVID-19 (Cao et al., 2020). Our study strengthens current knowledge about cytokine signaling in renal epithelium, and we believe that it can become a basis for further transcriptomic studies reaching beyond the current efforts to thwart and understand the COVID-19 pandemic.

Limitations of the study

There are several limitations to our study. First, the availability of only a single public RNA-seq data set from patients with AKI is a clear limitation, as AKI is an extremely diverse condition. Additionally, there are no large-scale renal COVID-19 transcriptomics data. Second, reliance on a single batch of primary cells may introduce bias. Third, in an *in vivo* setting, JAK inhibitors have a broader effect than inhibition of genes induced by IFNβ and may affect other cytokines and genetic programs. Finally, the belief in direct SARS-CoV-2 infection of the kidney is not universal despite published evidence.

STAR★METHODS

Detailed methods are provided in the online version of this paper and include the following:

- KEY RESOURCES TABLE
- RESOURCE AVAILABILITY
  - Lead contact
  - Materials availability
  - Data and code availability
- EXPERIMENTAL MODEL AND SUBJECT DETAILS
  - Cell culture
- METHOD DETAILS
  - Cytokine stimulation
  - RNA isolation and qRT-PCR
  - PCR amplification
  - RNA-seq library preparation and data analysis
  - ChIP-seq library preparation and data analysis
- QUANTIFICATION AND STATISTICAL ANALYSIS

SUPPLEMENTAL INFORMATION

Supplemental information can be found online at https://doi.org/10.1016/j.isci.2021.102928.

ACKNOWLEDGMENTS

We thank Ilhan Akan, Sijung Yun, and Harold Smith from the NIDDK genomics core for NGS. Cytokines were gifted by Dr. Marc Ferrer and Olive Jung (NIH/NCATS). This work utilized the computational resources of the NIH HPC Biowulf cluster (http://hpc.nih.gov). This work was supported by the Intramural Research Program (IRP) of the National Institute of Diabetes and Digestive and Kidney Diseases (NIDDK), the NIH Graduate Partnership Program (GPP), and the Austrian Science Fund (P30373).

AUTHOR CONTRIBUTIONS

Conceptualization and methodology: J.J., H.K.L., J.W., and L.H.; Formal analysis and validation, data curation, and visualization: J.J. and H.K.L.; Investigation: J.J.; Resources: L.H.; Writing – original draft: J.J. and H.K.L.; Writing – review and editing: J.J., H.K.L., J.W., and L.H.; Supervision, administration, and funding acquisition: J.W. and L.H. All authors approved the final version of the manuscript.

DECLARATION OF INTERESTS

The authors declare no competing interests.

Received: January 28, 2021
Revised: June 2, 2021
Accepted: July 23, 2021
Published: August 20, 2021

REFERENCES

Ahmadian, E., Hosseiniyan Khatibi, S.M., Razi Soofiyani, S., Abediazar, S., Shoja, M.M., Ardalan, M., and Zununi Vahed, S. (2021). Covid-19 and kidney injury: Pathophysiology and molecular mechanisms. Rev. Med. Virol. *31*, e2176.

Anders, S., Pyl, P.T., and Huber, W. (2015). HTSeq–a Python framework to work with high-throughput sequencing data. Bioinformatics *31*, 166–169.

Blume, C., Jackson, C.L., Spalluto, C.M., Legebeke, J., Nazlamova, L., Conforti, F., Perotin-Collard, J.-M., Frank, M., Crispin, M., Coles, J., et al. (2020). A novel isoform of ACE2 is expressed in human nasal and bronchial respiratory epithelia and is upregulated in response to RNA respiratory virus infection. bioRxiv, 2020.2007.2031.230870.

Bolger, A.M., Lohse, M., and Usadel, B. (2014). Trimmomatic: a flexible trimmer for Illumina sequence data. Bioinformatics *30*, 2114–2120.

Braun, F., Lutgehetmann, M., Pfefferle, S., Wong, M.N., Carsten, A., Lindenmeyer, M.T., Norz, D., Heinrich, F., Meissner, K., Wichmann, D., et al. (2020). SARS-CoV-2 renal tropism associates with acute kidney injury. Lancet *396*, 597–598.

Cao, Y., Wei, J., Zou, L., Jiang, T., Wang, G., Chen, L., Huang, L., Meng, F., Huang, L., Wang, N., et al. (2020). Ruxolitinib in treatment of severe coronavirus disease 2019 (COVID-19): a multicenter, single-blind, randomized controlled trial. J. Allergy Clin. Immunol. *146*, 137–146 e133.

Chen, Q.L., Li, J.Q., Xiang, Z.D., Lang, Y., Guo, G.J., and Liu, Z.H. (2020). Localization of cell receptor-related genes of SARS-CoV-2 in the kidney through single-cell transcriptome analysis. Kidney Dis. (Basel, Switzerland) *6*, 258–270.

Chong, W.H., and Saha, B.K. (2021). Relationship between severe acute respiratory syndrome coronavirus 2 (SARS-CoV-2) and the etiology of acute kidney injury (AKI). Am. J. Med. Sci. *361*, 287–296.

Chu, P., and Le, T. (2014). Role of collectrin, an ACE2 homologue, in blood pressure homeostasis. Curr. Hypertens. Rep. *16*, 490.

Desai, N., Neyaz, A., Szabolcs, A., Shih, A.R., Chen, J.H., Thapar, V., Nieman, L.T., Solovyov, A., Mehta, A., Lieb, D.J., et al. (2020). Temporal and spatial heterogeneity of host response to SARS-CoV-2 pulmonary infection. Nat. Commun. *11*, 6319.

Dobin, A., Davis, C.A., Schlesinger, F., Drenkow, J., Zaleski, C., Jha, S., Batut, P., Chaisson, M., and Gingeras, T.R. (2013). STAR: ultrafast universal RNA-seq aligner. Bioinformatics *29*, 15–21.

Donoghue, M., Hsieh, F., Baronas, E., Godbout, K., Gosselin, M., Stagliano, N., Donovan, M., Woolf, B., Robison, K., Jeyaseelan, R., et al. (2000). A novel angiotensin-converting enzyme-related carboxypeptidase (ACE2) converts angiotensin I to angiotensin 1-9. Circ. Res. *87*, E1–E9.

Eini, H., Tejman-Yarden, N., Lewis, E., Chaimovitz, C., Zlotnik, M., and Douvdevani, A. (2010). Association between renal injury and reduced interleukin-15 and interleukin-15 receptor levels in acute kidney injury. J. Interferon. Cytokine. Res. *30*, 1–8.

Fignani, D., Licata, G., Brusco, N., Nigi, L., Grieco, G.E., Marselli, L., Overbergh, L., Gysemans, C., Colli, M.L., Marchetti, P., et al. (2020). SARS-CoV-2 receptor Angiotensin I-Converting Enzyme type 2 (ACE2) is expressed in human pancreatic β-cells and in the human pancreas microvasculature. bioRxiv, 2020.2007.2023.208041.

Forero, A., Ozarkar, S., Li, H., Chia Heng, L., Hemann, E., Nadjsombati, M., Hendricks, M., So, L., Green, R., Roy, C., et al. (2019). Differential activation of the transcription factor IRF1 underlies the distinct immune responses elicited by type I and type III interferons. Immunity *51*, 451–464.

Freitas, M.C., Uchida, Y., Lassman, C., Danovitch, G.M., Busuttil, R.W., and Kupiec-Weglinski, J.W. (2011). Type I interferon pathway mediates renal ischemia/reperfusion injury. Transplantation *92*, 131–138.

Gibson, P.G., Qin, L., and Puah, S.H. (2020). COVID-19 acute respiratory distress syndrome (ARDS): clinical features and differences from typical pre-COVID-19 ARDS. Med. J. Aust. *213*, 54–56 e51.

He, Q., Mok, T.N., Yun, L., He, C., Li, J., and Pan, J. (2020). Single-cell RNA sequencing analysis of human kidney reveals the presence of ACE2 receptor: a potential pathway of COVID-19 infection. Mol. Genet. Genomic Med. e1442.

Heinz, S., Benner, C., Spann, N., Bertolino, E., Lin, Y.C., Laslo, P., Cheng, J.X., Murre, C., Singh, H., and Glass, C.K. (2010). Simple combinations of lineage-determining transcription factors prime cis-regulatory elements required for macrophage and B cell identities. Mol. Cell *38*, 576–589.

Hoffmann, M., Kleine-Weber, H., Schroeder, S., Kruger, N., Herrler, T., Erichsen, S., Schiergens, T.S., Herrler, G., Wu, N.H., Nitsche, A., et al. (2020). SARS-CoV-2 cell entry depends on ACE2 and TMPRSS2 and is blocked by a clinically proven protease inhibitor. Cell *181*, 271–280.e8.

Hoste, E.A.J., Kellum, J.A., Selby, N.M., Zarbock, A., Palevsky, P.M., Bagshaw, S.M., Goldstein, S.L., Cerda, J., and Chawla, L.S. (2018). Global epidemiology and outcomes of acute kidney injury. Nat. Rev. Nephrol. *14*, 607–625.

Huber, W., Carey, V.J., Gentleman, R., Anders, S., Carlson, M., Carvalho, B.S., Bravo, H.C., Davis, S., Gatto, L., Girke, T., et al. (2015). Orchestrating high-throughput genomic analysis with Bioconductor. Nat. Methods *12*, 115–121.

Kim, J.S., Lee, J.Y., Yang, J.W., Lee, K.H., Effenberger, M., Szpirt, W., Kronbichler, A., and Shin, J.I. (2021). Immunopathogenesis and treatment of cytokine storm in COVID-19. Theranostics *11*, 316–329.

Koka, V., Huang, X.R., Chung, A.C., Wang, W., Truong, L.D., and Lan, H.Y. (2008). Angiotensin II up-regulates angiotensin I-converting enzyme (ACE), but down-regulates ACE2 via the AT1-ERK/p38 MAP kinase pathway. Am. J. Pathol. *172*, 1174–1183.

Langmead, B., Trapnell, C., Pop, M., and Salzberg, S.L. (2009). Ultrafast and memory-efficient alignment of short DNA sequences to the human genome. Genome Biol. *10*, R25.

Lee, H.K., Jung, O., and Hennighausen, L. (2021). JAK inhibitors dampen activation of interferon-stimulated transcription of ACE2 isoforms in human airway epithelial cells. Commun. Biol. *4*, 654.

Lee, J.W., Chou, C.L., and Knepper, M.A. (2015). Deep sequencing in microdissected renal tubules identifies nephron segment-specific transcriptomes. J. Am. Soc. Nephrol. *26*, 2669–2677.

Li, H., Handsaker, B., Wysoker, A., Fennell, T., Ruan, J., Homer, N., Marth, G., Abecasis, G., Durbin, R., and Genome Project Data Processing, S. (2009). The sequence alignment/map format and SAMtools. Bioinformatics *25*, 2078–2079.

Love, M.I., Huber, W., and Anders, S. (2014). Moderated estimation of fold change and dispersion for RNA-seq data with DESeq2. Genome Biol. *15*, 550.

Lynch, M.R., and Tang, J. (2020). COVID-19 and kidney injury. Rhode Isl. Med. J. *103*, 24–28.

Malakauskas, S., Quan, H., Fields, T., McCall, S., Yu, M., Kourany, W., Frey, C., and Le, T. (2007). Aminoaciduria and altered renal expression of luminal amino acid transporters in mice lacking novel gene collectrin. Am. J. Physiol. Renal. Physiol. *292*, F533–F544.

Mizuiri, S., Hemmi, H., Arita, M., Aoki, T., Ohashi, Y., Miyagi, M., Sakai, K., Shibuya, K., Hase, H., and Aikawa, A. (2011). Increased ACE and decreased ACE2 expression in kidneys from patients with IgA nephropathy. Nephron Clin. Pract. *117*, c57–66.

Mizuiri, S., Hemmi, H., Arita, M., Ohashi, Y., Tanaka, Y., Miyagi, M., Sakai, K., Ishikawa, Y., Shibuya, K., Hase, H., et al. (2008). Expression of ACE and ACE2 in individuals with diabetic kidney disease and healthy controls. Am. J. Kidney Dis. *51*, 613–623.

Mizuiri, S., and Ohashi, Y. (2015). ACE and ACE2 in kidney disease. World J. Nephrol. *4*, 74–82.

Mokhtari, T., Hassani, F., Ghaffari, N., Ebrahimi, B., Yarahmadi, A., and Hassanzadeh, G. (2020). COVID-19 and multiorgan failure: a narrative review on potential mechanisms. J. Mol. Histol. *51*, 613–628.

Moon, J.Y., Jeong, K.H., Lee, S.H., Lee, T.W., Ihm, C.G., and Lim, S.J. (2008). Renal ACE and ACE2 expression in early diabetic rats. Nephron Exp. Nephrol. *110*, e8–e16.

Mount, D. (2007). Collectrin and the kidney. Curr. Opin. Nephrol. Hypertens. *16*, 427–429.

Ng, K.W., Attig, J., Bolland, W., Young, G.R., Major, J., Wrobel, A.G., Gamblin, S., Wack, A., and Kassiotis, G. (2020). Tissue-specific and interferon-inducible expression of nonfunctional ACE2 through endogenous retroelement co-option. Nat. Genet. *52*, 1294–1302.

Onabajo, O.O., Banday, A.R., Stanifer, M.L., Yan, W., Obajemu, A., Santer, D.M., Florez-Vargas, O., Piontkivska, H., Vargas, J.M., Ring, T.J., et al. (2020). Interferons and viruses induce a novel truncated ACE2 isoform and not the full-length SARS-CoV-2 receptor. Nat. Genet. *52*, 1283–1293.

Park, M., Kwon, C.H., Ha, H.K., Han, M., and Song, S.H. (2020). RNA-Seq identifies condition-specific biological signatures of ischemia-reperfusion injury in the human kidney. BMC Nephrol. *21*, 398.

Peng, L., Liu, J., Xu, W., Luo, Q., Chen, D., Lei, Z., Huang, Z., Li, X., Deng, K., Lin, B., et al. (2020). SARS-CoV-2 can be detected in urine, blood, anal swabs, and oropharyngeal swabs specimens. J. Med. Virol. *92*, 1676–1680.

Renteria, A., Mfuna Endam, L., Adam, D., Filali-Mouhim, A., Maniakas, A., Rousseau, S., Brochiero, E., Gallo, S., and Desrosiers, M. (2020). Azithromycin downregulates gene expression of IL-1β and pathways involving TMPRSS2 and TMPRSS11D required by SARS-CoV-2. Am. J. Respir. Cell. Mol. Biol. *63*, 707–709.

Risso, D., Ngai, J., Speed, T.P., and Dudoit, S. (2014). Normalization of RNA-seq data using factor analysis of control genes or samples. Nat. Biotechnol. *32*, 896–902.

Su, H., Yang, M., Wan, C., Yi, L.X., Tang, F., Zhu, H.Y., Yi, F., Yang, H.C., Fogo, A.B., Nie, X., et al. (2020). Renal histopathological analysis of 26 postmortem findings of patients with COVID-19 in China. Kidney Int. *98*, 219–227.

Sun, J., Zhu, A., Li, H., Zheng, K., Zhuang, Z., Chen, Z., Shi, Y., Zhang, Z., Chen, S.B., Liu, X., et al. (2020). Isolation of infectious SARS-CoV-2 from urine of a COVID-19 patient. Emerg. Microbes Infect *9*, 991–993.

Sungnak, W., Huang, N., Becavin, C., Berg, M., Queen, R., Litvinukova, M., Talavera-Lopez, C., Maatz, H., Reichart, D., Sampaziotis, F., et al. (2020). SARS-CoV-2 entry factors are highly expressed in nasal epithelial cells together with innate immune genes. Nat. Med. *26*, 681–687.

Thorvaldsdottir, H., Robinson, J.T., and Mesirov, J.P. (2013). Integrative Genomics Viewer (IGV): high-performance genomics data visualization and exploration. Brief Bioinform *14*, 178–192.

Thurman, R.E., Rynes, E., Humbert, R., Vierstra, J., Maurano, M.T., Haugen, E., Sheffield, N.C., Stergachis, A.B., Wang, H., Vernot, B., et al. (2012). The accessible chromatin landscape of the human genome. Nature *489*, 75–82.

Tipnis, S.R., Hooper, N.M., Hyde, R., Karran, E., Christie, G., and Turner, A.J. (2000). A human homolog of angiotensin-converting enzyme. Cloning and functional expression as a captopril-insensitive carboxypeptidase. J. Biol. Chem. *275*, 33238–33243.

Vinayagam, S., and Sattu, K. (2020). SARS-CoV-2 and coagulation disorders in different organs. Life Sci. *260*, 118431.

Wang, Y., John, R., Chen, J., Richardson, J., Shelton, J., Bennett, M., Zhou, X., Nagami, G., Zhang, Y., Wu, Q., et al. (2009). IRF-1 promotes inflammation early after ischemic acute kidney injury. J. Am. Soc. Nephrol. *20*, 1544–1555.

Wang, G., Kwan, B.C., Lai, F.M., Choi, P.C., Chow, K.M., Li, P.K., and Szeto, C.C. (2010). Intrarenal expression of miRNAs in patients with hypertensive nephrosclerosis. Am. J. Hypertens. *23*, 78–84.

Wu, H., Chen, G., Wyburn, K., Yin, J., Bertolino, P., Eris, J., Alexander, S., Sharland, A., and Chadban, S. (2007). TLR4 activation mediates kidney ischemia/reperfusion injury. J. Clin. Invest. *117*, 2847–2859.

Zhang, M., Wang, X., Wang, Y., Niu, A., Wang, S., Zou, C., and Harris, R. (2017). IL-4/IL-13-mediated polarization of renal macrophages/dendritic cells to an M2a phenotype is essential for recovery from acute kidney injury. Kidney Int. *91*, 357–386.

Ziegler, C.G.K., Allon, S.J., Nyquist, S.K., Mbano, I.M., Miao, V.N., Tzouanas, C.N., Cao, Y., Yousif, A.S., Bals, J., Hauser, B.M., et al. (2020). SARS-CoV-2 receptor ACE2 is an interferon-stimulated gene in human airway epithelial cells and is detected in specific cell subsets across tissues. Cell *181*, 1016–1035.e9.

STAR★METHODS

KEY RESOURCES TABLE

REAGENT or RESOURCE	SOURCE	IDENTIFIER
Antibodies		
Anti-Trimethyl-Histone H3 (Lys4)	Millipore	Cat# 07-473; RRID:AB_1977252
Anti-RNA polymerase II CTD repeat	Abcam	Cat# ab5408; RRID:AB_304868
Anti-Histone H3K27ac	Active Motif	Cat# 39133; RRID:AB_2561016
Anti-Histone H3K4me1	Active Motif	Cat# 39297; RRID:AB_2615075
Chemicals, peptides, and recombinant proteins		
Human IFNα	Stem Cell Tech.	Cat# 78077
Human IFNβ	Peprotech	Cat# 300-02BC
Human IFNγ	Peprotech	Cat# 300-02
Human IL-1β	Peprotech	Cat# 200-01B
Human TNFα	Peprotech	Cat# 300-01A
Human IL-6	Peprotech	Cat# 200-06
Ruxolitinib	Peprotech	Cat# 9414958
Critical commercial assays		
SsoAdvanced Universal Probes Supermix	Bio-rad	Cat# 172-5281
PureLink RNA Mini Kit	Invitrogen	Cat# 12183018A
SuperScript III First-Strand Synthesis SuperMix	Invitrogen	Cat# 18080-400
NEBNext® Ultra™ II DNA Library Prep Kit	New England Bio.	Cat# E7645L
TruSeq total RNA Library Prep Kit	Illumina	Cat# 20020597
Deposited data		
Original ChIP-seq data – cytokine-stimulated human proximal tubule cells	NCBI GEO data set	GSE161915
Original RNA-seq data – cytokine-stimulated human proximal tubule cells	NCBI GEO data set	GSE161916
RNA-seq – human AKI kidney	NCBI GEO data set	GSE142077
RNA-seq – human COVID-19 kidney	NCBI GEO data set	GSE150316
RNA-seq – lung epithelium + IFNβ	NCBI GEO data set	GSE161665
RNA-seq – liver epithelium + IFNβ	NCBI GEO data set	GSE115198
CTCF ChIP-seq - HEK293	NCBI GEO data set	GSE68976
DHS - Human Renal Cortical Epithelial cells	NCBI GEO data set	GSE29692
Hi-C - human adrenal gland	Northwestern University Yue Lab database	http://3dgenome.fsm.northwestern.edu/view.php
Human reference genome NCBI build 37, GRCh37	Genome Reference Consortium	http://www.ncbi.nlm.nih.gov/projects/genome/assembly/grc/human/
Experimental models: Cell lines		
Human Primary Proximal Tubule (HPPT) Cells	ATCC	Cat# PCS-400-010
Oligonucleotides		
Human *GAPDH* Taqman probe mix	Thermo Fisher	Hs02786624_g1
Human *ACE2* Taqman probe mix	Thermo Fisher	Hs01085333_m1
Human *TMPRSS2* Taqman probe mix	Thermo Fisher	Hs01122322_m1
Human *STAT1* Taqman probe mix	Thermo Fisher	Hs01013996_m1
Custom *dACE2* qRT-PCR probe	Eurofins Genomics	N/A

(*Continued on next page*)

Continued

REAGENT or RESOURCE	SOURCE	IDENTIFIER
Custom full-length *ACE2* qRT-PCR probe	Eurofins Genomics	N/A
Custom dACE2 PCR primers	Eurofins Genomics	N/A
Custom ACE2 PCR primers	Eurofins Genomics	N/A
Software and algorithms		
Trimmomatic (version 0.36)	Bolger et al., 2014	http://www.usadellab.org/cms/?page=trimmomatic
Bowtie (version 1.1.2)	Langmead et al., 2009	http://bowtie-bio.sourceforge.net/manual.shtml
Integrative Genomics Viewer	Thorvaldsdóttir et al., 2013	http://software.broadinstitute.org/software/igv/
STAR (2.5.4a)	Dobin et al., 2013	https://anaconda.org/bioconda/star/files?version=2.5.4a
HTSeq	Anders et al., 2015	https://htseq.readthedocs.io/en/master/
Bioconductor	Huber et al., 2015	https://www.bioconductor.org/
RUVSeq	Risso et al., 2014	https://bioconductor.org/packages/release/bioc/html/RUVSeq.html
DESeq2	Love et al., 2014	https://bioconductor.org/packages/release/bioc/html/DESeq2.html
Samtools	Li et al., 2009	http://www.htslib.org/
PRISM GraphPad (8.4.3)	GraphPad Software	https://www.graphpad.com/scientific-software/prism/

RESOURCE AVAILABILITY

Lead contact

Further information and requests for resources and reagents should be directed to and will be fulfilled by the Lead Contact, Lothar Hennighausen (lotharh@nih.gov).

Materials availability

This study did not generate new unique reagents.

Data and code availability

The original RNA-seq and ChIP-seq data from HPPT cells were submitted to the Gene Expression Omnibus under GEO: GSE161917 (ChIP-seq - GEO: GSE161915, RNA-seq - GEO: GSE161916), and are publicly available. Accession numbers are also listed in the key resources table. Additional supplemental items are available from Mendeley Data: https://doi.org/10.17632/zhvggb5b44.1. DHS from human renal cortical epithelial cells and CTCF ChIP-seq from HEK293 cells were obtained under GEO: GSE29692 and GEO: GSE68976, respectively. RNA-seq data for IFNβ-stimulated lung and liver cell were obtained from GEO: GSE161665 and GEO: GSE115198, respectively. Human AKI and COVID-19 data were found under GEO: GSE142077 and GEO: GSE150316, respectively. Hi-C data from human adrenal gland tissues were obtained from Hi-C data browser (http://3dgenome.fsm.northwestern.edu/view.php).

Any additional information required to reanalyze the data reported in this paper is available from the lead contact upon request.

EXPERIMENTAL MODEL AND SUBJECT DETAILS

Cell culture

HPPT cells (ATCC® PCS-400-010™) from a male donor were cultured in low-serum medium consisting of Renal Epithelial Cell Basal Medium (ATCC® PCS-400-030™) with Renal Epithelial Cell Growth Kit (ATCC® PCS-400-040™), Penicillin-Streptomycin-Amphotericin B Solution (ATCC® PCS-999-002™), and Phenol red (ATCC® PCS-999-001™) added. Cells were obtained at passage 2, cultured according to the manufacturer's instructions, and used between passages 4 and 6. In addition to characteristic cobblestone growth pattern when confluent, cells were confirmed to express several proximal tubule markers including γ-glutamyltransferase-1 and *SLC3a1* as assessed with RNA-seq (Lee et al., 2015).

METHOD DETAILS

Cytokine stimulation

Cells were stimulated with IFNα (Stem Cell Technologies), IFNβ, IFNγ, TNFα, IL-6, and IL-1β (all obtained from Peprotech) for 12 hours in concentration of 10 ng/ml. Cells were treated with ruxolitinib (Peprotech) at 10 μM for 12 hours together with IFNβ. At least three biological replicates were prepared for all experiments.

RNA isolation and qRT-PCR

After cytokine stimulation, cells were washed twice with phosphate buffered saline (PBS) before RNA isolation to remove medium and debris. mRNA was isolated using PureLink™ RNA Mini Kit (Invitrogen), and 500 ng was transcribed into cDNA using SuperScript™ III First-Strand Synthesis SuperMix (Invitrogen). qRT-PCR reaction was prepared with SsoAdvanced Universal Probes Supermix (Bio-Rad) and the following Taqman probes (ThermoFisher): *GAPDH* (Hs02786624_g1), *ACE2* (Hs01085333_m1), *TMPRSS2* (Hs01122322_m1), and *STAT1* (Hs01013996_m1) or the following primers: *dACE2* forward: 5′ GGAAGCAG GCTGGGACAAA 3′, *dACE2* reverse: 5′ AGCTGTCAGGAAGTCGTCCATT 3′, ACE2 forward: 5′ GGGCGAC TTCAGGATCCTTAT 3′, ACE2 reverse: 5′ GGATATGCCCCATCTCATGATG 3′. Custom qRT-PCR probe sequences were as follows: *ACE2*: 5′ [6∼FAM] ATGGACGACTTCCTGACAG [MGBE∼Q] 3′, *dACE2*: 5′ [6∼FAM] AGGGAGGATCCTTATGTG [MGBE∼Q] 3′. Reaction conditions were as follows: initial denaturation for 3 minutes at 95°C and 40 cycles of 10 seconds at 95°C and 30 seconds at 60°C.

PCR amplification

ACE2 PCR was performed with cDNA obtained as described earlier. Fifty nanograms of cDNA was used in the following reaction: initial denaturation – 3 minutes, 98°C and 35 cycles of denaturation – 30 seconds at 98°C, annealing – 30 seconds at 58°C, extension – 72°C for 2 minutes, ending with final extension of 72°C for 10 minutes. Amplified fragments were run on a 1.5% agarose in 1x TAE gel with 100-kb DNA ladder to assess product size. Bands were cut out, and PCR products cleaned with MinElute Gel Extraction Kit (Quiagen) and Sanger sequenced by Quintara Biosciences. Primers used were as follows: dACE2 forward: 5′-TGTGAGAGCCTTAGGTTGGATTCC-3′, dACE2 reverse: 5′-TCTCTCCTTGGCCATGTTGT-3′ (Onabajo et al., 2020).

RNA-seq library preparation and data analysis

mRNA was prepared as described earlier and quality assessed using Bioanalyzer 2100 (Agilent). Samples with adequate RIN values were transcribed into libraries using TruSeq total RNA Library Prep Kit according to the manufacturer's instructions. Libraries were pooled in equimolar amounts and sequenced using HiSeq 2000 (Illumina).

The raw data were subjected to QC analyses using the FastQC tool (version 0.11.9) (https://www.bioinformatics.babraham.ac.uk/projects/fastqc/). Trimmomatic (version 0.36) (Bolger et al., 2014) was used to assess total RNA-seq read quality, and STAR RNA-seq (version 2.5.4a) (Dobin et al., 2013) using 50-bp paired-end mode was used to align the reads (hg19). HTSeq (Anders et al., 2015) was used to retrieve the raw counts, and R package DESeq2 (Huber et al., 2015; Love et al., 2014) was used to normalize data. Additionally, the RUVSeq (Risso et al., 2014) package was applied to remove confounding factors. A minimum of five reads was an additional basis for filtering artifacts. The visualization was done using dplyr (https://CRAN.R-project.org/package=dplyr) and ggplot2 (Risso et al., 2014). Significantly differential expressed genes with an adjusted p-value (pAdj, FDR) below 0.05 and a fold change > 2 for upregulated genes were categorized using GSEA (https://www.gsea-msigdb.org/gsea/msigdb). Sequence read numbers were calculated using Samtools (Li et al., 2009) software with sorted bam files.

ChIP-seq library preparation and data analysis

Cells were washed twice with PBS and fixed with 0.75% formaldehyde in Dulbecco's Modified Eagle Medium (DMEM) for 10 minutes in room temperature. Next, glycine was added to quench fixation in a final concentration of 125 mM, and plates were incubated in room temperature for another 10 minutes. Cells were then scraped and centrifuged at 4°C, for 1 minute, at 3000 rpm, and then washed twice with cold PBS. Pellets were resuspended in 2 ml of Farnham Lysis Buffer with protease inhibitors and incubated on ice for 10 minutes. Then, the cells were pelleted again at 4°C, for 5 minutes, at 3500 rpm and resuspended in TE buffer with protease inhibitors. Chromatin was sonicated for 3 minutes using a probe sonicator

(Active Motif). Finally, after centrifugation at 4°C, 13000 g for 10 minutes, the supernatant was used for immunoprecipitation.

Briefly, 600-1000 μg of chromatin was incubated with antibody-coated Dynabeads™ Protein A (Invitrogen) at 4°C overnight. The beads were then washed with radioimmunoprecipitation assay buffer (RIPA), high-NaCl RIPA, LiCl buffer, and PBS. Next, DNA was eluted from the beads and reverse cross-linked by incubating with proteinase K at 65°C overnight. DNA was then purified with MinElute PCR Purification Kit (Quiagen), and library preparation was performed according to the manufacturer's instructions for NEBNext® Ultra™ II DNA Library Prep Kit for Illumina® (New England Biotechnology). Proper library size distribution with a peak in 300- to 500-bp range was confirmed using Bioanalyzer 2100 (Aligent), libraries pooled and sequenced with HiSeq 2000 (Illumina). Antibodies used were as follows: anti-Trimethyl-Histone H3 (Lys4) (Millipore, 07-473), Anti-RNA polymerase II CTD repeat (Abcam, ab5408), Anti-Histone H3K27ac (Active Motif, 39133), Anti-Histone H3K4me1 (Active Motif, 39297)

Quality filtering and alignment of the raw reads was performed using Trimmomatic (Bolger et al., 2014) (version 0.36) and Bowtie (Langmead et al., 2009) (version 1.1.2), with the parameter '-m 1' to keep only uniquely mapped reads, using the reference genome hg19. Picard tools (Broad Institute, Picard, http://broadinstitute.github.io/picard/. 2016) was used to remove duplicates and subsequently, and Homer (Heinz et al., 2010) (version 4.8.2) software was applied to generate bedGraph files. Integrative Genomics Viewer (Thorvaldsdottir et al., 2013) was used for visualization.

QUANTIFICATION AND STATISTICAL ANALYSIS

Statistical analysis of data was performed using Prism 8. First, normal distribution of data was assessed. Next, statistical significance was evaluated with 1-way or 2-way AVOVA followed by Tukey's multiple comparisons, or a T-test, depending on the experimental setup. n and points on a graph always represent biological replicates – seeded wells of a 6-well culture plate. Values of *$p < 0.05$, **$p < 0.01$, ***$p < 0.001$, ****$p < 0.0001$ were considered statistically significant.

Publication 2

Enhancer and super-enhancer dynamics in repair after ischemic acute kidney injury.

Julia Wilflingseder, Michaela Willi, Hye Kyung Lee, Hannes Olauson, Jakub Jankowski, Takaharu Ichimura, Reinhold Erben, M. Todd Valerius, Lothar Hennighausen, Joseph V. Bonventre

Nature Communications 2020, 11:3383

nature COMMUNICATIONS

ARTICLE

https://doi.org/10.1038/s41467-020-17205-5 OPEN

Enhancer and super-enhancer dynamics in repair after ischemic acute kidney injury

Julia Wilflingseder[1,2,3,5✉], Michaela Willi[2,5], Hye Kyung Lee[2], Hannes Olauson[1,4], Jakub Jankowski[2,3], Takaharu Ichimura[1], Reinhold Erben[3], M. Todd Valerius[1], Lothar Hennighausen[2] & Joseph V. Bonventre[1✉]

The endogenous repair process can result in recovery after acute kidney injury (AKI) with adaptive proliferation of tubular epithelial cells, but repair can also lead to fibrosis and progressive kidney disease. There is currently limited knowledge about transcriptional regulators regulating these repair programs. Herein we establish the enhancer and super-enhancer landscape after AKI by ChIP-seq in uninjured and repairing kidneys on day two after ischemia reperfusion injury (IRI). We identify key transcription factors including HNF4A, GR, STAT3 and STAT5, which show specific binding at enhancer and super-enhancer sites, revealing enhancer dynamics and transcriptional changes during kidney repair. Loss of bromodomain-containing protein 4 function before IRI leads to impaired recovery after AKI and increased mortality. Our comprehensive analysis of epigenetic changes after kidney injury in vivo has the potential to identify targets for therapeutic intervention. Importantly, our data also call attention to potential caveats involved in use of BET inhibitors in patients at risk for AKI.

[1] Brigham and Women's Hospital, Renal Division, Harvard Medical School, 4 Blackfan Circle, Boston, MA 02115, USA. [2] Laboratory of Genetics and Physiology, NIDDK, NIH, 8 Center Dr, Bethesda, MD 20814, USA. [3] Department of Physiology and Pathophysiology, University of Veterinary Medicine, Veterinärplatz 1, 1210 Vienna, Austria. [4] Division of Renal Medicine, Department of Clinical Science, Intervention and Technology, Karolinska Institutet, Solnavägen 1, 171 77 Stockholm, Sweden. [5] These authors contributed equally: Julia Wilflingseder, Michaela Willi. ✉email: julia.wilflingseder@vetmeduni.ac.at; joseph_bonventre@hms.harvard.edu

Acute kidney injury (AKI) is common, present in up to 10% of hospitalized patients[1], up to 17.5% of patients with cancer, and is associated with high morbidity and mortality[2,3]. Common causes of AKI include ischemia reperfusion injury (IRI), sepsis, and exposure to nephrotoxic substances.

The physiological and cellular hallmarks of AKI include the loss of renal glomerular and tubular function, cell death of kidney epithelia cells, vasoconstriction, and initiation of an inflammatory response. AKI is defined clinically by a rise in serum creatinine reflecting the reduction of glomerular filtration. Although a decrease of renal function can be reversed through the endogenous repair processes of the kidney, AKI is associated with a substantially increased risk of developing fibrosis and chronic kidney disease (CKD), especially if there is severe or repeated injury resulting in 'maladaptive' repair processes[4,5].

Surviving tubular epithelial cells are the main cellular source of the repair process in the kidney with robust proliferation to replace the cells lost as a result of the injury[6]. In this process the proliferating tubular epithelial cells are able to rapidly activate transcriptional repair programs[7]. Investigation of gene expression and function have generated molecular models of kidney injury and repair[8]; yet, there is limited understanding of the epigenetic regulatory events that activate and regulate kidney tissue repair programs.

Recent advances in chromatin analyses suggest that gene regulatory elements are highly prevalent in the genome and, of these elements, distal-acting regulatory sequences, or enhancers, represent the most abundant class[9,10]. Enhancers can induce direct expression of their target genes by increasing transcription[11], and have been predominantly examined as a means for stage- and tissue-specific regulation during embryonic development[12,13]. Studies have also implicated enhancers in health and disease[14,15]. Such findings raise the possibility of existing enhancer elements that engage with transcription factors in response to tissue damage to regulate genetic programs for kidney repair.

To investigate the role of enhancer activation in kidney repair we made use of pharmacological enhancer inhibition through BET (bromodomain and extra terminal) inhibitors. BET protein family members couple with acetyl-lysine residues on histone tails[16] and interact with several key proteins involved in transcriptional regulation (initiation and elongation of transcription) at enhancer sites[17,18]. Bromodomain containing protein 4 (BRD4) is the most widely studied member of the BET protein family. Pharmacological inhibition of BET proteins shows therapeutic activity in a variety of different pathologies, particularly in models of cancer and inflammation[19–21]. Several of these BET inhibitors have been or are being evaluated in clinical trials with more than twenty studies currently registered at clinicaltrials.gov. Most studies evaluate the effect of BET inhibitors in different forms of cancer, but two trials are also testing this class of drugs for cardiovascular diseases and CKD (NCT02586155 and NCT03160430).

In this study, we demonstrate that kidney injury leads to genome-wide changes in the enhancer and super-enhancer repertoire with activation of injury responsive regulatory elements shaping the transcriptional response after injury and during repair. Further, we find that the transcription factors, hepatocyte nuclear factor 4 alpha (HNF4A), glucocorticoid receptor (GR), and signal transducer and activator of transcription (STAT) 3 and 5 bind at the identified enhancer elements. Inhibition of BRD4 function, and therefore blockage of enhancer dynamics after kidney injury, affects critical repair responses resulting in impaired recovery after AKI. These results are the first comprehensive characterization of enhancer and super-enhancer elements in the kidney in vivo before and after injury, thereby providing a rich resource for the research community and critical insight in the regulation of kidney repair.

Results

Kidney injury leads to enhancer repertoire changes in vivo. In order to define the dynamic enhancer and super-enhancer landscape after kidney injury, we performed chromatin immunoprecipitation with next-generation DNA sequencing (ChIP-seq) in SHAM and bilateral-IRI samples at day two after surgery. We used day two post injury samples to capture the proliferating repair phase of the kidney[7]. Kidney cortex samples, consisting in a healthy kidney of at least 90% epithelia cells, were used to capture the chromatin state of mainly proximal (predominant) and distal tubular cells[22].

First, we established a chromatin landscape for the kidney using H3K4me3 to identify promoters, H3K27ac to reveal active enhancer regions and Pol II to define regions of active transcription. We then assessed the genome-wide localization of the representative BET protein, BRD4, also by ChIP-seq and performed sample matched RNA-seq in SHAM and IRI treated kidney samples (Fig. 1a).

H3K27ac marks strongly correlated with binding sites of BRD4 in both SHAM and IRI samples (Fig. 1b, Supplementary Fig. 1) indicating that both ChIP-seq profiles classify active enhancers in the kidney[23,24]. We applied broad peak calling on H3K27ac marks to identify active enhancer regions. Possible promoter regions were identified by H3K4me3 marks and H3K27ac peaks ±2500 bp from the transcription start site (TSS) of genes and verified by overlapping them. We identified 29,925 H3K27ac binding sites shared between SHAM and IRI samples, and 7,439 and 11,406 sites with preferential binding in SHAM or IRI, respectively (Fig. 1c). For further analysis, we named the three groups of binding sites: SHARED (present in both SHAM and IRI samples); IRI-decreased (preferential binding in SHAM samples); and IRI-increased (preferential binding in IRI samples) (Fig. 1d).

Amongst the SHARED sites, 56% are enhancers, and 44% (40% with H3K4me3 and 4% without) were identified as promoters (Fig. 1d, left). In both IRI- decreased and IRI-increased binding sites, the proportion of promoter to enhancers was very different compared to the SHARED group. The analysis of the peaks identified in the IRI-decreased group revealed 88% enhancers and only 12% promoters (2% showing H3K4me3 binding) (Fig. 1d, center). The peaks characteristic for IRI-increased sites consisted of 86% enhancers, and 14% promoters (7.5% with and 6.5% without H3K4me3 binding) (Fig. 1d, right), indicating a higher dynamic at enhancer sites compared to promoter sites after injury.

In order to verify the identified classes of enhancers and promoters we used peak profiles to show the underlying H3K27ac, BRD4, and Pol II marks for SHAM and IRI. Based on the ChIP-seq results for SHAM, the enhancers identified in the SHARED group show the highest coverage (solid orange line), followed by IRI-decreased (dashed black line). The enhancers present in IRI-increased are, as expected, the lowest (dotted red line; Supplementary Fig. 2a). Using IRI ChIP-seq samples, the enhancers gained in IRI (IRI-increased, dotted red line) have a higher coverage than those lost after injury (IRI-decreased, dashed black line). The SHARED enhancers are again those with the highest binding profile (solid orange line; Supplementary Fig. 2b). Based on these results, we conclude that the response to IRI leads to genome-wide alterations in the enhancer landscape in kidney epithelia cells.

Gained enhancers regulate expression of injury-induced genes. To determine the functional relevance of the identified enhancer

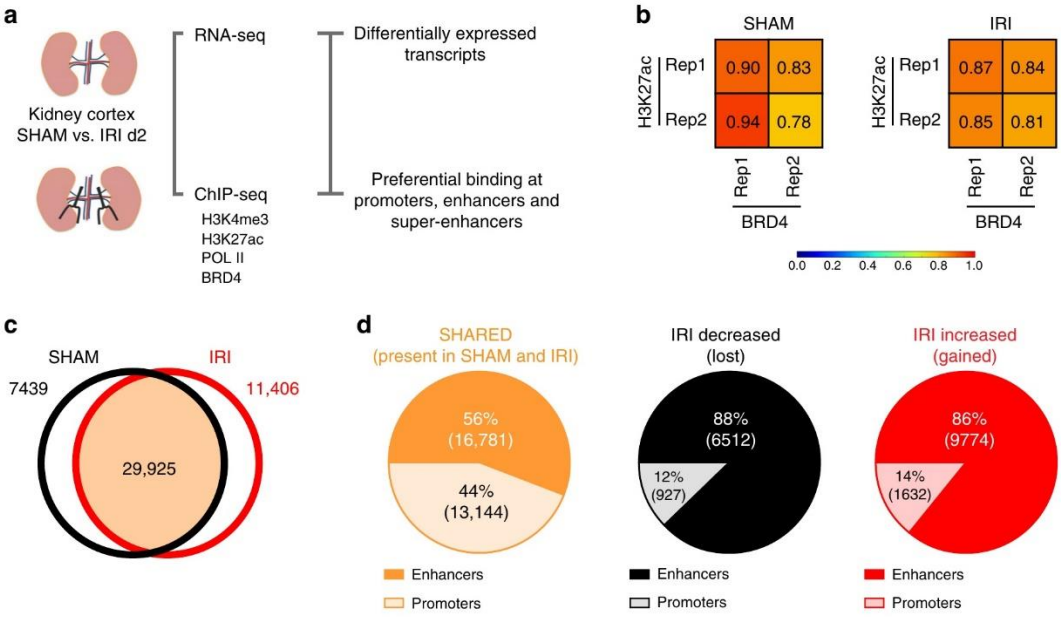

Fig. 1 Identification of enhancer elements. a Workflow of the experimental approach. **b** H3K27ac marks and BRD4 binding sites strongly correlate in both SHAM and IRI samples. **c** Broad peak calling was applied on H3K27ac SHAM and IRI samples. 29,925 peaks overlapped between them; 7439 and 11,406 were only identified in SHAM or IRI samples, respectively. **d** 56% of the identified peaks SHARED between both samples are enhancer elements, whereas 44% are promoter elements. Peaks identified with preferential binding in SHAM samples (IRI-decreased) consist of 88% enhancers and 12% promoter regions. Out of 11,406 peaks identified with preferential binding in IRI samples (IRI-increased) 86% are enhancers and 14% are promoters.

elements we leveraged sample-matched RNA-Seq gene expression data. The RNA-seq data revealed 919 significantly downregulated genes and 1716 significantly upregulated genes when comparing IRI day 2 vs SHAM treated kidneys with false discovery rate (FDR) < 5% and fold change ±2 (Fig. 2a, Supplementary Data 1 and 2). It is interesting that the two most highly upregulated genes are *Lcn2 (NGAL)* and *Havcr1 (KIM-1)*, both of which are generally considered the two most highly upregulated genes after kidney injury[25,26].

Enhancers elements were assigned to genes using GREAT[27]. The majority of enhancers in each group were assigned to at least one gene (Fig. 2b). Only a few enhancers remained unannotated as they were more than 100 kb away from the nearby gene. The vast majority of enhancers were assigned to genes present within 5–50 kb (Fig. 2c).

We found that 571 enhancers were associated with 919 differentially downregulated genes (62%) and 1076 enhancers with 1716 upregulated genes (63%) in IRI day 2 vs SHAM treated kidneys (Fig. 2d). Overall, genes associated with increased enhancers showed significantly increased expression, and decreased enhancers showed statistically significant downregulation of the assigned genes, compared to genes associated with SHARED enhancers (Fig. 2e, Supplementary Data 3–5). As examples of putative enhancers at kidney related genes we show *Slc34a1* (which encodes the proximal tubule sodium-dependent phosphate transporter 2A) and *Kl* (klotho) locus. *Havcr1* genomic locus is shown as a kidney injury related gene. *Slc34a1* and *Kl* were significantly downregulated and *Havcr1 (KIM-1)* significantly upregulated after kidney injury on gene expression level (Fig. 2f) with corresponding protein level changes for KL and KIM-1 (Havcr1) (Supplementary Fig. 3). BRD4 and H3K27ac signals at enhancers near down-regulated *Slc34a1* and *Kl* (Fig. 2g, h) were significantly decreased after IRI, which is consistent with reduced promoter binding of H3K4me3 and significantly lower gene expression after an ischemic insult (Fig. 2f). In contrast, we found injury-induced enrichment of BRD4 and H3K27ac binding at enhancers and promoter near upregulated *Havcr1* genes (Fig. 2i). *Havcr1* (*KIM-1*) is expressed in injured proximal tubular cells[25], where it is involved in clearing apoptotic cells and cell debri from the tubular lumen. Therefore, it plays an important role in the repair phase of tubular cells[28], although prolonged expression of *KIM-1* leads to interstitial fibrosis and CKD[29].

These data suggest an association between BRD4 and H3K27ac enrichment at enhancers and the expression levels of their associated genes. Thus, the enhancer landscape changes in concert with the gene expression changes caused by kidney injury.

Super-enhancer regulation in kidney repair. Multiple and enriched H3K27ac/BRD4 signals in genomic proximity are coined super-enhancers and are associated with cell identity genes in normal and disease states[30,31]. To determine whether super-enhancers might play a role in the response to kidney injury, we undertook a systematic mapping of super-enhancers in IRI day 2 and in SHAM kidneys. We used H3K27ac and BRD4 co-occupied regions with preferential binding either in SHAM or IRI, or present in SHAM and IRI to identify super-enhancers using the ROSE algorithm[30,31]. This algorithm stitches enhancers present within 12.5 kb of each other and ranks them according to the BRD4 and H3K27ac signals (Fig. 3a). We identified 216 injury-associated super-enhancers consisting of 565 single enhancers, 164 super-enhancers lost during injury consisting of 419 enhancers and 385 SHARED super-enhancers consisting of 1630 enhancers, which are present in the kidney at baseline and in IRI day 2 samples. These results indicate widespread changes in H3K27ac and BRD4 occupancy at several super-enhancers after injury. Injury gained super-enhancers showed increased enrichment of H3K27ac and BRD4 at their different enhancer sites. By contrast, lost super-enhancers after IRI exhibited decreased enrichment of H3K27ac and BRD4 at their enhancer sites. The average profile of H3K27ac, BRD4 and Pol II is enriched over all

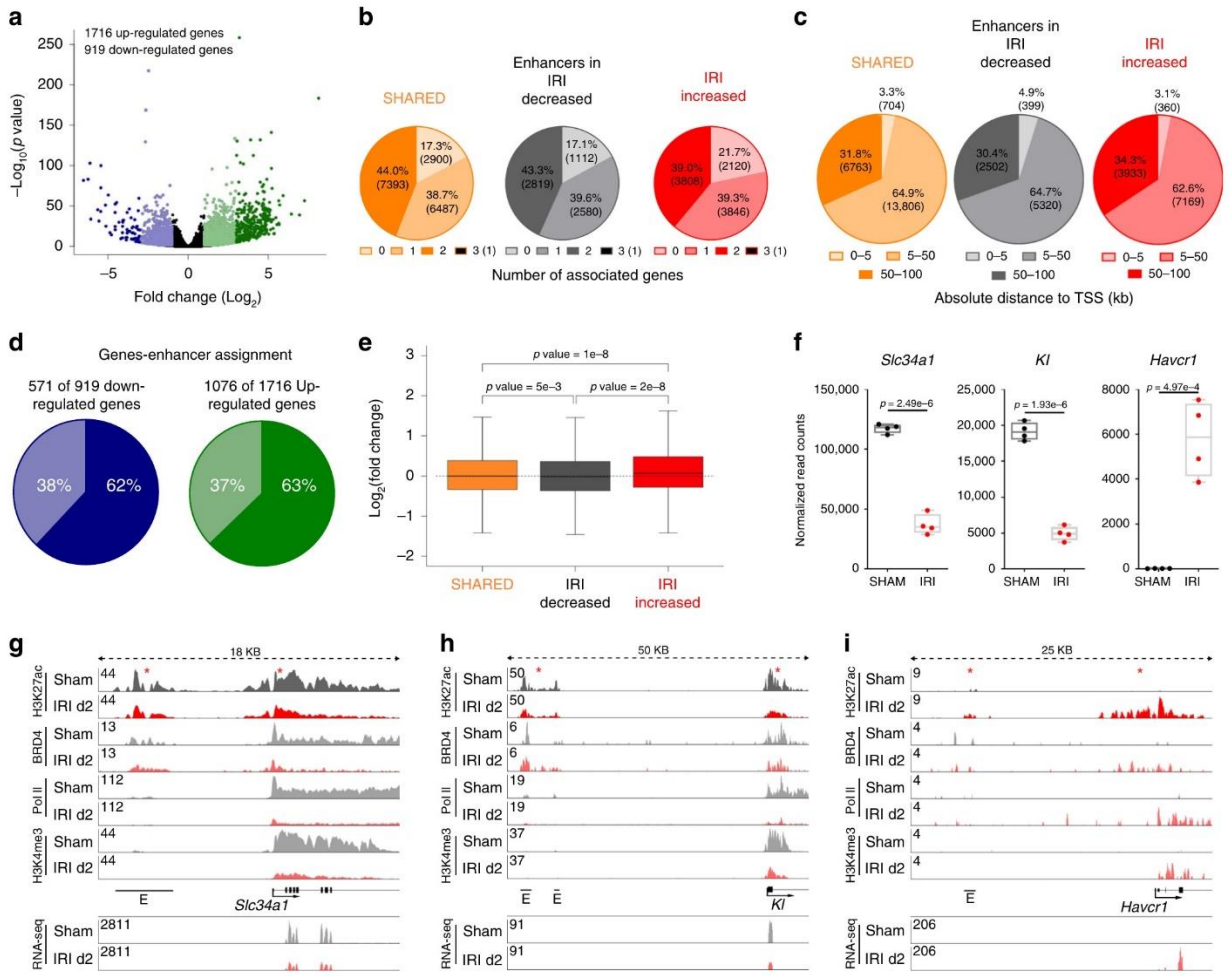

Fig. 2 Enhancer—gene annotation. a The volcano plot illustrates the 919 down- (blue) and 1716 upregulated genes (green) using RNA-seq data. **b** GREAT was used to annotate enhancers to genes. The pie plot shows how many genes were annotated to enhancer elements. **c** The pie plot illustrates the distance between the enhancers and their annotated genes (in kb to the transcriptional start site (TSS)). **d** 571 enhancer elements are annotated to the 919 downregulated genes (62%, dark blue). 1076 enhancers are assigned to 1716 upregulated genes (63%, dark green). **e** Genes associated with IRI-decreased enhancers ($n = 6512$) are significantly downregulated, whereas genes assigned to IRI-increased enhancers ($n = 9774$) have a significantly higher gene expression compared to genes assigned to SHARED enhancers ($n = 16781$). Median, middle line inside each box; IQR (interquartile range), the box containing 50% of the data; whiskers, 1.5 times the IQR. One-way ANOVA with Tukey post hoc test was applied. **f** *Slc34a1* and *Kl* are representative genes that were down-regulated in IRI day 2 when compared with SHAM. *Havcr1(encoding* KIM-1*)* is a gene significantly upregulated at IRI day 2. Two-sample *t*-test was applied (two-sided). Individual data points and box-plot with mean ± max, min are shown. $n = 4$ biologically independent samples **g** Illustration of the enhancer landscape of *Slc34a1*. The indicated enhancers show a lower coverage of H3K27ac, and a strongly reduced coverage of BRD4 and Pol II with IRI compared to SHAM. The coverage of BRD4, Pol II and H3K4me3 is also strongly reduced over the promoter with IRI. RNA-seq track shows reduced expression on exon elements after injury. **h** Depiction of the enhancers associated to *Kl*. These enhancers show a strong decrease of H3K27ac, BRD4, and Pol II. In addition the promoter loses H3K27ac, BRD4, Pol II, and H3K4me3 binding. RNA-seq track shows reduced expression on exon elements after injury. **i** *Havcr1* gains an enhancer element at IRI day 2. Also the promoter shows an increased coverage of H3K27ac, BRD4, Pol II, and H3K4me3. RNA-seq track shows increased expression on exon elements after injury.

identified super-enhancers compared to lone enhancers (Supplementary Fig. 4).

Integration with RNA-Seq data showed that the expression changes for super-enhancer associated genes were more pronounced than lone enhancer associated genes (Fig. 3b). Moreover, genes associated with gained super-enhancers had significantly higher fold changes in expression compared to genes associated with lost or unaffected super-enhancers (Fig. 3c). One example for a gene with increased expression and a gained super-enhancer is *Spp1* (Fig. 3d, e). The *Spp1* gene product had the highest abundance according to normalized read counts after kidney injury compared to all other genes. Also the Spp1 protein plasma levels are significantly increased of this secretory protein (Supplementary Fig. 3c). *Hnf1b*, an important transcription factor in the kidney epithelium, which controls expression of genes responsible for development, solute transport and metabolism, is a representative gene for the class of unchanged genes and of SHARED super-enhancer where there is no change with IRI (Fig. 3d, f, Supplementary Fig. 3)[32]. Overall, 83% of the identified super-enhancers (SHARED combined with IRI-decreased super-enhancers in SHAM samples) and 71% of SHARED combined with IRI-increased super-enhancers in IRI samples can be annotated to at least one highly abundant gene (top 20%) in SHAM and IRI day 2 samples, respectively

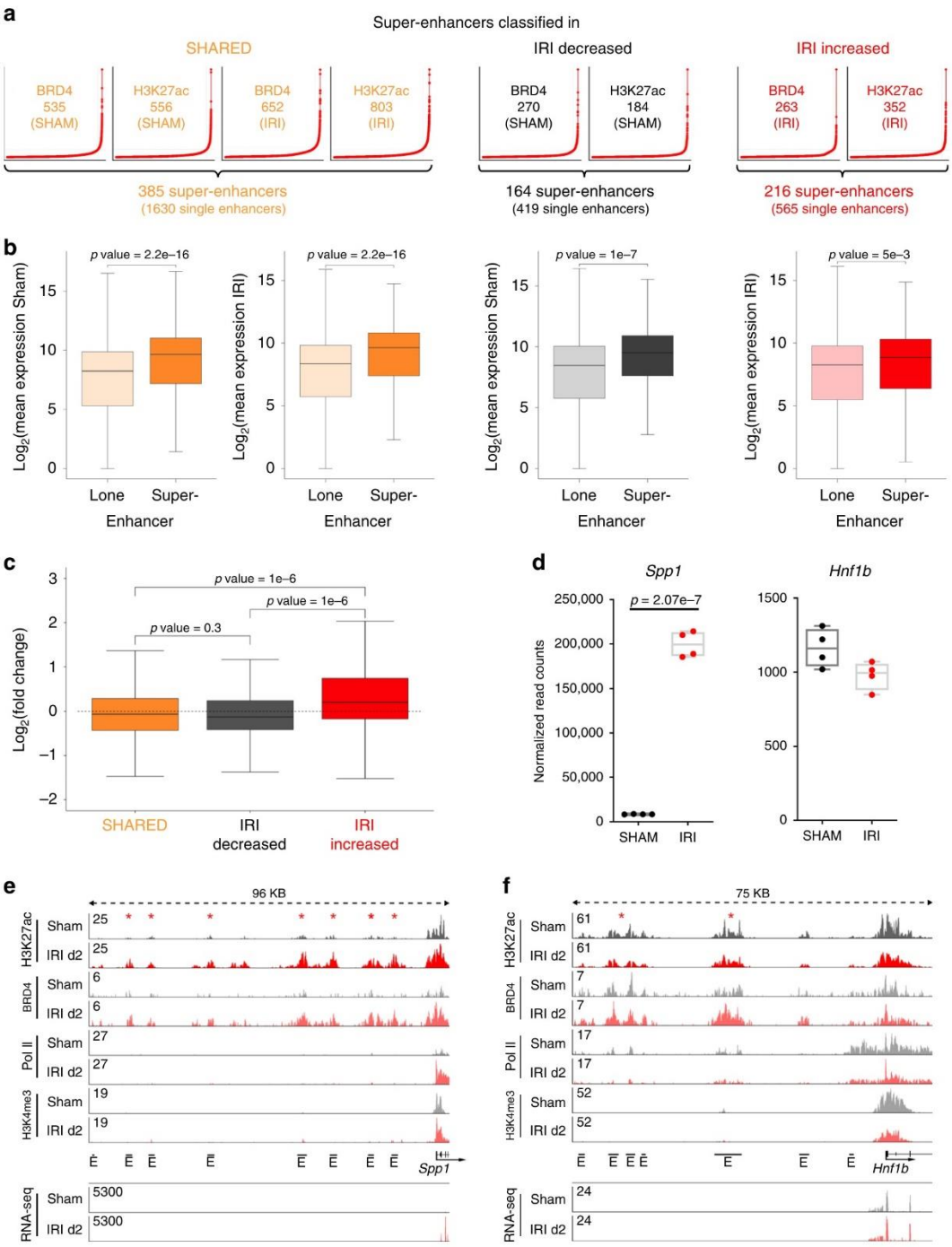

(Supplementary Data 6–8), reflecting super-enhancer association to high abundant gene expression and the important role of super-enhancers in kidney epithelial cells.

Transcription factor binding predicted by motif analysis. Little is known about the characteristics of transcription factor binding at specific enhancer sites in the regulation of repair. Therefore and to further validate the identified enhancer and super-enhancer sites we studied potential transcription factor (TF) binding motifs in our enhancer repertoire and subsequently measured a selection of predicted TFs with ChIP-seq.

First, we identified candidate TFs regulating the enhancer landscape in kidney cells via motif discovery analysis. The identified transcription factor motifs in the SHARED, IRI-decreased, and IRI-increased enhancer groups are shown in Supplementary Data 9. Further, Supplementary Fig. 5a shows the top ten transcription factor motifs in the SHARED, IRI-decreased and IRI-increased enhancer groups as defined by *p*-value. The *p*-value reflects the enrichment of the TF motif in the enhancer sequences compared to the background sequences. In contrast, Supplementary Fig. 5b shows the percentage of enhancer sequences having the underlying TF motif. Among the predicted

Fig. 3 Identification of super-enhancers and their annotation to genes. a Super-enhancers were identified for all three enhancer categories using H3K27ac enhancer elements with the underlying H3K27ac and BRD4 signal. The resulting individual super-enhancers using H3K27ac or BRD4 were overlapped to identify the 385 super-enhancers based on enhancers identified in SHARED, the 164 super-enhancers based on IRI-decreased enhancers and 216 super-enhancers identified in IRI upregulated enhancers. **b** The box plots depict significantly higher expression for genes associated with super-enhancers. Unpaired *t*-tests were applied (two-sided). SHARED lone enhancer: $n = 15151$, SHARED super-enhancer: $n = 385$; IRI-decreased lone enhancer: $n = 6093$, IRI-decreased super-enhancer: $n = 164$; IRI-increased lone enhancer: $n = 9209$, IRI-increased super-enhancer: $n = 216$. Median, middle line inside each box; IQR (interquartile range), the box containing 50% of the data; whiskers, 1.5 times the IQR. **c** The box plot shows that genes assigned to super-enhancers from the IRI-decreased group ($n = 164$) have a lower gene expression level, whereas genes assigned to IRI- increased super-enhancers ($n = 216$) have significantly higher gene expression level compared to SHARED super-enhancers ($n = 385$). Median, middle line inside each box; IQR (interquartile range), the box containing 50% of the data; whiskers, 1.5 times the IQR. One-way ANOVA with Tukey post hoc test was applied. **d** *Spp1* as a representative gene for gaining transcriptional marks is significantly upregulated at IRI d2 (based on RNA-seq data). *Hnf1b* is a representative gene assigned to a SHARED super-enhancer. Two-sample *t*-test was applied (two-sided). Individual data points and box-plot with mean ± max, min are shown. $n = 4$ biologically independent samples. **e** The induced expression of *Spp1* goes along with gained enhancer elements at IRI d2. The enhancers are characterized by strongly increased H3K27ac and BRD4 coverage. The gene body shows strongly increased Pol II binding. RNA-seq track shows increased expression on exon elements after injury. **f** *Hnf1b* enhancers show mild reductions in BRD4, Pol II and H3K27ac binding. RNA-seq track shows unchanged expression on exon elements after injury.

transcription factors many of them are also differentially regulated after injury (Supplementary Fig. 5c).

Based on the motif discovery analysis and availability of suitable antibodies we selected transcription factors in each group for validation in ChIP-seq experiments. Out of the selected transcription factors, namely HNF4A[33,34], GR, Fos-related antigen 1 (FRA1), Fos-related antigen 2 (FOSL2), Jun proto-oncogne (JUN), and STAT 3 and 5 we were able to generate high quality ChIP-seq profiles for four transcription factors which have important roles in kidney epithelial cell fate and response to injury- HNF4A[33], GR[35], STAT3[36], and STAT5[37]. We analyzed the genome-wide binding of these four transcription factors on the identified enhancer elements in the three categories: SHARED, IRI-decreased, and IRI-increased (Fig. 4a). We observed reduced binding of HNF4A and GR at SHARED and IRI-decreased enhancer elements. STAT3 showed decreased binding at IRI-decreased enhancer elements and increased binding at IRI-increased enhancer elements. We could not observe a dynamic binding pattern of STAT5 after IRI. Representative enhancer loci with binding of the four transcription factors are shown in Fig. 4b and Supplementary Fig. 6. At the enhancer element next to Slc34a1 we observed reduced binding of HNF4A, GR, and STAT3. At the Junb locus we find additional STAT3 binding after IRI indicating Junb activation by STAT3 (Fig. 4b). Interestingly at the regulatory element next to Havcr1 we observed GR binding before injury and reduced GR binding after IRI indicating GR may have a repressive function on Havcr1 before injury (Supplementary Fig. 6a). Super-enhancer elements occupied by the identified transcription factors are shown in the Spp1 and Hnf1b locus (Supplementary Fig. 6a). Bcl6 and Neat1 control loci provide visual proof of the technical quality of the ChIP-seq in SHAM and IRI kidney cortex samples (Supplementary Fig. 6b).

In summary, we predicted distinct transcription factor panels and demonstrate three transcription factors, HNF4a, GR, and STAT3, which are potentially involved in enhancer dynamics and therefore potentially significantly contribute to shaping the enhancer landscape in the kidney before and after kidney injury.

BET inhibition increases mortality after experimental AKI. As proof of principle of the role of the observed enhancer and super-enhancer dynamic after kidney injury, we selectively disrupted the BET family, and examined the phenotypic consequences of BET dependent enhancer inhibition. The BET inhibitor, JQ1, was administered prior to injury or later during recovery from IRI in mice. First, we clarified the importance of the different BET family members (BRD2, BRD3, and BRD4) in the kidney. We performed immunofluorescence staining and ChIP-seq experiments for BRD4, BRD2, and BRD3. We found that BRD4 is the dominant member of the BET family in the kidney with higher protein abundance and genome-wide binding at regulatory elements compared to BRD2 and BRD3 which have low protein abundance and low binding at the genome before and after IRI (Supplementary Fig. 7).

Wild-type adult male C57BL/6 mice were injected with JQ1 (50 mg/kg BW) daily starting at the day of IRI surgery (day 0) (Fig. 5a), a dose and schedule well tolerated in the previous studies[31,38,39]. Compared to SHAM mice we detected a 10 to 20-fold increase in serum creatinine at day 1 after IRI, indicating we sucessfully induced AKI in our IRI animals (Fig. 5b). The increase of serum creatinine at day 1 after IRI was equal between IRI vehicle and IRI JQ1 group, suggesting BET inhibition did not modify the ischemia-induced initial renal injury (Fig. 5b). Strikingly, while vehicle-treated mice showed the expected 20% mortality after 26 min bilateral warm ischemia, mice treated with JQ1 had 80% mortality dying 2–3 days post surgery (Fig. 5c, log rank $p = 0.0186$), indicating kidneys exposed to JQ1 treatment have an impaired recovery response after injuy. Of note, surviving mice in the IRI JQ1 group were the ones with the lowest creatinine at day 1 post surgery.

To investigate whether the effects seen were specific to BET inhibition rather than nonspecifically induced by transcriptional inhibition we compared the response to inhibition of BETs to the response to CDK9 inhibition with flavopiridol. It was shown recently that BET proteins act as master transcription elongation factors independent of CDK9 recruitment[40]. We observed no significant increase in mortality with two tested concentrations of CDK9 inhibitor (flavopiridol 2.5 mg/kg and 1 mg/kg body weight per day when we started the treatment 3 h before the surgery (IRI SHAM: 75% survival, $n = 4$; IRI flavopiridol 1 mg/kg: 83% survival, $n = 6$; IRI flavopiridol 2.5 mg/kg: 67% survival, $n = 6$)).

To evaluate the effect of delayed treatment of JQ1 after AKI in mice and to estimate the time window in which JQ1 had a detrimental effect on the survival after AKI we treated C57BL/6 mice with JQ1 starting at day 1, day 2, day 3 or day 4 after IRI surgery (Fig. 5d). Again, serum creatinine at day 1 after injury was not different between the vehicle and JQ1 treatment groups (Fig. 5e). There was a significant increase in mortality rate after IRI at 83% (log rank $p = 0.0096$) in mice exposed to delayed JQ1 treatment starting at day 1. When JQ1 treatment was started at day 2 there was a higher mortality rate (50%), but without reaching statistical significance. When JQ1 was initiated on day 3 or 4 post IRI the survival rate did not change compared to the vehicle-treated group (Fig. 5f). The higher mortality rate when

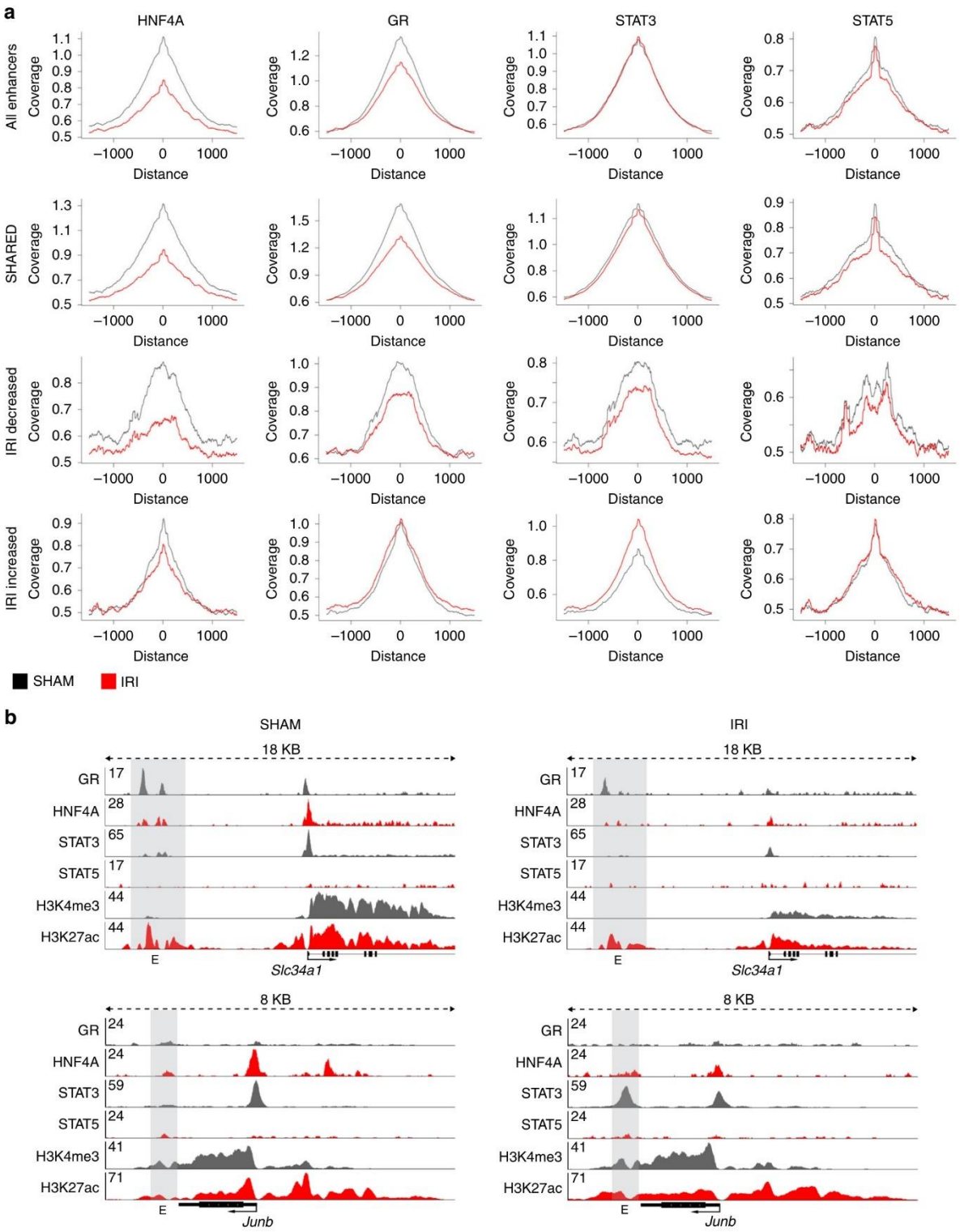

Fig. 4 HNF4A, GR, STAT3, and STAT5 binding at enhancer elements. a Genome-wide coverage plots at all, SHARED, IRI-decreased and IRI-increased enhancers. The coverage for HNF4A and GR decreased in SHARED and IRI-decreased enhancer group after IRI. In contrast, STAT3 shows increased coverage at IRI-increased enhancers. STAT5 peak height at enhancer elements is unchanged after kidney injury. **b** Representative examples of transcription factor binding at enhancer sites in kidney epithelia cells. The Slc34a1 and Junb genomic locus are shown for HNF4A, GR, STAT3, and STAT5 binding together with H3K4me3 and H3K27ac in the SHAM (left) and IRI (right) condition. Enhancer elements are indicated by gray bars.

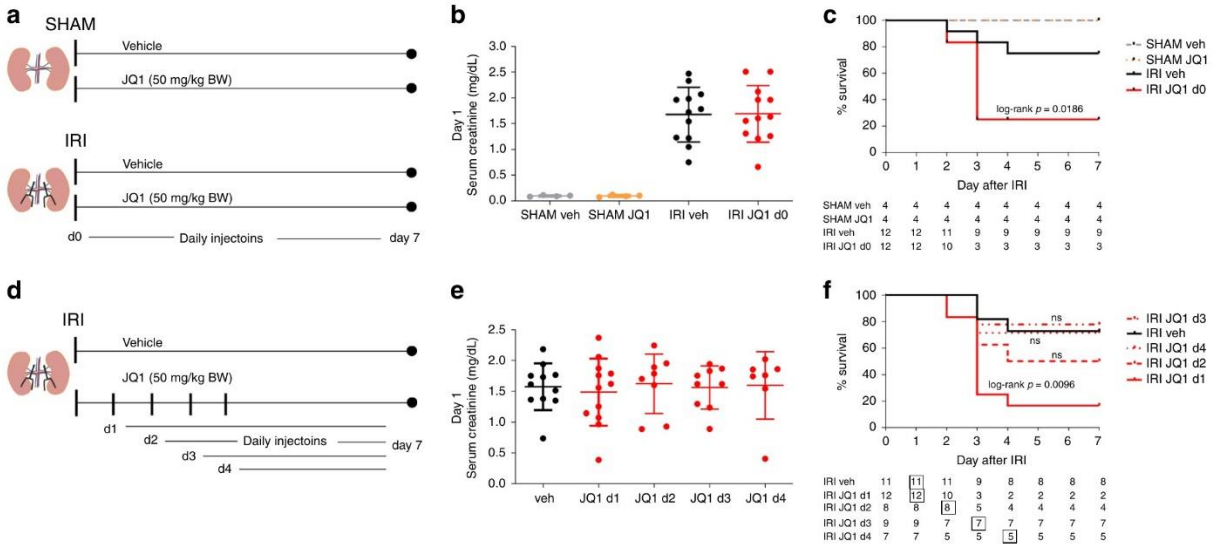

Fig. 5 Phenotypic consequences of BET inhibition after experimental AKI. a C57BL/6N mice (10- to 12-week-old males) were treated daily starting at the day of SHAM or IRI surgery (d0) with JQ1 (50 mg/kg BW) or vehicle (DMSO/10% ß-cyclo dextrin 1:10). **b** Serum creatinine (mg/dL) values in SHAM and IRI animals with vehicle or JQ1 at day 1 after surgery are shown (individual data points and mean ± SD). SHAM: $n = 4$; IRI: $n = 12$ biologically independent samples. **c** Survival curves after IRI surgery (ischemic time was 26 min at 37 °C). JQ1 treatment leads to 80% mortality after IRI surgery. Table shows number of animals alive at indicated days. **d** Experimental design of delayed treatment with JQ1 (50 mg/kg BW) after IRI starting at day 1, day 2, day 3 or day 4. **e** Serum creatinine levels at day 1 after IRI, verifying that AKI was induced to a roughly equivalent extent in each of the groups of animals that were subsequently treated with JQ1 (individual data points and mean ± SD). IRI veh: $n = 11$; IRI d1: $n = 12$; IRI d2: $n = 8$; IRI d3: $n = 9$; IRI d4: $n = 7$ biologically independent samples. **f** Survival curve after delayed JQ1 treatment starting day 1, day 2, day 3 or day 4. Table indicates number of animals alive at each day. Box indicates start of vehicle or JQ1 treatment. Source data are provided as a Source data file.

mice are treated with JQ1 within 48 h of IRI suggests that within this window of time BET dependent transcriptional activation is essential to control gene expression central to the early survival after IRI-induced AKI. The lack of mortality with JQ1 administration at later times after the initial ischemia also points to the lack of generalized toxicity and is compatible with an inhibitory effect on early repair as an explanation for the mortality seen with early JQ1 exposure after injury.

Transcriptional consequences of BET inhibition. To gain insights into the transcriptional consequences of BET inhibition in kidney injury and repair, we performed transcriptional profiling of vehicle- and JQ1-treated kidney cortex samples from animals at day 2 after IRI. Principal component analysis (PCA) shows clear separation between SHAM, IRI, and IRI JQ1 (d0) treated kidney profiles by visualizing principal component (PC) 1 (67% variance) and PC 2 (29% variance) (Fig. 6a). Also at day 2 after IRI we couldn't detect any significant difference in serum creatinine with JQ1 d0 treatment compared to the vehicle group (Fig. 6b). By contrast, at the transcriptional level a total of 2635 transcripts (1716 up, 919 down) were differentially regulated between SHAM vs. IRI and 3054 transcripts (676 up, 2378 down) were differentially regulated between IRI vs IRI JQ1 (Supplementary Data 1, 2, 10, and 11). 73% of downregulated genes (fold change > 2) after JQ1 treatment can be assigned to active enhancer elements (Chi-square: $p < 0.001$). Of the 1716 upregulated transcripts after IRI (Fig. 6c), 718 genes showed reduced expression if JQ1 treatment accompanied the IRI (Chi-square $p < 0.001$) (Fig. 6d), which means that approximately 40% of injury-induced genes were suppressed by JQ1 (Fig. 6c). JQ1 suppressed genes are associated with pathways central in kidney repair such as cell cycle, TNF-alpha signaling, ECM-receptor interaction, chemokine signaling, NOD-like receptor signaling, protein digestion and absorption, DNA replication, cytokine–cytokine receptor interaction, PI3K-Akt signaling and p53 signaling pathway (Fig. 6e)[8,29,41,42]. The top 30 upregulated genes with the highest fold changes after kidney injury are shown in Fig. 6f. Out of the 30 genes 23 were suppressed by JQ1 treatment (FDR < 5%, at least 2-fold reduction), with many of the suppressed genes central to kidney repair such as *Cdk1* (Cyclin-dependent kinase involved in cell cycle progression)[6]. Also at the protein level JQ1 leads to a reduced expression of *KIM-1* and to a marked reduction of proliferating (Ki67+) cells (Fig. 6g). Corresponding transcript expression levels of *KIM-1* and *Mki67* are significantly reduced as validated by qRT-PCR (Fig. 6h).

To further illustrate the consequence of BET inhibition we performed Pol II ChIP-seq with JQ1 treated kidneys after IRI. Through competitive binding of the two extra terminal bromodomains of the BET proteins, JQ1 inhibits the transcriptional elongation process resulting in genome-wide Pol II pausing[43]. We found that JQ1 treatment leads to higher coverage of Pol II on the TSS (0% distance) and lower coverage in the middle of the gene body (50% distance) indicating genome-wide Pol II pausing two days after IRI in the kidney (Fig. 6i). Further, we show the Spp1 gene body for Pol II binding in SHAM, IRI, and IRI + JQ1 treatment (Fig. 6j). Spp1 mRNA expression was also downregulated by JQ1 (Fig. 6k). Together, these results clearly illustrate that BET inhibition impairs the transcriptional response to injury and disrupts acute repair programs in the kidney after IRI.

To also explore the function of BET proteins in the maintenance of kidney specific transcriptional programs without injury we compared SHAM vehicle vs SHAM JQ1 d0 treated kidneys at day 2 after SHAM surgery. Surprisingly, also in the healthy kidney BET inhibition leads to significant changes on the transcriptional level. A total of 2441 transcripts (774 up, 1667 down) were differentially regulated comparing SHAM vehicle vs. SHAM JQ1 (Supplementary Data 12 and 13). Among the 1667

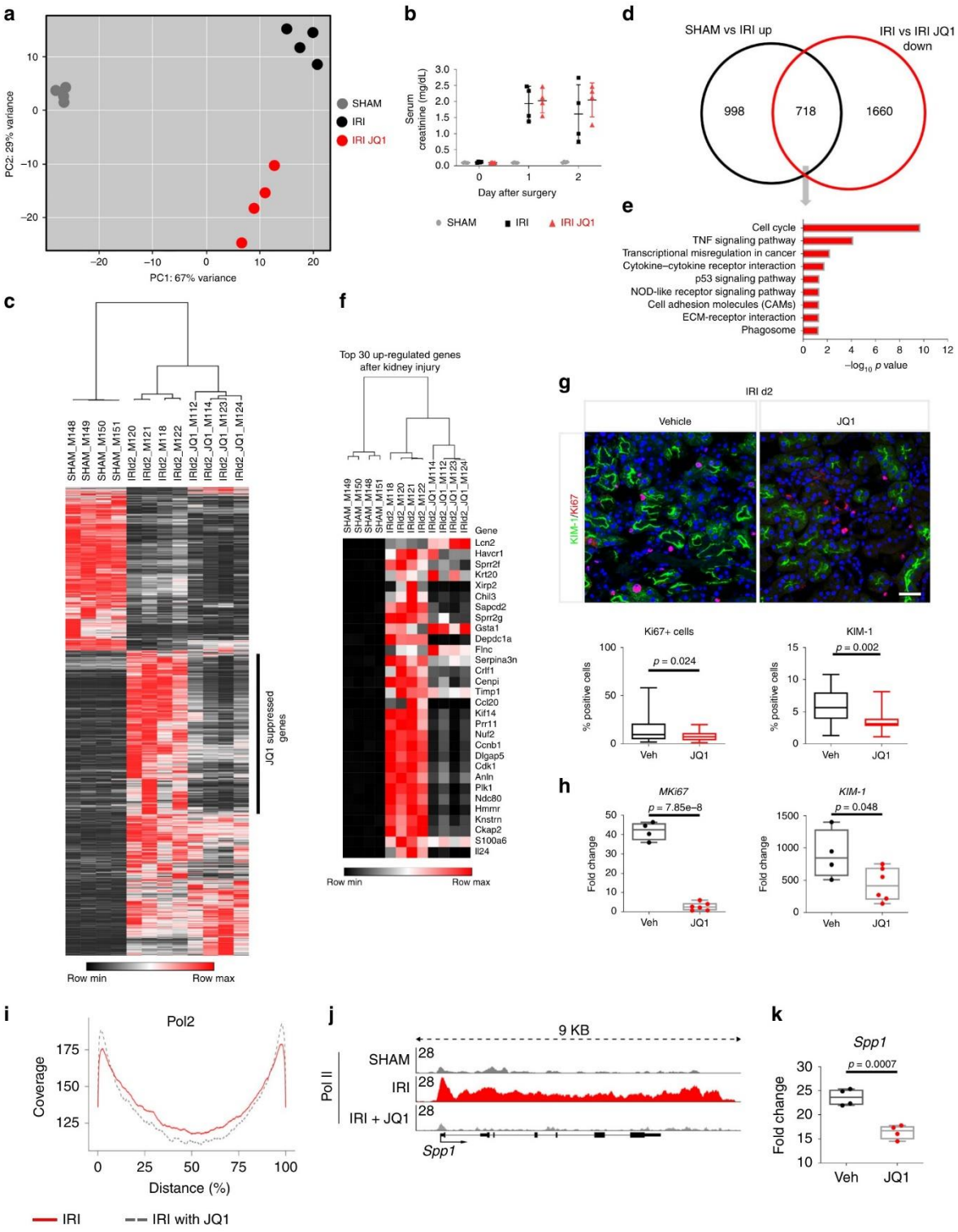

downregulated transcripts many genes are involved in the normal functions of the kidney such as genes with kidney specific transporter activity (Supplementary Data 14). Of the 334 transcripts identified as kidney related in a whole-body tissue comparision[44] 99 were significant down-regulated by JQ1 in the kidney (Supplementary Data 15, Chi-square $p < 0.001$). Therefore, our data suggest that BET proteins are important in the maintenance of kidney specific transcriptional programs and essential in the transcriptional regulation of early kidney repair.

Evaluation of BET inhibition in kidney fibrosis. To evaluate kidney fibrosis development after IRI we treated C57BL/6 mice with JQ1 starting at day 4 after injury once the initial phase of post-ischemic transcriptional response had subsided[4]. Mice were

Fig. 6 Transcriptional consequences of sBET Inhibition. a Principal component (PC) analysis of normalized RNA-seq data matrix of SHAM, IRI and IRI JQ1 kidney cortex samples on day 2 after IRI. **b** Serum creatinine values at days 0, 1, and 2 after IRI comparing SHAM, IRI and IRI JQ1-treated groups. **c** Genes significantly differentially regulated between SHAM and IRI are shown in a heatmap of SHAM, IRI, and IRI JQ1; JQ1 leads to suppression of ~40% upregulated genes after injury. **d** Comparison of significantly upregulated genes 2 days after injury (SHAM vs. IRI up) and significantly down-regulated genes after JQ1 treatment (IRI vs IRI JQ1 down) with an overlap of 718 transcripts (Chi-square test $P < 0.001$) shown in a Venn diagram. **e** KEGG pathways enriched for the 718 genes upregulated after injury and down-regulated by JQ1. **f** Top 30 upregulated genes after injury shown in a heatmap of SHAM, IRI and IRI JQ1 samples. **g** Representative KIM-1/Ki67-immunostained IRI kidney cortex treated with vehicle or JQ1 at day 2 after injury, Quantification of Ki67+ cells (Ki67+ cells/total number of cells (DAPI)) and KIM-1+ surface area per hpf ($n = 4$, 7 high power fields (hpf) per sample). Scale bar: 50 µm. **h** Fold change of Mki67 and KIM-1 after IRI comparing vehicle and JQ1 treated animals at day 2 after injury (vehicle: $n = 4$, JQ1: $n = 6$). **i** Genome-wide assessment of Pol II binding: Genome-wide coverage blots of Pol II on the gene body. Pol II binding after JQ1 treatment is increased at the TSS and decreased across the gene body indicating Pol II pausing **j** Pol II ChIP-seq tracks at the Spp1 gene body. **k** Fold change of Spp1 after IRI comparing vehicle and JQ1 treated animals at day 2 after injury. $n = 4$. Data represent the mean ± min, max. Box contains 50% of the data. *t*-test (two-sided) (**g**, **h**, **k**). Source data are provided as a Source data file.

randomly assigned to vehicle or JQ1-treated groups (Supplementary Fig. 8a). Two mice died before the start of the treatment at day 3 after IRI. BUN trajectories were not different between vehicle and JQ1 group after injury (Supplementary Fig. 8b). Interestingly, also gene expression levels at day 21 of fibrosis-associated genes, such as *KIM-1*, *Acta2*, *Ctgf*, *Col1a1*, and *c-Myc* were not differentially regulated with JQ1 treatment (Supplementary Fig. 8c). Furthermore, we evaluated the amount of fibrosis in these kidneys by Masson Trichrome-staining at day 21 and saw no significant reduction by JQ1 treatment (Supplementary Fig. 8d). Also of note, the severity of fibrosis seen at day 21 after AKI induced by IRI was moderate with only ~5% Masson Trichrome-positive area in the vehicle group; therefore, we evaluated the effect of fibrosis development under JQ1 treatment in two different kidney fibrosis models where the fibrosis is more severe, namely aristolochic acid toxic nephropathy (AAN) and unilateral ureteral obstruction (UUO).

A single injection of aristolochic acid (AA) (3 mg/kg BW) to BALB/c mice was combined with a daily treatment of JQ1 in two treatment arms: (1) starting the same day as the AA injection (group: JQ1 d0) or (2) starting on day 7 after AA injection (group: JQ1 d7) (Fig. 7a). AA treatment alone resulted in severe kidney injury, as indicated by increased serum creatinine levels (Fig. 7b), but was not associated with mortality as there was 100% survival in the vehicle-treated mice (Fig. 7c). Daily JQ1 treatment commencing on day 0 or 7 after AA injection did not alter serum creatinine (Fig. 7b). Thirty-three percent mortality was detected in the early JQ1 treated mice (JQ1 d0; two out of six mice died, log rank $p = 0.072$), compared to no mortality in the delayed JQ1 treated mice (JQ1 d7). At the protein level JQ1 d0 and JQ1 d7 compared to vehicle lead to similar reductions of *Acta2*, and *Ki67*+ cells (Fig. 7d, e) on day 21, confirming reduced myelofibroblasts and proliferation in these kidneys.

To further evaluate the anti-fibrotic effects of JQ1, permanent injury was induced to the left kidney, through irreversible obstruction of the ureter resulting in a severe fibrotic phenotype within 10 days after obstruction (Fig. 7f). BET inhibition significantly reduced the severity of fibrosis in JQ1 treated C57BL/6N mice after UUO as reflected by decreased trichome-positive area and collagen deposition (assessed by Sirius red-staining) (Fig. 7g, h) which is consistent with the current literature[45–47]. No mortality was observed in the treatment arms as kidney function was maintained by the contralateral, uninjured kidney. In summary, these data derived from IRI, UUO and AAN models suggest that BET dependent gene regulation is essential in kidney repair and also plays a part in the development of kidney fibrosis post injury.

Discussion

Surviving kidney tubular cells have to undergo phenotypic and transcriptional changes to initiate the repair of the tubular structure and restore kidney function after AKI. We have determined epigenetic changes that occur after kidney injury during the early repair phase. We profiled the enhancer and super-enhancer repertoire in normal kidney and during the proliferating repair phase 2 days after IRI. This yields a rich resource of epigenomic data of distal regulatory elements controlling the expression of critical genes and pathways involved in kidney injury and repair. Our data suggest that enhancer regulation and genes controlled by these enhancer elements are disproportionally enriched during repair. Early after an insult to the kidney, a cascade of downstream signaling events, involving cytokine, chemokine and kinase-dependent signaling[48], are activated[4]. These signals recruit key signal-dependent transcription factors, such as STAT3 or AP-1 transcription factors, mainly to distal regulatory enhancer and super-enhancer elements that further lead to histone acetylation and binding of mediator proteins, including BRD4. This transcriptional regulation cascade promotes transcription of genes key to kidney repair. We also observe a loss of enhancer and super-enhancer elements with injury reflected by decreased H3K27ac and BRD4 marks. We observed reduced binding of HNF4A and GR at IRI-decreased enhancer elements, changes that likely facilitate the dedifferentiation process necessary for surviving kidney cells to proliferate[42].

How transcription factors involved in kidney repair act on enhancer elements and their target genes in kidney cells is unknown[42]. Our motif discovery analyses within enhancer and super-enhancer elements provides insight into which transcription factors might contribute to the transcriptional initiation of kidney repair and maintaining kidney specific gene expression programs. The HNF4A transcription factor was the top predicted motif in our SHARED and IRI-decreased enhancer group suggesting enhancer regulation in kidney epithelia cells. In humans heterozygous mutations in this transcription factor causes variable multisystem phenotypes including maturity-onset diabetes of the young and a variety of renal phenotypes (including renal cysts and mimicking of Fanconi syndrome)[49]. This attests to the importance of HNF4A in the transcriptional regulation of kidney epithelia-specific genes. However, as HNF4A is not kidney specific and also has important roles in other organs such as the pancreas and the liver, it is likely that a panel of transcription factors are necessary for the regulation of kidney epithelia-specific transcription programs. We provide the first evidence that HNF4A and GR are part of such a transcription factor panel providing insight into the differentiation process of the kidney and therefore important information for regeneration medicine.

Related to the differentiation process into kidney epithelia cells, kidney repair requires specific transcriptional changes of surviving kidney epithelia cells that allows them to proliferate. We found a dynamic binding of STAT3 at injury regulated enhancer elements. We show an interesting relationship with STAT3

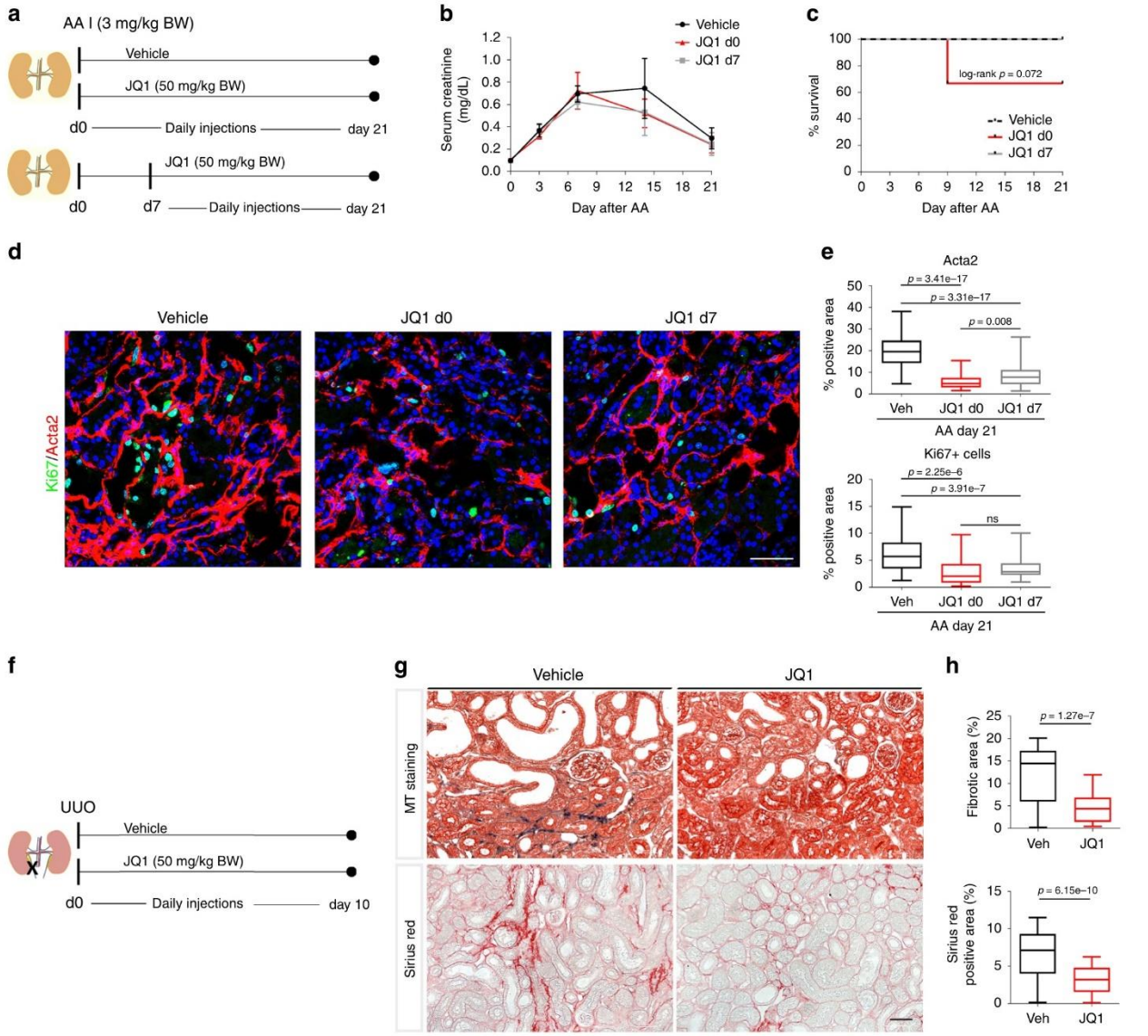

Fig. 7 BET inhibition blocks fibrosis development in AAN and UUO. a BALB/c mice (10- to 12-week-old males) were treated daily with JQ1 (50 mg/kg) or vehicle (DMSO/10% ß-cyclo dextrin 1:10) starting on the day of aristolochic acid (AA) injection (3 mg/kg BW) or day 7 after AA injection. Mice were sacrificed on day 21 after AA injection. **b** Serum creatinine (mg/dL) trajectories of vehicle and JQ1 treated mice from day 0 until day 21 after AA (mean ± SD). vehicle: $n = 7$; JQ1 d0: $n = 6$; JQ1 d7: $n = 8$ biologically independent samples. **c** Survival curves after AA injection: 100% survial in vehicle and JQ1 d7 group, 67% survival in mice treated with JQ1 from day 0 until day 21 after AA injection. **d** Representative Ki67-1/Acta2-immunostained AAN kidneys treated with vehicle or JQ1 d0 or JQ1 d7. **e** Quantification of α-SMA+ (Acta2) surface area. Percentage of Ki67+ cells (Ki67+ cells/total number of cells (DAPI) per hpf). vehicle: $n = 7$ (60 hpf); JQ1 d0: $n = 4$ (33 hpf); JQ1 d7: $n = 8$ (64 hpf) at least 8 hpf per sample. **f** C57BL/6N mice (8- to 10-week-old males) were treated daily starting at the day of UUO surgery with JQ1 (50 mg/kg) or vehicle, and were sacrificed on day 10 after surgery. **g** Representative trichrome-stained and Sirius-red stained sections. **h** Quantification of fibrotic area (masson trichrome +-stained) ($n = 7$, 5 hpf per sample) and Sirius red+ area (collagen) ($n = 7$, at least 7 hpf per sample. *t*-test (two-sided). Data represent the mean ± min, max. Box contains 50% of the data. Scale bars: 100 µm (**d**), 50 µm (**g**). Source data are provided as a Source data file.

binding next to Junb, a member of the AP-1 transcription factor family. AP-1 transcription factor motifs were highly enriched at injury-induced enhancer elements. Further, AP-1 transcription factors can complex with the GR leading to either activation or repression of target genes[50]. GR binding is highly dynamic at lost and gained enhancer elements after injury suggesting a crosstalk between GR and AP-1 transcription factors during kidney repair. We provide data of the binding of these transcription factors at enhancer sites in the kidney and novel clues as to how these regulatory circuits orchestrate transcriptional kidney programs and response to injury.

Emerging evidence indicates that enhancer and super-enhancer regulation is crucial in health and disease[31] and directs cell-specific gene expression[30]. Here we show that enhancer and super-enhancer formation is BRD4 dependent in the kidney before and after kidney injury. Importantly, BET inhibitor administration had very different molecular effects in the kidney depending on timing after injury. BET inhibition in the early

recovery phase after AKI leads to impaired recovery and increased mortality whereas later after injury BET inhibition can block development of fibrosis. These different effects may be explained through the modification of the chromatin state of the cell by BET inhibitors[43,51]. It is interesting that KIM-1 expression is reduced with JQ1 treatment since early upregulation of KIM-1 after injury is protective in IRI[28]. Liu et al. have suggested a protective effect of JQ1 treatment administered seven days before IRI since they measured a decrease in creatinine level rise 24 h after IRI[52]. However, in their study survival after IRI was not assessed beyond 24 h after injury. Furthermore, pretreatment with JQ1 for 7 days may change the chromatin state of the renal cells and thereby alter the response to ischemia.

Studies in humans have documented broad changes in plasma protein concentrations 24 h after abapetalone (BET inhibitor) administration in CKD patients and healthy controls[53]. Osteopontin (*Spp1*) was one of the most affected proteins and was significantly down-regulated with the BET inhibitor in CKD and control patients, suggesting super-enhancer dependency of *Spp1* and sensitivity to BET inhibitors also in humans. In general this study and various pre-clinical studies published by us and others present a rationale for antifibrotic effects of BET inhibitors and therefore a rationale for further human clinical investigation of this class of agents in CKD[45–47,54,55]. Different BET inhibitors, which specifically inhibit either the first (BD1) or the second (BD2) bromodomain of the BET proteins can have different functional contributions to the biological effects of BET inhibitors[56]. BD2 inhibitors were predominantly effective in inflammation-related disorders[56]. Apabetalone is an example of a BD2 inhibitor used in clinical trials[57]. Further, different genomic BRD4 binding and loads of cell-state-determining enhancers, depending on their molecular context in the kidney cell, can dramatically affect the outcome of the BET inhibitor therapy.

For patients at risk for AKI, our data call attention to potential caveats for use of small molecule inhibitors of BET proteins that are currently being tested in clinical trials, primarily in cancer. As AKI is quite common among hospitalized and cancer patients this requires further considerations and might effect clinical management.

In summary, we describe enhancer and super-enhancer elements and transcription factor binding at enhancer elements in the kidney before and after injury in vivo, yielding important clues to the regulation of cell-fate of kidney cells after injury. This work opens up a level of transcriptional understanding of kidney repair. In addition, the information obtained provides targets for therapeutic intervention.

Methods

Animal experiments. Bilateral IRI was induced in male C57BL/6N mice by clamping of both renal arteries for 26 min at 37 °C with a retroperitoneal approach using pentobarbitol anesthesia. Reperfusion was verified by visual inspection of kidneys. One ml of 37 °C saline was administered by intraperitoneal injection (IP) after surgery for volume repletion. In SHAM operations both kidneys were exposed without induction of ischemia. For the unilateral ureteral obstruction model the left ureter of male C57BL/6N mice was exposed and ligated with a non-absorbable suture. One ml of 37 °C saline was given (IP) after surgery for volume repletion. Aristolochic Acid nephropathy was induced by a single injection of 3 mg/kg aristolochic acid I in saline intraperitoneally in male BALB/c mice. The BET inhibitor JQ1 or vehicle was provided to us by Dr. Jay Bradner (formerly at Brigham and Women's Hospital now at the Novartis Institutes for Biomedical Research). JQ1 was administered daily during the treatment periods. Pharmacokinetic studies in mice have shown that a dosage of 50 mg/kg/day of JQ1 is sufficient to achieve an effective blockade of BRD4[20,31]. We prepared a stock solution of JQ1 (50 mg/ml in DMSO) and further diluted it in 10% ß-cyclo-dextrin 1:9 to achieve solubility of the compound. 6 to 12 mice were used in each group in most experiments. Male C57BL/6 N or BALB/c mice aged 8 to 10 weeks weighing 20–22 g were purchased from Charles River Laboratories. Mice were kept under standard housing conditions (22–24 °C ambient temperature, 50-60% humidity, 12 h dark/light cycle). All mouse work was performed in accordance with all relevant ethical regulations for animal testing and research. The animal use protocol was approved by the Institutional Animal Care and User Committee of the Harvard Medical School/Brigham and Women's Hospital.

ChIP-seq. Chip assays were performed as described previously[58]. Briefly, snap-frozen kidney cortex from SHAM or IRI mice (day 2) were ground into powder in liquid nitrogen. After 15 min chromatin cross-linking was carried out in 1% formaldehyde at room temperature and the reaction was quenched with 0.125 M glycine. After cell lysis and 22 min of sonication, sheared chromatin was incubated with 10 µg of following antibodies: anti-H3K27ac (Abcam, ab4729), anti-H3K4me3 (Millipore, 17-614), anti-BRD4 (Bethyl Laboratory, A301-985A), anti-RNA Polymerase II (Abcam, ab5408), anti-BRD2 (Bethyl Laboratory, A301-583A), anti-BRD3 (Bethyl Laboratory, A301-368A), anti-HNF4A (Abcam, ab41898), anti-GR (Thermo Scientific, PA1-511A), anti-STAT3 (Santa Cruz, sc-482) and anti-STAT5 (Santa Cruz, sc-835). Libraries for next-generation sequencing were prepared with NEBNext Ultra II DNA Library Prep Kit (New England BioLabs, E7645) and sequenced on HiSeq 2500 machine (Illumina).

ChIP-seq data analysis. The ChIP-seq analysis workflow comprised trimming using trimmomatic (version 0.36)[59] in order to filter low quality reads, followed by the application of bowtie aligner (version 1.1.2)[60] with the parameter of -m 1 to retrieve only uniquely mapped reads (mm10 reference genome), and finally Homer software (version 4.8.2)[61] and Integrative Genomics Viewer (version 2.3.81)[62] for the visualization. DeepTools (version 2.1.0)[63] was used to obtain the correlation between the replicates.

In order to identify regions of ChIP-seq enrichment over the background, the MACS2 (version 2.1.1)[64] peak finding algorithm was used. Broad peak calling of H3K27ac with a q-value cutoff of 0.1 and 0.05 for SHAM and IRI day 2 was done in replicates, which were subsequently overlapped using BEDtools (version 2.26.0)[65] to identify high-confident peaks. Promoters were filtered using the coordinates of the GFF file and overlapping them with the peak files using BEDtools. Annotation of the identified enhancer elements to their target genes was done with GREAT[27] using the setting of "Basal plus extension" and a maximum distal distance of 100 kb. Coverage plots (normalized to 10 million reads) and motif analysis with default background were done using Homer software (version 4.8.2)[61]. HOMER[61] was used for motif analysis using the default settings.

The ROSE algorithm[30,31] was applied for super-enhancer analysis. We used enhancer elements identified by H3K27ac, and the default stitching size of 12.5 kb and H3K27ac and BRD4 BAM files as input. Graphs were generated using R (R Project for Statistical Computing, https://www.R-project.org/) and the packages ggplot2[66] and dplyr (https://CRAN.R-project.org/package=dplyr). Box plots were used to illustrate data (Median, middle bar inside each box; IQR (interquartile range)), the box containing 50% of the data; whiskers, 1.5 times the IQR). Two sample t-tests was applied where appropriate. One-way ANOVA with Tukey post hoc test was applied where appropriate.

Gene expression profiling. Total RNA was isolated from kidney cortex samples with the PureLink RNA Mini Kit (Thermo Fisher Scientific, 12183018A) or TRIzol reagent (Thermo Fisher Scientific, 15596029) for RNA-Seq or qRT-PCR. For qRT-PCR 2 µg of total RNA was reverse transcribed with the M-MLV reverse transcriptase Kit and oligo dT primers (Invitrogen). Gene expression was analyzed by qPCR using SYBR Green reagent (Bio-Rad) with gene-specific primers in 25 µl reactions in triplicate on Bio-Rad real-time detection system.

Libraries for next-generation sequencing were prepared with TruSeq Stranded RNA LT Kit (Illumina, 15032611) and sequenced on HiSeq 2500 machine (Illumina).

RNA-seq analysis. RNA-seq data were trimmed using trimmomatic (version 0.36)[59] and subsequently aligned to the reference genome mm10 applying STAR RNA-seq aligner (version 2.5.3a)[59]. HTSeq (version 0.6.1p1)[67] and DESeq2[68] were applied for the RNA-seq analysis.

Renal function and histology. The plasma creatinine and BUN concentration was determined by Mass Spectrometry at the University of Alabama and BUN infinity kit from ThermoFisher Scientific, respectively. Kidney histology was examined on methacarn-fixed sections stained for PAS, H&E, Masson's trichrome and Sirius red. The degree of interstitial fibrosis was scored quantitatively on Masson's trichrome stained tissue or Sirius red-stained tissue (Collagen) with Image J.

Immunofluorescence staining. Immunofluorescence staining of the kidney was performed on fixed-frozen sections. Briefly, the tissue sections were activated and labeled with antibodies, including rabbit anti-Ki-67 (Vector, VP-K451, 1 in 200), rabbit anti-KIM-1 (R9[25], 1 in 200), rabbit anti-α-SMA (Sigma, 1 in 400), rat anti-F4/80 (Abcam, ab6640, 1 in 1000), rabbit anti-Hnf1b (Thermo Fisher Scientific, 720259), rabbit anti-GR (Thermo Fisher Scientific, PA1-511A), rabbit anti-Slc34a1 (Novusbio, NBP2-13328), rabbit anti-Spp1 (Abcam, ab8448) and rat anti-Kl (BioLogo, KM2076). The slides were then exposed to FITC or Cy3-labeled secondary antibodies (Jackson ImmunoResearch). The staining was examined with fluorescence microscopes (Nikon TE 1000 and Nikon C1 confocal). At least 7

high-power fields/section for each sample were examined in each evaluation and quantification (positive area or cell count) was performed with an in-house Macro in Image J. Spp1 plasma concentration was measured by ELISA (R&D Systems, MOST00).

Reporting summary. Further information on research design is available in the Nature Research Life Sciences Reporting Summary linked to this article.

Data availability

The data that support this work is available from the corresponding authors upon reasonable request. ChIP-seq and RNA-seq raw data files are available in the Gene Expression Omnibus (GEO) at NCBI with the accession number GSE114294. The source data underlying Fig. 5b, e, 6b, g, h, 7b, e, h and Supplementary Figs. 3b, c and 8b–d are provided as a Source data file.

Code availability

A summary of our analysis approach can be found in the Supplementary information. We only applied existing tools to analyze our data.

Received: 8 April 2019; Accepted: 9 June 2020;
Published online: 07 July 2020

References

1. Chertow, G. M., Burdick, E., Honour, M., Bonventre, J. V. & Bates, D. W. Acute kidney injury, mortality, length of stay, and costs in hospitalized patients. *J. Am. Soc. Nephrol.* **16**, 3365–3370 (2005).
2. Coresh, J. et al. Prevalence of chronic kidney disease in the United States. *JAMA* **298**, 2038–2047 (2007).
3. Rosner, M. H. & Perazella, M. A. Acute kidney injury in patients with cancer. *N. Engl. J. Med* **376**, 1770–1781 (2017).
4. Liu J. et al. Molecular characterization of the transition from acute to chronic kidney injury following ischemia/reperfusion. *JCI Insight* **2**, e94716 (2017).
5. Yang L., Besschetnova T. Y., Brooks C. R., Shah J. V. & Bonventre J. V. Epithelial cell cycle arrest in G2/M mediates kidney fibrosis after injury. *Nat Med.* **16**, 535–543 (2010).
6. Humphreys, B. D. et al. Intrinsic epithelial cells repair the kidney after injury. *Cell Stem Cell* **2**, 284–291 (2008).
7. Kumar, S. et al. Sox9 activation highlights a cellular pathway of renal repair in the acutely injured mammalian kidney. *Cell Rep.* **12**, 1325–1338 (2015).
8. Chang-Panesso, M. & Humphreys, B. D. Cellular plasticity in kidney injury and repair. *Nat. Rev. Nephrol.* **13**, 39–46 (2017).
9. Consortium, T. E. An integrated encyclopedia of DNA elements in the human genome. *Nature* **489**, 57–74 (2012).
10. Kundaje, A. et al. Integrative analysis of 111 reference human epigenomes. *Nature* **518**, 317–330 (2015).
11. Larsson, A. J. M. et al. Genomic encoding of transcriptional burst kinetics. *Nature* **565**, 251–254 (2019).
12. Lagha, M., Bothma, J. P. & Levine, M. Mechanisms of transcriptional precision in animal development. *Trends Genet.* **28**, 409–416 (2012).
13. Visel, A., Rubin, E. M. & Pennacchio, L. A. Genomic views of distant-acting enhancers. *Nature* **461**, 199–205 (2009).
14. Lonfat, N., Montavon, T., Darbellay, F., Gitto, S. & Duboule, D. Convergent evolution of complex regulatory landscapes and pleiotropy at Hox loci. *Science* **346**, 1004–1006 (2014).
15. Rebeiz, M., Pool, J. E., Kassner, V. A., Aquadro, C. F. & Carroll, S. B. Stepwise modification of a modular enhancer underlies adaptation in a *Drosophila* population. *Science* **326**, 1663–1667 (2009).
16. Filippakopoulos, P. et al. Histone recognition and large-scale structural analysis of the human bromodomain family. *Cell* **149**, 214–231 (2012).
17. Jung, M. et al. Affinity map of bromodomain protein 4 (BRD4) interactions with the histone H4 tail and the small molecule inhibitor JQ1. *J. Biol. Chem.* **289**, 9304–9319 (2014).
18. Wu, S. Y. & Chiang, C. M. The double bromodomain-containing chromatin adaptor Brd4 and transcriptional regulation. *J. Biol. Chem.* **282**, 13141–13145 (2007).
19. De Raedt, T. et al. PRC2 loss amplifies Ras-driven transcription and confers sensitivity to BRD4-based therapies. *Nature* **514**, 247–251 (2014).
20. Filippakopoulos, P. et al. Selective inhibition of BET bromodomains. *Nature* **468**, 1067–1073 (2010).
21. Mertz, J. A. et al. Targeting MYC dependence in cancer by inhibiting BET bromodomains. *Proc. Natl Acad. Sci. USA* **108**, 16669–16674 (2011).
22. Park, J. et al. Single-cell transcriptomics of the mouse kidney reveals potential cellular targets of kidney disease. *Science* **360**, 758–763 (2018).
23. Lee, J. E. et al. Brd4 binds to active enhancers to control cell identity gene induction in adipogenesis and myogenesis. *Nat. Commun.* **8**, 2217 (2017).
24. Najafova, Z. et al. BRD4 localization to lineage-specific enhancers is associated with a distinct transcription factor repertoire. *Nucleic Acids Res.* **45**, 127–141 (2017).
25. Ichimura, T., Hung, C. C., Yang, S. A., Stevens, J. L. & Bonventre, J. V. Kidney injury molecule-1: a tissue and urinary biomarker for nephrotoxicant-induced renal injury. *Am. J. Physiol. Ren. Physiol.* **286**, F552–F563 (2004).
26. Mishra, J. et al. Identification of neutrophil gelatinase-associated lipocalin as a novel early urinary biomarker for ischemic renal injury. *J. Am. Soc. Nephrol.* **14**, 2534–2543 (2003).
27. McLean, C. Y. et al. GREAT improves functional interpretation of cis-regulatory regions. *Nat. Biotechnol.* **28**, 495–501 (2010).
28. Yang, L. et al. KIM-1-mediated phagocytosis reduces acute injury to the kidney. *J. Clin. Invest.* **125**, 1620–1636 (2015).
29. Humphreys, B. D. et al. Chronic epithelial kidney injury molecule-1 expression causes murine kidney fibrosis. *J. Clin. Invest.* **123**, 4023–4035 (2013).
30. Whyte, W. A. et al. Master transcription factors and mediator establish super-enhancers at key cell identity genes. *Cell* **153**, 307–319 (2013).
31. Loven, J. et al. Selective inhibition of tumor oncogenes by disruption of super-enhancers. *Cell* **153**, 320–334 (2013).
32. Clissold, R. L., Hamilton, A. J., Hattersley, A. T., Ellard, S. & Bingham, C. HNF1B-associated renal and extra-renal disease-an expanding clinical spectrum. *Nat. Rev. Nephrol.* **11**, 102–112 (2015).
33. Kaminski, M. M. et al. Direct reprogramming of fibroblasts into renal tubular epithelial cells by defined transcription factors. *Nat. Cell Biol.* **18**, 1269–1280 (2016).
34. Marable S. S., Chung E., Adam M., Potter S. S. & Park J. S. Hnf4a deletion in the mouse kidney phenocopies Fanconi renotubular syndrome. *JCI Insight* **3**, e97497 (2018).
35. Zager, R. A. & Johnson, A. C. M. Acute kidney injury induces dramatic p21 upregulation via a novel, glucocorticoid-activated, pathway. *Am. J. Physiol. Renal Physiol.* **316**, F674–f681 (2019).
36. Chen, J., Chen, J. K., Conway, E. M. & Harris, R. C. Survivin mediates renal proximal tubule recovery from AKI. *J. Am. Soc. Nephrol.* **24**, 2023–2033 (2013).
37. Huen, S. C. et al. GM-CSF promotes macrophage alternative activation after renal ischemia/reperfusion injury. *J. Am. Soc. Nephrol.* **26**, 1334–1345 (2015).
38. Chapuy, B. et al. Discovery and characterization of super-enhancer-associated dependencies in diffuse large B cell lymphoma. *Cancer Cell* **24**, 777–790 (2013).
39. Delmore, J. E. et al. BET bromodomain inhibition as a therapeutic strategy to target c-Myc. *Cell* **146**, 904–917 (2011).
40. Winter, G. E. et al. BET bromodomain proteins function as master transcription elongation factors independent of CDK9 recruitment. *Mol. Cell* **67**, 5–18 (2017). e19.
41. Bonventre, J. V. & Yang, L. Cellular pathophysiology of ischemic acute kidney injury. *J. Clin. Invest.* **121**, 4210–4221 (2011).
42. Kumar, S. Cellular and molecular pathways of renal repair after acute kidney injury. *Kidney Int.* **93**, 27–40 (2018).
43. Kanno, T. et al. BRD4 assists elongation of both coding and enhancer RNAs by interacting with acetylated histones. *Nat. Struct. amp; Mol. Biol.* **21**, 1047–1057 (2014).
44. Uhlen, M. et al. Proteomics. Tissue-based map of the human proteome. *Science* **347**, 1260419 (2015).
45. Lemos D. R., et al. Interleukin-1beta activates a MYC-dependent metabolic switch in kidney stromal cells necessary for progressive tubulointerstitial fibrosis. *J Am. Soc. Nephrol.* **29**,1690–1705 (2018).
46. Xiong, C. et al. Pharmacological targeting of BET proteins inhibits renal fibroblast activation and alleviates renal fibrosis. *Oncotarget* **7**, 69291–69308 (2016).
47. Zhou, B. et al. Brd4 inhibition attenuates unilateral ureteral obstruction-induced fibrosis by blocking TGF-beta-mediated Nox4 expression. *Redox Biol.* **11**, 390–402 (2017).
48. Ferenbach, D. A. & Bonventre, J. V. Mechanisms of maladaptive repair after AKI leading to accelerated kidney ageing and CKD. *Nat. Rev. Nephrol.* **11**, 264–276 (2015).
49. Hamilton, A. J. et al. The HNF4A R76W mutation causes atypical dominant Fanconi syndrome in addition to a beta cell phenotype. *J. Med Genet* **51**, 165–169 (2014).
50. Ray, A. & Prefontaine, K. E. Physical association and functional antagonism between the p65 subunit of transcription factor NF-kappa B and the glucocorticoid receptor. *Proc. Natl Acad. Sci. USA* **91**, 752–756 (1994).
51. Shi, J. & Vakoc, C. R. The mechanisms behind the therapeutic activity of BET bromodomain inhibition. *Mol. Cell* **54**, 728–736 (2014).

52. Liu, H. et al. Inhibition of Brd4 alleviates renal ischemia/reperfusion injury-induced apoptosis and endoplasmic reticulum stress by blocking FoxO4-mediated oxidative stress. *Redox Biol.* **24**, 101195 (2019).
53. Wasiak, S. et al. Benefit of apabetalone on plasma proteins in renal disease. *Kidney Int. Rep.* **3**, 711–721 (2018).
54. Zhou, X. et al. Therapeutic targeting of BET bromodomain protein, Brd4, delays cyst growth in ADPKD. *Hum. Mol. Genet.* **24**, 3982–3993 (2015).
55. Suarez-Alvarez, B. et al. Inhibition of bromodomain and extraterminal domain family proteins ameliorates experimental renal damage. *J. Am. Soc. Nephrol.* **28**, 504–519 (2017).
56. Gilan, O. et al. Selective targeting of BD1 and BD2 of the BET proteins in cancer and immunoinflammation. *Science* **368**, 387–394 (2020).
57. Ray, K. K. et al. Effect of selective BET protein inhibitor apabetalone on cardiovascular outcomes in patients with acute coronary syndrome and diabetes: Rationale, design, and baseline characteristics of the BETonMACE trial. *Am. Heart J.* **217**, 72–83 (2019).
58. Shin, H. Y. et al. Hierarchy within the mammary STAT5-driven Wap super-enhancer. *Nat. Genet.* **48**, 904–911 (2016).
59. Dobin, A. et al. STAR: ultrafast universal RNA-seq aligner. *Bioinformatics* **29**, 15–21 (2013).
60. Langmead, B., Trapnell, C., Pop, M. & Salzberg, S. L. Ultrafast and memory-efficient alignment of short DNA sequences to the human genome. *Genome Biol.* **10**, R25 (2009).
61. Heinz, S. et al. Simple combinations of lineage-determining transcription factors prime cis-regulatory elements required for macrophage and B cell identities. *Mol. Cell* **38**, 576–589 (2010).
62. Thorvaldsdottir, H., Robinson, J. T. & Mesirov, J. P. Integrative Genomics Viewer (IGV): high-performance genomics data visualization and exploration. *Brief. Bioinform.* **14**, 178–192 (2013).
63. Ramirez, F., Dundar, F., Diehl, S., Gruning, B. A. & Manke, T. deepTools: a flexible platform for exploring deep-sequencing data. *Nucleic Acids Res* **42**, W187–W191 (2014).
64. Zhang, Y. et al. Model-based analysis of ChIP-Seq (MACS). *Genome Biol.* **9**, R137 (2008).
65. Quinlan, A. R. & Hall, I. M. BEDTools: a flexible suite of utilities for comparing genomic features. *Bioinformatics* **26**, 841–842 (2010).
66. Wickham H. *ggplot2: Elegant Graphics for Data Analysis* (2009).
67. Anders, S., Pyl, P. T. & Huber, W. HTSeq-a Python framework to work with high-throughput sequencing data. *Bioinformatics* **31**, 166–169 (2015).
68. Love, M. I., Huber, W. & Anders, S. Moderated estimation of fold change and dispersion for RNA-seq data with DESeq2. *Genome Biol.* **15**, 550 (2014).

Acknowledgements

This research was supported by a Marie Curie International Outgoing Fellowship within the 7th European Community Framework Programme (#328613) and the Austrian Science Fund (FWF) P30373 to J.W., US National Institutes of Health awards DK039773, DK072381, and TR002155 to J.V.B. and through the Intramural Research Programs of NIDDK/NIH (MW, HKL, LH). This work utilized the computational resources of the NIH HPC Biowulf cluster. (http://hpc.nih.gov).

Author contributions

J.W., L.H., and J.V.B. designed the experiments, and J.W. carried out the majority of the experiments. M.W. and HK.L. performed the computational analyses, and H.O., J.J., and T.I. performed immunofluorescence staining of some of the samples. M.T.V. contributed important insights and helped with data interpretation. R.E. reviewed the paper. J.W., M.W., and J.V.B. wrote the paper. All authors carefully reviewed the manuscript.

Competing interests

J.V.B. is co-inventor on KIM-1 patents assigned to Partners Healthcare. He is co-founder of Goldfinch Bio. He is a consultant for Cadent, Aldeyra and an advisor with equity in Medibeacon Inc, Rubius, Theravance, Goldilocks, DxNow, and Sentien. All other authors have no competing interests.

Additional information

Supplementary information is available for this paper at https://doi.org/10.1038/s41467-020-17205-5.

Correspondence and requests for materials should be addressed to J.W. or J.V.B.

Peer review information *Nature Communications* thanks the anonymous reviewer(s) for their contribution to the peer review of this work. Peer reviewer reports are available.

Reprints and permission information is available at http://www.nature.com/reprints

Publisher's note Springer Nature remains neutral with regard to jurisdictional claims in published maps and institutional affiliations.

Discussion

1. Changes in global transcriptional regulation in renal tubular epithelial cells

Both publications included in this thesis delve into the transcriptional regulation in murine or human renal epithelium, altered after inducing injury or cytokine stimulation. They deliver much needed insight into kidney epigenetic landscape. The genomic datasets provided by us are of immense utility, as amount of kidney data is overshadowed by other organs such as brain, liver or heart in repositories like ENCODE (Luo et al., 2020). They have unique value as a fundament for future comparative analyses, as the worth of the genomic data increases exponentially the more similar datasets are available, allowing for exploration of the differences between conditions and treatments. The data presented here can also easily stand on their own and many new pieces of information can be learned from our experiments alone.

2. Cytokine stimulation of human RTEC

2.1. Renal dACE2

Our study was the first to describe the human renal dACE2 locus in detail. This alternative, interferon-inducible, short *ACE2* isoform did not gain recognition until mid-2020, when it was first reported in a pre-print repository publication (Onabajo et al., 2020). This is despite ACE2 playing a regulatory role on the crossroads of several vital processes and being known as a potential receptor for coronaviruses. Western blot remains the prevalent method of protein detection in the literature, but very few pre-pandemic publications report an ACE2 variant approximately 50 kDa in size. Even then it is usually dismissed as a product of proteolysis (Gutta et al., 2018). Additionally, since ACE2 protein has an expected size of 100 kDa, the common practice of cropping non-specific bands to show only the predicted protein sizes, even when not malicious, has contributed to this delayed detection.

The discovery was likely further slowed down by the unknown function of dACE2. It lacks the extracellular catalytic domain making the full-length protein a coronavirus target, thus its expression must have a different role. It was proposed to be a part of antiviral response (Mpekoulis

et al., 2021), more generalized IFN-induced inflammation (Bitossi et al., 2021), or to not have a distinct function at all (Oliveto et al., 2022). The last option is not likely, as dACE2, in addition to being interferon-responsive and present in a wide variety of cancer cells, has been reported to be abundantly expressed in healthy pancreatic β-cells and as having a defined expression pattern on human spermatozoa (Fignani et al., 2020; Ramal-Sanchez et al., 2022). Whatever its role may be, if not for genomic studies such as ours, the existence of dACE2 would stay hidden even longer.

Our research is an example showing how little we understand about epigenetic regulation of genes that we know take part in vital homeostatic processes. Comparing our data to other organs, such as the lung, we were able to propose tissue-preferential putative enhancers surrounding ACE2 locus in human epithelial cells (Lee et al., 2021). Collectrin, an ACE2 homologue located upstream of the gene, is co-regulated by interferons in the kidney and the lung, but not in the liver. Further dissection of enhancer elements driving this tandem upregulation of expression might shed additional light at blood pressure regulation in an inflammatory setting (Chu & Le, 2014).

2.2. Interferon stimulation of RTEC

One of the main impulses to perform our study was a report of interferons increasing *ACE2* expression. This would complicate using interferons as therapeutic agents, as they could increase the quantity of the viral receptor (Ziegler et al., 2020). As it was reported several months later, it was the then-unknown dACE2 which prompted the change in expression independently of full-length ACE2. Currently, the efficacy of interferons in COVID-19 therapy is uncertain, as the result of clinical trials range from positive recommendations (Alavi Darazam et al., 2021) to neutral and negative (Consortium et al., 2021; Kalil et al., 2021). Regardless, interferons are a key part of immune response expressed by inflammatory milieu. Despite that, detailed information about the epigenetic changes stimulated by common immune mediators is scarce.

Our dataset allowed us a direct comparison of RNA-seq results with only two other human tissues treated with the same cytokine concentrations for the same period. We were able to find a subset of genes upregulated after IFNβ stimulation in kidney, lung and liver, forming a core epithelial interferon response to be investigated in future research. Additionally, a large subset of IFN-induced genes was kidney-specific and enriched in genes key for epithelial-mesenchymal transition and immune signaling pathways such as complement. Interferons themselves had an unexpectedly distinct impact on the RTEC gene expression, despite us finding strong overlaps as

well. Deciphering the common and unique transcriptional trends of processes such as inflammation will lead to development of new approaches to systemic or targeted medicine. To illustrate this principle, we also compared interferon stimulation to severe COVID-19 and renal ischemia-reperfusion, surprisingly finding larger overlap of upregulated genes with injury. This approach may partially mitigate the multifactorial nature of AKI preventing therapy development, though it has its caveats. What may be common for two kidney injury triggers, might not be for the third. To increase our predictive power, we simply need more data. As of now, attempts to find ChIP-seq information relating to COVID-19 and the kidney in the arguably largest genomic dataset repository, Gene Expression Omnibus (GEO), yield only our study (Edgar et al., 2002).

3. Epigenetic landscape of murine kidney

3.1. Enhancer loss and activation in murine kidney injury

The murine changes in epigenetic landscape, though easier to investigate, are no less complex than the human. Fortunately, mouse models remain an excellent tool allowing for dissection of mechanisms governing both renal homeostasis and disease (Kuure & Sariola, 2020; Rabe & Schaefer, 2016). It is also important to remember that despite numerous transpositions and other DNA re-shuffling, mouse and human DNA contain abundance of conserved regions (Lund et al., 2000). Curiously, those conserved regions might play different roles in different species, further pointing out the need of experimental validation of all cis-regulatory element findings (Yan et al., 1997).

Such individual validation is only possible due to studies like ours, adapting a multi-modal approach to investigation and prediction of key cis-regulatory elements. Majority of the published manuscripts rely on ATAC-seq or detection of DNase Hypersensitive Sites (DHS), often paired with RNA-seq (Morabito et al., 2021; Wu et al., 2016). This only illustrates the open transcriptional windows, without allowing for detailed distinction of, for example, gene promoters versus putative enhancers. In our study, we visualize thousands of enhancers gaining or losing function after renal injury. Several of those candidate enhancer elements are located near known renal injury markers, such as *Havcr1*, *Kl* and *Slc34a1*. This confirms our accuracy and suggests that investigating the others may yield yet unknown AKI regulators. Additionally, we indicate several transcription factors which drive this epigenetic shift. Among them are the hepatic nuclear factor 4a (HNF4a), glucocorticoid receptor (GR), Fos-related antigens (FRA1, FOSL), and Signal Transducer and

Activator of Transcription proteins (STATs). They are promising therapeutic targets, as JAK/STAT pathway inhibitors are already in clinical use and several other TF inhibitors are currently being tested in clinical trials or and are commercially available for laboratory testing (Debono et al., 2013; Kiselyuk et al., 2012; Serra Lopez-Matencio et al., 2019).

3.2. BET inhibition in renal injury

Bromodomain and Extraterminal protein (BET) inhibition was also a subject of multiple clinical trials (Bechter & Schoffski, 2020). BET proteins act as chromatin readers by interacting with acetylated histones. With the exception of one study investigating Fabry disease, all the remaining studies currently registered in the NIH's clinical trial database concern cancer. BET inhibitors were tested in clinical trials aiming to treat a range of kidney conditions, but no BET inhibitors were approved by large regulatory bodies like the FDA (Food and Drug Administration) or EMA (European Medicines Agency). They were reported to delay polycystic kidney disease development, attenuate fibrosis and prevent hyperuricemic injury (Xiong et al., 2021; Xiong et al., 2016; Zhou et al., 2015).

Our study shows the importance of an additional factor, timing. While early treatment caused increased mortality in mice, most likely due to impaired repair mechanisms, later application helped ameliorate renal fibrosis. This was accompanied by more shifts in epigenetic landscape, clearly painting its picture as a very dynamic process. Unfortunately, this also confounds any future clinical studies on AKI. While systemic administration of BET inhibitors may aid patients with isolated, resolving AKI, global attenuation of BET activity or drug interactions may lead to unforeseen side-effects and toxicity in patients suffering from comorbidities (Doroshow et al., 2017). Therefore, discerning the exact epigenetic changes made by this class of drugs is vital for their future use in AKI or CKD treatment.

4. Conclusions

In this thesis, we provide novel insights into epigenetic regulation of kidney epithelial cells. We begin by dissecting the genetic locus of *ACE2*, a receptor key for viral entry in the current SARS-CoV-2 pandemic. We demonstrate how little is known about cis-regulatory elements present in known disease factor locus, how it differs compared to the lung and we propose promoter and enhancer elements of the recently discovered, interferon-inducible short isoform *dACE2*. Further, we broaden the scope of the interferon stimulation research to global RNA-seq analysis and line up our results with different tissues and disease conditions to build a foundation for investigation of shared and unique gene expression patterns. Next, we present the shifts in epigenetic landscape of murine kidney in an ischemia-reperfusion model of acute kidney injury. We show the thousands of cis-regulatory elements gaining and losing their activity and propose transcription factors driving these changes. We also manipulate this process using pharmaceutical inhibition of BET proteins, showing the deleterious results of stopping early repair programs and the benefits of fibrosis attenuation. Taken together, those results pave the way for enhanced understanding of renal epithelial transcriptome and form a new cornerstone for future data to be compared and related to. We believe that this work will contribute to development of therapeutic strategies aiming at the source of kidney disease: the epigenetic changes governing gene expression.

References

Abbate, M., Rottoli, D., & Gianatti, A. (2020). COVID-19 Attacks the Kidney: Ultrastructural Evidence for the Presence of Virus in the Glomerular Epithelium. *Nephron*, *144*(7), 341-342. https://doi.org/10.1159/000508430

Ahmadian, E., Hosseiniyan Khatibi, S. M., Razi Soofiyani, S., Abediazar, S., Shoja, M. M., Ardalan, M., & Zununi Vahed, S. (2021). Covid-19 and kidney injury: Pathophysiology and molecular mechanisms. *Rev Med Virol*, *31*(3), e2176. https://doi.org/10.1002/rmv.2176

Alavi Darazam, I., Shokouhi, S., Pourhoseingholi, M. A., Naghibi Irvani, S. S., Mokhtari, M., Shabani, M., Amirdosara, M., Torabinavid, P., Golmohammadi, M., Hashemi, S., Azimi, A., Jafarazadeh Maivan, M. H., Rezaei, O., Zali, A., Hajiesmaeili, M., Shabanpour Dehbsneh, H., Hoseyni Kusha, A., Taleb Shoushtari, M., Khalili, N., . . . Khoshkar, A. (2021). Role of interferon therapy in severe COVID-19: the COVIFERON randomized controlled trial. *Sci Rep*, *11*(1), 8059. https://doi.org/10.1038/s41598-021-86859-y

Anders, H. J., Huber, T. B., Isermann, B., & Schiffer, M. (2018). CKD in diabetes: diabetic kidney disease versus nondiabetic kidney disease. *Nat Rev Nephrol*, *14*(6), 361-377. https://doi.org/10.1038/s41581-018-0001-y

Atkinson, M. A., & Warady, B. A. (2018). Anemia in chronic kidney disease. *Pediatr Nephrol*, *33*(2), 227-238. https://doi.org/10.1007/s00467-017-3663-y

Bar-On, Y. M., Flamholz, A., Phillips, R., & Milo, R. (2020). SARS-CoV-2 (COVID-19) by the numbers. *Elife*, *9*. https://doi.org/10.7554/eLife.57309

Barutcu, A. R., Maass, P. G., Lewandowski, J. P., Weiner, C. L., & Rinn, J. L. (2018). A TAD boundary is preserved upon deletion of the CTCF-rich Firre locus. *Nat Commun*, *9*(1), 1444. https://doi.org/10.1038/s41467-018-03614-0

Bechter, O., & Schoffski, P. (2020). Make your best BET: The emerging role of BET inhibitor treatment in malignant tumors. *Pharmacol Ther*, *208*, 107479. https://doi.org/10.1016/j.pharmthera.2020.107479

Best Rocha, A., Stroberg, E., Barton, L. M., Duval, E. J., Mukhopadhyay, S., Yarid, N., Caza, T., Wilson, J. D., Kenan, D. J., Kuperman, M., Sharma, S. G., & Larsen, C. P. (2020). Detection of SARS-CoV-2 in

formalin-fixed paraffin-embedded tissue sections using commercially available reagents. *Lab Invest*, *100*(11), 1485-1489. https://doi.org/10.1038/s41374-020-0464-x

Bitossi, C., Frasca, F., Viscido, A., Oliveto, G., Scordio, M., Belloni, L., Cimino, G., Pietropaolo, V., Gentile, M., d'Ettorre, G., Midulla, F., Trancassini, M., Antonelli, G., Pierangeli, A., & Scagnolari, C. (2021). SARS-CoV-2 Entry Genes Expression in Relation with Interferon Response in Cystic Fibrosis Patients. *Microorganisms*, *9*(1). https://doi.org/10.3390/microorganisms9010093

Bolisetty, S., & Agarwal, A. (2009). Neutrophils in acute kidney injury: not neutral any more. *Kidney Int*, *75*(7), 674-676. https://doi.org/10.1038/ki.2008.689

Bouquegneau, A., Erpicum, P., Grosch, S., Habran, L., Hougrand, O., Huart, J., Krzesinski, J. M., Misset, B., Hayette, M. P., Delvenne, P., Bovy, C., Kylies, D., Huber, T. B., Puelles, V. G., Delanaye, P., & Jouret, F. (2021). COVID-19-associated Nephropathy Includes Tubular Necrosis and Capillary Congestion, with Evidence of SARS-CoV-2 in the Nephron. *Kidney360*, *2*(4), 639-652. https://doi.org/10.34067/KID.0006992020

Bowe, B., Xie, Y., Xu, E., & Al-Aly, Z. (2021). Kidney Outcomes in Long COVID. *J Am Soc Nephrol*, *32*(11), 2851-2862. https://doi.org/10.1681/ASN.2021060734

Cantuti-Castelvetri, L., Ojha, R., Pedro, L. D., Djannatian, M., Franz, J., Kuivanen, S., van der Meer, F., Kallio, K., Kaya, T., Anastasina, M., Smura, T., Levanov, L., Szirovicza, L., Tobi, A., Kallio-Kokko, H., Osterlund, P., Joensuu, M., Meunier, F. A., Butcher, S. J., . . . Simons, M. (2020). Neuropilin-1 facilitates SARS-CoV-2 cell entry and infectivity. *Science*, *370*(6518), 856-860. https://doi.org/10.1126/science.abd2985

Cassol, C. A., Gokden, N., Larsen, C. P., & Bourne, T. D. (2020). Appearances Can Be Deceiving - Viral-like Inclusions in COVID-19 Negative Renal Biopsies by Electron Microscopy. *Kidney360*, *1*(8), 824-828. https://doi.org/10.34067/KID.0002692020

Castellano, G., Franzin, R., Sallustio, F., Stasi, A., Banelli, B., Romani, M., De Palma, G., Lucarelli, G., Divella, C., Battaglia, M., Crovace, A., Staffieri, F., Grandaliano, G., Stallone, G., Ditonno, P., Cravedi, P., Cantaluppi, V., & Gesualdo, L. (2019). Complement component C5a induces aberrant epigenetic modifications in renal tubular epithelial cells accelerating senescence by Wnt4/betacatenin signaling after ischemia/reperfusion injury. *Aging (Albany NY)*, *11*(13), 4382-4406. https://doi.org/10.18632/aging.102059

Chagnac, A., Zingerman, B., Rozen-Zvi, B., & Herman-Edelstein, M. (2019). Consequences of Glomerular Hyperfiltration: The Role of Physical Forces in the Pathogenesis of Chronic Kidney Disease in Diabetes and Obesity. *Nephron*, *143*(1), 38-42. https://doi.org/10.1159/000499486

Cheng, A. Y., Sloan, L., & Anderson, J. (2021). Management of Type 2 Diabetes in People With Renal Impairment. *J Fam Pract*, *70*(4 Suppl). https://doi.org/10.12788/jfp.0212

Chesnaye, N. C., van Stralen, K. J., Bonthuis, M., Harambat, J., Groothoff, J. W., & Jager, K. J. (2018). Survival in children requiring chronic renal replacement therapy. *Pediatr Nephrol*, *33*(4), 585-594. https://doi.org/10.1007/s00467-017-3681-9

Chu, C. D., Powe, N. R., McCulloch, C. E., Crews, D. C., Han, Y., Bragg-Gresham, J. L., Saran, R., Koyama, A., Burrows, N. R., Tuot, D. S., Centers for Disease, C., & Prevention Chronic Kidney Disease Surveillance, T. (2021). Trends in Chronic Kidney Disease Care in the US by Race and Ethnicity, 2012-2019. *JAMA Netw Open*, *4*(9), e2127014. https://doi.org/10.1001/jamanetworkopen.2021.27014

Chu, P. L., & Le, T. H. (2014). Role of collectrin, an ACE2 homologue, in blood pressure homeostasis. *Curr Hypertens Rep*, *16*(11), 490. https://doi.org/10.1007/s11906-014-0490-4

Consortium, W. H. O. S. T., Pan, H., Peto, R., Henao-Restrepo, A. M., Preziosi, M. P., Sathiyamoorthy, V., Abdool Karim, Q., Alejandria, M. M., Hernandez Garcia, C., Kieny, M. P., Malekzadeh, R., Murthy, S., Reddy, K. S., Roses Periago, M., Abi Hanna, P., Ader, F., Al-Bader, A. M., Alhasawi, A., Allum, E., . . . Swaminathan, S. (2021). Repurposed Antiviral Drugs for Covid-19 - Interim WHO Solidarity Trial Results. *N Engl J Med*, *384*(6), 497-511. https://doi.org/10.1056/NEJMoa2023184

Corman, V. M., Muth, D., Niemeyer, D., & Drosten, C. (2018). Hosts and Sources of Endemic Human Coronaviruses. *Adv Virus Res*, *100*, 163-188. https://doi.org/10.1016/bs.aivir.2018.01.001

Coskun, Z. M., Ersoz, M., Adas, M., Hancer, V. S., Boysan, S. N., Gonen, M. S., & Acar, A. (2019). Kruppel-Like Transcription Factor-4 Gene Expression and DNA Methylation Status in Type 2 Diabetes and Diabetic Nephropathy Patients. *Arch Med Res*, *50*(3), 91-97. https://doi.org/10.1016/j.arcmed.2019.05.012

Cullis, B., Al-Hwiesh, A., Kilonzo, K., McCulloch, M., Niang, A., Nourse, P., Parapiboon, W., Ponce, D., & Finkelstein, F. O. (2021). ISPD guidelines for peritoneal dialysis in acute kidney injury: 2020 update (adults). *Perit Dial Int*, *41*(1), 15-31. https://doi.org/10.1177/0896860820970834

Danser, A. H., van Kats, J. P., Admiraal, P. J., Derkx, F. H., Lamers, J. M., Verdouw, P. D., Saxena, P. R., & Schalekamp, M. A. (1994). Cardiac renin and angiotensins. Uptake from plasma versus in situ synthesis. *Hypertension*, *24*(1), 37-48. https://doi.org/10.1161/01.hyp.24.1.37

Debono, M., Chadarevian, R., Eastell, R., Ross, R. J., & Newell-Price, J. (2013). Mifepristone reduces insulin resistance in patient volunteers with adrenal incidentalomas that secrete low levels of cortisol: a pilot study. *PLoS One*, *8*(4), e60984. https://doi.org/10.1371/journal.pone.0060984

Deichmann, U. (2016). Epigenetics: The origins and evolution of a fashionable topic. *Dev Biol*, *416*(1), 249-254. https://doi.org/10.1016/j.ydbio.2016.06.005

Diao, B., Wang, C., Wang, R., Feng, Z., Zhang, J., Yang, H., Tan, Y., Wang, H., Wang, C., Liu, L., Liu, Y., Liu, Y., Wang, G., Yuan, Z., Hou, X., Ren, L., Wu, Y., & Chen, Y. (2021). Human kidney is a target for novel severe acute respiratory syndrome coronavirus 2 infection. *Nat Commun*, *12*(1), 2506. https://doi.org/10.1038/s41467-021-22781-1

Donoghue, M., Hsieh, F., Baronas, E., Godbout, K., Gosselin, M., Stagliano, N., Donovan, M., Woolf, B., Robison, K., Jeyaseelan, R., Breitbart, R. E., & Acton, S. (2000). A novel angiotensin-converting enzyme-related carboxypeptidase (ACE2) converts angiotensin I to angiotensin 1-9. *Circ Res*, *87*(5), E1-9. https://doi.org/10.1161/01.res.87.5.e1

Doroshow, D. B., Eder, J. P., & LoRusso, P. M. (2017). BET inhibitors: a novel epigenetic approach. *Ann Oncol*, *28*(8), 1776-1787. https://doi.org/10.1093/annonc/mdx157

Ebert, T., Pawelzik, S. C., Witasp, A., Arefin, S., Hobson, S., Kublickiene, K., Shiels, P. G., Back, M., & Stenvinkel, P. (2020). Inflammation and Premature Ageing in Chronic Kidney Disease. *Toxins (Basel)*, *12*(4). https://doi.org/10.3390/toxins12040227

Edeling, M., Ragi, G., Huang, S., Pavenstadt, H., & Susztak, K. (2016). Developmental signalling pathways in renal fibrosis: the roles of Notch, Wnt and Hedgehog. *Nat Rev Nephrol*, *12*(7), 426-439. https://doi.org/10.1038/nrneph.2016.54

Edgar, R., Domrachev, M., & Lash, A. E. (2002). Gene Expression Omnibus: NCBI gene expression and hybridization array data repository. *Nucleic Acids Res*, *30*(1), 207-210. https://doi.org/10.1093/nar/30.1.207

El-Achkar, T. M., & Dagher, P. C. (2015). Tubular cross talk in acute kidney injury: a story of sense and sensibility. *Am J Physiol Renal Physiol*, *308*(12), F1317-1323. https://doi.org/10.1152/ajprenal.00030.2015

Fenrich, M., Mrdenovic, S., Balog, M., Tomic, S., Zjalic, M., Roncevic, A., Mandic, D., Debeljak, Z., & Heffer, M. (2020). SARS-CoV-2 Dissemination Through Peripheral Nerves Explains Multiple Organ Injury. *Front Cell Neurosci*, *14*, 229. https://doi.org/10.3389/fncel.2020.00229

Fignani, D., Licata, G., Brusco, N., Nigi, L., Grieco, G. E., Marselli, L., Overbergh, L., Gysemans, C., Colli, M. L., Marchetti, P., Mathieu, C., Eizirik, D. L., Sebastiani, G., & Dotta, F. (2020). SARS-CoV-2 Receptor Angiotensin I-Converting Enzyme Type 2 (ACE2) Is Expressed in Human Pancreatic beta-Cells and in the Human Pancreas Microvasculature. *Front Endocrinol (Lausanne)*, *11*, 596898. https://doi.org/10.3389/fendo.2020.596898

Flores-Munoz, M., Smith, N. J., Haggerty, C., Milligan, G., & Nicklin, S. A. (2011). Angiotensin1-9 antagonises pro-hypertrophic signalling in cardiomyocytes via the angiotensin type 2 receptor. *J Physiol*, *589*(Pt 4), 939-951. https://doi.org/10.1113/jphysiol.2010.203075

Galang, G., Mandla, R., Ruan, H., Jung, C., Sinha, T., Stone, N. R., Wu, R. S., Mannion, B. J., Allu, P. K. R., Chang, K., Rammohan, A., Shi, M. B., Pennacchio, L. A., Black, B. L., & Vedantham, V. (2020). ATAC-Seq Reveals an Isl1 Enhancer That Regulates Sinoatrial Node Development and Function. *Circ Res*, *127*(12), 1502-1518. https://doi.org/10.1161/CIRCRESAHA.120.317145

Giri, A. K., & Aittokallio, T. (2019). DNMT Inhibitors Increase Methylation in the Cancer Genome. *Front Pharmacol*, *10*, 385. https://doi.org/10.3389/fphar.2019.00385

Gironacci, M. M. (2015). Angiotensin-(1-7): beyond its central effects on blood pressure. *Ther Adv Cardiovasc Dis*, *9*(4), 209-216. https://doi.org/10.1177/1753944715599875

Glick, D., Barth, S., & Macleod, K. F. (2010). Autophagy: cellular and molecular mechanisms. *J Pathol*, *221*(1), 3-12. https://doi.org/10.1002/path.2697

Godwin, J. G., Ge, X., Stephan, K., Jurisch, A., Tullius, S. G., & Iacomini, J. (2010). Identification of a microRNA signature of renal ischemia reperfusion injury. *Proc Natl Acad Sci U S A*, *107*(32), 14339-14344. https://doi.org/10.1073/pnas.0912701107

Gollin, S. M. (2004). Chromosomal instability. *Curr Opin Oncol*, *16*(1), 25-31. https://doi.org/10.1097/00001622-200401000-00006

Guan, Q., Nguan, C. Y., & Du, C. (2010). Expression of transforming growth factor-beta1 limits renal ischemia-reperfusion injury. *Transplantation*, *89*(11), 1320-1327. https://doi.org/10.1097/TP.0b013e3181d8e9dc

Gutta, S., Grobe, N., Kumbaji, M., Osman, H., Saklayen, M., Li, G., & Elased, K. M. (2018). Increased urinary angiotensin converting enzyme 2 and neprilysin in patients with type 2 diabetes. *Am J Physiol Renal Physiol*, *315*(2), F263-F274. https://doi.org/10.1152/ajprenal.00565.2017

Heintzman, N. D., Stuart, R. K., Hon, G., Fu, Y., Ching, C. W., Hawkins, R. D., Barrera, L. O., Van Calcar, S., Qu, C., Ching, K. A., Wang, W., Weng, Z., Green, R. D., Crawford, G. E., & Ren, B. (2007). Distinct and predictive chromatin signatures of transcriptional promoters and enhancers in the human genome. *Nat Genet*, *39*(3), 311-318. https://doi.org/10.1038/ng1966

Himmelfarb, J., McMonagle, E., Freedman, S., Klenzak, J., McMenamin, E., Le, P., Pupim, L. B., Ikizler, T. A., & The, P. G. (2004). Oxidative stress is increased in critically ill patients with acute renal failure. *J Am Soc Nephrol*, *15*(9), 2449-2456. https://doi.org/10.1097/01.ASN.0000138232.68452.3B

Hod, T., & Goldfarb-Rumyantzev, A. S. (2015). Clinical issues in renal transplantation in the elderly. *Clin Transplant*, *29*(2), 167-175. https://doi.org/10.1111/ctr.12481

Hoffmann, M. J., & Schulz, W. A. (2005). Causes and consequences of DNA hypomethylation in human cancer. *Biochem Cell Biol*, *83*(3), 296-321. https://doi.org/10.1139/o05-036

Hommos, M. S., Glassock, R. J., & Rule, A. D. (2017). Structural and Functional Changes in Human Kidneys with Healthy Aging. *J Am Soc Nephrol*, *28*(10), 2838-2844. https://doi.org/10.1681/ASN.2017040421

Hoste, E. A. J., Kellum, J. A., Selby, N. M., Zarbock, A., Palevsky, P. M., Bagshaw, S. M., Goldstein, S. L., Cerda, J., & Chawla, L. S. (2018). Global epidemiology and outcomes of acute kidney injury. *Nat Rev Nephrol*, *14*(10), 607-625. https://doi.org/10.1038/s41581-018-0052-0

Hyndman, K. A., Kasztan, M., Mendoza, L. D., & Monteiro-Pai, S. (2019). Dynamic changes in histone deacetylases following kidney ischemia-reperfusion injury are critical for promoting proximal tubule proliferation. *Am J Physiol Renal Physiol*, *316*(5), F875-F888. https://doi.org/10.1152/ajprenal.00499.2018

Ikizler, T. A., Burrowes, J. D., Byham-Gray, L. D., Campbell, K. L., Carrero, J. J., Chan, W., Fouque, D., Friedman, A. N., Ghaddar, S., Goldstein-Fuchs, D. J., Kaysen, G. A., Kopple, J. D., Teta, D., Yee-Moon Wang, A., & Cuppari, L. (2020). KDOQI Clinical Practice Guideline for Nutrition in CKD: 2020 Update. *Am J Kidney Dis*, *76*(3 Suppl 1), S1-S107. https://doi.org/10.1053/j.ajkd.2020.05.006

Jean, G., Souberbielle, J. C., & Chazot, C. (2017). Vitamin D in Chronic Kidney Disease and Dialysis Patients. *Nutrients*, *9*(4). https://doi.org/10.3390/nu9040328

Jia, H. P., Look, D. C., Shi, L., Hickey, M., Pewe, L., Netland, J., Farzan, M., Wohlford-Lenane, C., Perlman, S., & McCray, P. B., Jr. (2005). ACE2 receptor expression and severe acute respiratory syndrome coronavirus infection depend on differentiation of human airway epithelia. *J Virol*, *79*(23), 14614-14621. https://doi.org/10.1128/JVI.79.23.14614-14621.2005

Kalaitzidis, R. G., & Elisaf, M. S. (2018). Treatment of Hypertension in Chronic Kidney Disease. *Curr Hypertens Rep*, *20*(8), 64. https://doi.org/10.1007/s11906-018-0864-0

Kalil, A. C., Mehta, A. K., Patterson, T. F., Erdmann, N., Gomez, C. A., Jain, M. K., Wolfe, C. R., Ruiz-Palacios, G. M., Kline, S., Regalado Pineda, J., Luetkemeyer, A. F., Harkins, M. S., Jackson, P. E. H., Iovine, N. M., Tapson, V. F., Oh, M. D., Whitaker, J. A., Mularski, R. A., Paules, C. I., . . . members, A.-s. g. (2021). Efficacy of interferon beta-1a plus remdesivir compared with remdesivir alone in

hospitalised adults with COVID-19: a double-bind, randomised, placebo-controlled, phase 3 trial. *Lancet Respir Med*, *9*(12), 1365-1376. https://doi.org/10.1016/S2213-2600(21)00384-2

Kawachi, H., & Fukusumi, Y. (2020). New insight into podocyte slit diaphragm, a therapeutic target of proteinuria. *Clin Exp Nephrol*, *24*(3), 193-204. https://doi.org/10.1007/s10157-020-01854-3

Khraiwesh, B., Arif, M. A., Seumel, G. I., Ossowski, S., Weigel, D., Reski, R., & Frank, W. (2010). Transcriptional control of gene expression by microRNAs. *Cell*, *140*(1), 111-122. https://doi.org/10.1016/j.cell.2009.12.023

Kipari, T., & Hughes, J. (2002). Macrophage-mediated renal cell death. *Kidney Int*, *61*(2), 760-761. https://doi.org/10.1046/j.1523-1755.2002.00180.x

Kiselyuk, A., Lee, S. H., Farber-Katz, S., Zhang, M., Athavankar, S., Cohen, T., Pinkerton, A. B., Ye, M., Bushway, P., Richardson, A. D., Hostetler, H. A., Rodriguez-Lee, M., Huang, L., Spangler, B., Smith, L., Higginbotham, J., Cashman, J., Freeze, H., Itkin-Ansari, P., . . . Levine, F. (2012). HNF4alpha antagonists discovered by a high-throughput screen for modulators of the human insulin promoter. *Chem Biol*, *19*(7), 806-818. https://doi.org/10.1016/j.chembiol.2012.05.014

Krivega, I., & Dean, A. (2012). Enhancer and promoter interactions-long distance calls. *Curr Opin Genet Dev*, *22*(2), 79-85. https://doi.org/10.1016/j.gde.2011.11.001

Ku, E., Lee, B. J., Wei, J., & Weir, M. R. (2019). Hypertension in CKD: Core Curriculum 2019. *Am J Kidney Dis*, *74*(1), 120-131. https://doi.org/10.1053/j.ajkd.2018.12.044

Kurzhagen, J. T., Dellepiane, S., Cantaluppi, V., & Rabb, H. (2020). AKI: an increasingly recognized risk factor for CKD development and progression. *J Nephrol*, *33*(6), 1171-1187. https://doi.org/10.1007/s40620-020-00793-2

Kuure, S., & Sariola, H. (2020). Mouse Models of Congenital Kidney Anomalies. *Adv Exp Med Biol*, *1236*, 109-136. https://doi.org/10.1007/978-981-15-2389-2_5

Kwong, Y. D., & Liu, K. D. (2017). AKI Adjudication: Do We Need It. *Nephron*, *137*(4), 294-296. https://doi.org/10.1159/000477831

Lanni, S., Goracci, M., Borrelli, L., Mancano, G., Chiurazzi, P., Moscato, U., Ferre, F., Helmer-Citterich, M., Tabolacci, E., & Neri, G. (2013). Role of CTCF protein in regulating FMR1 locus transcription. *PLoS Genet*, *9*(7), e1003601. https://doi.org/10.1371/journal.pgen.1003601

Lee, H. K., Jung, O., & Hennighausen, L. (2021). JAK inhibitors dampen activation of interferon-stimulated transcription of ACE2 isoforms in human airway epithelial cells. *Commun Biol*, *4*(1), 654. https://doi.org/10.1038/s42003-021-02167-1

Lee, H. K., Willi, M., Wang, C., Yang, C. M., Smith, H. E., Liu, C., & Hennighausen, L. (2017). Functional assessment of CTCF sites at cytokine-sensing mammary enhancers using CRISPR/Cas9 gene editing in mice. *Nucleic Acids Res*, *45*(8), 4606-4618. https://doi.org/10.1093/nar/gkx185

Li, M. Y., Li, L., Zhang, Y., & Wang, X. S. (2020). Expression of the SARS-CoV-2 cell receptor gene ACE2 in a wide variety of human tissues. *Infect Dis Poverty*, *9*(1), 45. https://doi.org/10.1186/s40249-020-00662-x

Li, W., Moore, M. J., Vasilieva, N., Sui, J., Wong, S. K., Berne, M. A., Somasundaran, M., Sullivan, J. L., Luzuriaga, K., Greenough, T. C., Choe, H., & Farzan, M. (2003). Angiotensin-converting enzyme 2 is a functional receptor for the SARS coronavirus. *Nature*, *426*(6965), 450-454. https://doi.org/10.1038/nature02145

Li, Z., Lu, X., Liu, Y., Zhao, J., Ma, S., Yin, H., Huang, S., Zhao, Y., & He, X. (2021). Gain of LINC00624 Enhances Liver Cancer Progression by Disrupting the Histone Deacetylase 6/Tripartite Motif Containing 28/Zinc Finger Protein 354C Corepressor Complex. *Hepatology*, *73*(5), 1764-1782. https://doi.org/10.1002/hep.31530

Lin, F., Wang, Z. V., & Hill, J. A. (2014). Seeing is believing: dynamic changes in renal epithelial autophagy during injury and repair. *Autophagy*, *10*(4), 691-693. https://doi.org/10.4161/auto.27749

Lomvardas, S., Barnea, G., Pisapia, D. J., Mendelsohn, M., Kirkland, J., & Axel, R. (2006). Interchromosomal interactions and olfactory receptor choice. *Cell*, *126*(2), 403-413. https://doi.org/10.1016/j.cell.2006.06.035

Long, H. K., Osterwalder, M., Welsh, I. C., Hansen, K., Davies, J. O. J., Liu, Y. E., Koska, M., Adams, A. T., Aho, R., Arora, N., Ikeda, K., Williams, R. M., Sauka-Spengler, T., Porteus, M. H., Mohun, T., Dickel, D. E., Swigut, T., Hughes, J. R., Higgs, D. R., . . . Wysocka, J. (2020). Loss of Extreme Long-Range Enhancers in Human Neural Crest Drives a Craniofacial Disorder. *Cell Stem Cell*, *27*(5), 765-783 e714. https://doi.org/10.1016/j.stem.2020.09.001

Lorenzen, J. M., Kaucsar, T., Schauerte, C., Schmitt, R., Rong, S., Hubner, A., Scherf, K., Fiedler, J., Martino, F., Kumarswamy, R., Kolling, M., Sorensen, I., Hinz, H., Heineke, J., van Rooij, E., Haller, H., & Thum, T. (2014). MicroRNA-24 antagonism prevents renal ischemia reperfusion injury. *J Am Soc Nephrol*, *25*(12), 2717-2729. https://doi.org/10.1681/ASN.2013121329

Luger, K., Dechassa, M. L., & Tremethick, D. J. (2012). New insights into nucleosome and chromatin structure: an ordered state or a disordered affair? *Nat Rev Mol Cell Biol*, *13*(7), 436-447. https://doi.org/10.1038/nrm3382

Lund, J., Chen, F., Hua, A., Roe, B., Budarf, M., Emanuel, B. S., & Reeves, R. H. (2000). Comparative sequence analysis of 634 kb of the mouse chromosome 16 region of conserved synteny with the human velocardiofacial syndrome region on chromosome 22q11.2. *Genomics*, *63*(3), 374-383. https://doi.org/10.1006/geno.1999.6044

Luo, Y., Hitz, B. C., Gabdank, I., Hilton, J. A., Kagda, M. S., Lam, B., Myers, Z., Sud, P., Jou, J., Lin, K., Baymuradov, U. K., Graham, K., Litton, C., Miyasato, S. R., Strattan, J. S., Jolanki, O., Lee, J. W., Tanaka, F. Y., Adenekan, P., . . . Cherry, J. M. (2020). New developments on the Encyclopedia of DNA Elements (ENCODE) data portal. *Nucleic Acids Res*, *48*(D1), D882-D889. https://doi.org/10.1093/nar/gkz1062

Mannon, R. B. (2018). Delayed Graft Function: The AKI of Kidney Transplantation. *Nephron*, *140*(2), 94-98. https://doi.org/10.1159/000491558

Martin, J. L., Gruszczyk, A. V., Beach, T. E., Murphy, M. P., & Saeb-Parsy, K. (2019). Mitochondrial mechanisms and therapeutics in ischaemia reperfusion injury. *Pediatr Nephrol*, *34*(7), 1167-1174. https://doi.org/10.1007/s00467-018-3984-5

Massoth, L. R., Desai, N., Szabolcs, A., Harris, C. K., Neyaz, A., Crotty, R., Chebib, I., Rivera, M. N., Sholl, L. M., Stone, J. R., Ting, D. T., & Deshpande, V. (2021). Comparison of RNA In Situ Hybridization and Immunohistochemistry Techniques for the Detection and Localization of SARS-CoV-2 in Human Tissues. *Am J Surg Pathol*, *45*(1), 14-24. https://doi.org/10.1097/PAS.0000000000001563

Meng, X. M., Nikolic-Paterson, D. J., & Lan, H. Y. (2016). TGF-beta: the master regulator of fibrosis. *Nat Rev Nephrol*, *12*(6), 325-338. https://doi.org/10.1038/nrneph.2016.48

Mercure, C., Yogi, A., Callera, G. E., Aranha, A. B., Bader, M., Ferreira, A. J., Santos, R. A., Walther, T., Touyz, R. M., & Reudelhuber, T. L. (2008). Angiotensin(1-7) blunts hypertensive cardiac remodeling by a direct effect on the heart. *Circ Res*, *103*(11), 1319-1326. https://doi.org/10.1161/CIRCRESAHA.108.184911

Miao, Z., Balzer, M. S., Ma, Z., Liu, H., Wu, J., Shrestha, R., Aranyi, T., Kwan, A., Kondo, A., Pontoglio, M., Kim, J., Li, M., Kaestner, K. H., & Susztak, K. (2021). Single cell regulatory landscape of the mouse kidney highlights cellular differentiation programs and disease targets. *Nat Commun*, *12*(1), 2277. https://doi.org/10.1038/s41467-021-22266-1

Miller, R. P., Tadagavadi, R. K., Ramesh, G., & Reeves, W. B. (2010). Mechanisms of Cisplatin nephrotoxicity. *Toxins (Basel)*, *2*(11), 2490-2518. https://doi.org/10.3390/toxins2112490

Moore, L. D., Le, T., & Fan, G. (2013). DNA methylation and its basic function. *Neuropsychopharmacology*, *38*(1), 23-38. https://doi.org/10.1038/npp.2012.112

Morabito, S., Miyoshi, E., Michael, N., Shahin, S., Martini, A. C., Head, E., Silva, J., Leavy, K., Perez-Rosendahl, M., & Swarup, V. (2021). Single-nucleus chromatin accessibility and transcriptomic characterization of Alzheimer's disease. *Nat Genet*, *53*(8), 1143-1155. https://doi.org/10.1038/s41588-021-00894-z

Mpekoulis, G., Frakolaki, E., Taka, S., Ioannidis, A., Vassiliou, A. G., Kalliampakou, K. I., Patas, K., Karakasiliotis, I., Aidinis, V., Chatzipanagiotou, S., Angelakis, E., Vassilacopoulou, D., & Vassilaki, N. (2021). Alteration of L-Dopa decarboxylase expression in SARS-CoV-2 infection and its association with the interferon-inducible ACE2 isoform. *PLoS One*, *16*(6), e0253458. https://doi.org/10.1371/journal.pone.0253458

Munro, D. A. D., & Hughes, J. (2017). The Origins and Functions of Tissue-Resident Macrophages in Kidney Development. *Front Physiol*, *8*, 837. https://doi.org/10.3389/fphys.2017.00837

Neufeld, M., Maclaren, N. K., Riley, W. J., Lezotte, D., McLaughlin, J. V., Silverstein, J., & Rosenbloom, A. L. (1980). Islet cell and other organ-specific antibodies in U.S. Caucasians and Blacks with insulin-dependent diabetes mellitus. *Diabetes*, *29*(8), 589-592. https://doi.org/10.2337/diab.29.8.589

Oliveto, G., Scagnolari, C., Frasca, F., Sorrentino, L., Matera, L., Nenna, R., Viscido, A., Scordio, M., Petrarca, L., Maria Zicari, A., Gentilini, E., D'Ettorre, G., Ceccarelli, G., Midulla, F., Antonelli, G., & Pierangeli, A. (2022). The non-functional ACE2 isoform, but not the SARS-CoV-2 receptor, is induced as an interferon-stimulated gene, in SARS-CoV-2 infected adults. *Cytokine*, *158*, 155997. https://doi.org/10.1016/j.cyto.2022.155997

Onabajo, O. O., Banday, A. R., Yan, W., Obajemu, A., Stanifer, M. L., Santer, D. M., Florez-Vargas, O., Piontkivska, H., Vargas, J., Kee, C., Tyrrell, D. L. J., Mendoza, J. L., Boulant, S., & Prokunina-Olsson, L. (2020). Interferons and viruses induce a novel primate-specific isoform dACE2 and not the SARS-CoV-2 receptor ACE2. *bioRxiv*. https://doi.org/10.1101/2020.07.19.210955

Ostermann, M., Bellomo, R., Burdmann, E. A., Doi, K., Endre, Z. H., Goldstein, S. L., Kane-Gill, S. L., Liu, K. D., Prowle, J. R., Shaw, A. D., Srisawat, N., Cheung, M., Jadoul, M., Winkelmayer, W. C., Kellum, J. A., & Conference, P. (2020). Controversies in acute kidney injury: conclusions from a Kidney Disease: Improving Global Outcomes (KDIGO) Conference. *Kidney Int*, *98*(2), 294-309. https://doi.org/10.1016/j.kint.2020.04.020

Ounzain, S., & Pedrazzini, T. (2016). Super-enhancer lncs to cardiovascular development and disease. *Biochim Biophys Acta*, *1863*(7 Pt B), 1953-1960. https://doi.org/10.1016/j.bbamcr.2015.11.026

Peck, K. M., Burch, C. L., Heise, M. T., & Baric, R. S. (2015). Coronavirus Host Range Expansion and Middle East Respiratory Syndrome Coronavirus Emergence: Biochemical Mechanisms and Evolutionary

Perspectives. *Annu Rev Virol*, *2*(1), 95-117. https://doi.org/10.1146/annurev-virology-100114-055029

Phelan, A. L., Katz, R., & Gostin, L. O. (2020). The Novel Coronavirus Originating in Wuhan, China: Challenges for Global Health Governance. *JAMA*, *323*(8), 709-710. https://doi.org/10.1001/jama.2020.1097

Piplani, S., Singh, P. K., Winkler, D. A., & Petrovsky, N. (2021). In silico comparison of SARS-CoV-2 spike protein-ACE2 binding affinities across species and implications for virus origin. *Sci Rep*, *11*(1), 13063. https://doi.org/10.1038/s41598-021-92388-5

Puelles, V. G., Lutgehetmann, M., Lindenmeyer, M. T., Sperhake, J. P., Wong, M. N., Allweiss, L., Chilla, S., Heinemann, A., Wanner, N., Liu, S., Braun, F., Lu, S., Pfefferle, S., Schroder, A. S., Edler, C., Gross, O., Glatzel, M., Wichmann, D., Wiech, T., . . . Huber, T. B. (2020). Multiorgan and Renal Tropism of SARS-CoV-2. *N Engl J Med*, *383*(6), 590-592. https://doi.org/10.1056/NEJMc2011400

Qazi, T. J., Quan, Z., Mir, A., & Qing, H. (2018). Epigenetics in Alzheimer's Disease: Perspective of DNA Methylation. *Mol Neurobiol*, *55*(2), 1026-1044. https://doi.org/10.1007/s12035-016-0357-6

Rabb, H., Griffin, M. D., McKay, D. B., Swaminathan, S., Pickkers, P., Rosner, M. H., Kellum, J. A., Ronco, C., & Acute Dialysis Quality Initiative Consensus, X. W. G. (2016). Inflammation in AKI: Current Understanding, Key Questions, and Knowledge Gaps. *J Am Soc Nephrol*, *27*(2), 371-379. https://doi.org/10.1681/ASN.2015030261

Rabe, M., & Schaefer, F. (2016). Non-Transgenic Mouse Models of Kidney Disease. *Nephron*, *133*(1), 53-61. https://doi.org/10.1159/000445171

Ramal-Sanchez, M., Castellini, C., Cimini, C., Taraschi, A., Valbonetti, L., Barbonetti, A., Bernabo, N., & Barboni, B. (2022). ACE2 Receptor and Its Isoform Short-ACE2 Are Expressed on Human Spermatozoa. *Int J Mol Sci*, *23*(7). https://doi.org/10.3390/ijms23073694

Rowley, M. J., & Corces, V. G. (2018). Organizational principles of 3D genome architecture. *Nat Rev Genet*, *19*(12), 789-800. https://doi.org/10.1038/s41576-018-0060-8

Rubin, S., Orieux, A., Prevel, R., Garric, A., Bats, M. L., Dabernat, S., Camou, F., Guisset, O., Issa, N., Mourissoux, G., Dewitte, A., Joannes-Boyau, O., Fleureau, C., Roze, H., Carrie, C., Petit, L., Clouzeau, B., Sazio, C., Bui, H. N., . . . Boyer, A. (2020). Characterization of acute kidney injury in critically ill patients with severe coronavirus disease 2019. *Clin Kidney J*, *13*(3), 354-361. https://doi.org/10.1093/ckj/sfaa099

Saeedi, P., Petersohn, I., Salpea, P., Malanda, B., Karuranga, S., Unwin, N., Colagiuri, S., Guariguata, L., Motala, A. A., Ogurtsova, K., Shaw, J. E., Bright, D., Williams, R., & Committee, I. D. F. D. A.

(2019). Global and regional diabetes prevalence estimates for 2019 and projections for 2030 and 2045: Results from the International Diabetes Federation Diabetes Atlas, 9(th) edition. *Diabetes Res Clin Pract*, *157*, 107843. https://doi.org/10.1016/j.diabres.2019.107843

Sanaei, M., & Kavoosi, F. (2019). Histone Deacetylases and Histone Deacetylase Inhibitors: Molecular Mechanisms of Action in Various Cancers. *Adv Biomed Res*, *8*, 63. https://doi.org/10.4103/abr.abr_142_19

Sarode, G. V., Neier, K., Shibata, N. M., Shen, Y., Goncharov, D. A., Goncharova, E. A., Mazi, T. A., Joshi, N., Settles, M. L., LaSalle, J. M., & Medici, V. (2021). Wilson Disease: Intersecting DNA Methylation and Histone Acetylation Regulation of Gene Expression in a Mouse Model of Hepatic Copper Accumulation. *Cell Mol Gastroenterol Hepatol*, *12*(4), 1457-1477. https://doi.org/10.1016/j.jcmgh.2021.05.020

Sarras, M. P., Jr., Leontovich, A. A., Olsen, A. S., & Intine, R. V. (2013). Impaired tissue regeneration corresponds with altered expression of developmental genes that persists in the metabolic memory state of diabetic zebrafish. *Wound Repair Regen*, *21*(2), 320-328. https://doi.org/10.1111/wrr.12027

Schefold, J. C., Filippatos, G., Hasenfuss, G., Anker, S. D., & von Haehling, S. (2016). Heart failure and kidney dysfunction: epidemiology, mechanisms and management. *Nat Rev Nephrol*, *12*(10), 610-623. https://doi.org/10.1038/nrneph.2016.113

Sengupta, S., & George, R. E. (2017). Super-Enhancer-Driven Transcriptional Dependencies in Cancer. *Trends Cancer*, *3*(4), 269-281. https://doi.org/10.1016/j.trecan.2017.03.006

Serra Lopez-Matencio, J. M., Morell Baladron, A., & Castaneda, S. (2019). JAK-STAT inhibitors for the treatment of immunomediated diseases. *Med Clin (Barc)*, *152*(9), 353-360. https://doi.org/10.1016/j.medcli.2018.10.020 (Inhibidores de la via de senalizacion JAK-STAT en el tratamiento de las enfermedades inmunomediadas.)

Sharfuddin, A. A., & Molitoris, B. A. (2011). Pathophysiology of ischemic acute kidney injury. *Nat Rev Nephrol*, *7*(4), 189-200. https://doi.org/10.1038/nrneph.2011.16

Sharma, P., Uppal, N. N., Wanchoo, R., Shah, H. H., Yang, Y., Parikh, R., Khanin, Y., Madireddy, V., Larsen, C. P., Jhaveri, K. D., Bijol, V., & Northwell Nephrology, C.-R. C. (2020). COVID-19-Associated Kidney Injury: A Case Series of Kidney Biopsy Findings. *J Am Soc Nephrol*, *31*(9), 1948-1958. https://doi.org/10.1681/ASN.2020050699

Sharma, S., Pavlasova, G. M., Seda, V., Cerna, K. A., Vojackova, E., Filip, D., Ondrisova, L., Sandova, V., Kostalova, L., Zeni, P. F., Borsky, M., Oppelt, J., Liskova, K., Kren, L., Janikova, A., Pospisilova, S.,

Fernandes, S. M., Shehata, M., Rassenti, L. Z., . . . Mraz, M. (2021). miR-29 modulates CD40 signaling in chronic lymphocytic leukemia by targeting TRAF4: an axis affected by BCR inhibitors. *Blood*, *137*(18), 2481-2494. https://doi.org/10.1182/blood.2020005627

Shin, H. Y., Willi, M., HyunYoo, K., Zeng, X., Wang, C., Metser, G., & Hennighausen, L. (2016). Hierarchy within the mammary STAT5-driven Wap super-enhancer. *Nat Genet*, *48*(8), 904-911. https://doi.org/10.1038/ng.3606

Sims, A. C., Baric, R. S., Yount, B., Burkett, S. E., Collins, P. L., & Pickles, R. J. (2005). Severe acute respiratory syndrome coronavirus infection of human ciliated airway epithelia: role of ciliated cells in viral spread in the conducting airways of the lungs. *J Virol*, *79*(24), 15511-15524. https://doi.org/10.1128/JVI.79.24.15511-15524.2005

Soutourina, J. (2018). Transcription regulation by the Mediator complex. *Nat Rev Mol Cell Biol*, *19*(4), 262-274. https://doi.org/10.1038/nrm.2017.115

Sovik, S., Isachsen, M. S., Nordhuus, K. M., Tveiten, C. K., Eken, T., Sunde, K., Brurberg, K. G., & Beitland, S. (2019). Acute kidney injury in trauma patients admitted to the ICU: a systematic review and meta-analysis. *Intensive Care Med*, *45*(4), 407-419. https://doi.org/10.1007/s00134-019-05535-y

Stengel, B. (2010). Chronic kidney disease and cancer: a troubling connection. *J Nephrol*, *23*(3), 253-262. https://www.ncbi.nlm.nih.gov/pubmed/20349418

Su, H., Yang, M., Wan, C., Yi, L. X., Tang, F., Zhu, H. Y., Yi, F., Yang, H. C., Fogo, A. B., Nie, X., & Zhang, C. (2020). Renal histopathological analysis of 26 postmortem findings of patients with COVID-19 in China. *Kidney Int*, *98*(1), 219-227. https://doi.org/10.1016/j.kint.2020.04.003

Summers, K. M., Bush, S. J., & Hume, D. A. (2020). Network analysis of transcriptomic diversity amongst resident tissue macrophages and dendritic cells in the mouse mononuclear phagocyte system. *PLoS Biol*, *18*(10), e3000859. https://doi.org/10.1371/journal.pbio.3000859

Tuddenham, L., Wheeler, G., Ntounia-Fousara, S., Waters, J., Hajihosseini, M. K., Clark, I., & Dalmay, T. (2006). The cartilage specific microRNA-140 targets histone deacetylase 4 in mouse cells. *FEBS Lett*, *580*(17), 4214-4217. https://doi.org/10.1016/j.febslet.2006.06.080

Tuo, X. M., Zhu, D. L., Chen, X. F., Rong, Y., Guo, Y., & Yang, T. L. (2020). The osteoporosis susceptible SNP rs4325274 remotely regulates the SOX6 gene through enhancers. *Yi Chuan*, *42*(9), 889-897. https://doi.org/10.16288/j.yczz.20-098

Wang, L., Li, X., Chen, H., Yan, S., Li, D., Li, Y., & Gong, Z. (2020). Coronavirus Disease 19 Infection Does Not Result in Acute Kidney Injury: An Analysis of 116 Hospitalized Patients from Wuhan, China. *Am J Nephrol*, *51*(5), 343-348. https://doi.org/10.1159/000507471

Weyemi, U., & Galluzzi, L. (2021). Chromatin and genomic instability in cancer. *Int Rev Cell Mol Biol*, *364*, ix-xvii. https://doi.org/10.1016/S1937-6448(21)00116-7

Whyte, W. A., Orlando, D. A., Hnisz, D., Abraham, B. J., Lin, C. Y., Kagey, M. H., Rahl, P. B., Lee, T. I., & Young, R. A. (2013). Master transcription factors and mediator establish super-enhancers at key cell identity genes. *Cell*, *153*(2), 307-319. https://doi.org/10.1016/j.cell.2013.03.035

Wu, J., Huang, B., Chen, H., Yin, Q., Liu, Y., Xiang, Y., Zhang, B., Liu, B., Wang, Q., Xia, W., Li, W., Li, Y., Ma, J., Peng, X., Zheng, H., Ming, J., Zhang, W., Zhang, J., Tian, G., . . . Xie, W. (2016). The landscape of accessible chromatin in mammalian preimplantation embryos. *Nature*, *534*(7609), 652-657. https://doi.org/10.1038/nature18606

Xiong, C., Deng, J., Wang, X., Shao, X., Zhou, Q., Zou, H., & Zhuang, S. (2021). Pharmacologic Targeting of BET Proteins Attenuates Hyperuricemic Nephropathy in Rats. *Front Pharmacol*, *12*, 636154. https://doi.org/10.3389/fphar.2021.636154

Xiong, C., Masucci, M. V., Zhou, X., Liu, N., Zang, X., Tolbert, E., Zhao, T. C., & Zhuang, S. (2016). Pharmacological targeting of BET proteins inhibits renal fibroblast activation and alleviates renal fibrosis. *Oncotarget*, *7*(43), 69291-69308. https://doi.org/10.18632/oncotarget.12498

Xu, K., Rosenstiel, P., Paragas, N., Hinze, C., Gao, X., Huai Shen, T., Werth, M., Forster, C., Deng, R., Bruck, E., Boles, R. W., Tornato, A., Gopal, T., Jones, M., Konig, J., Stauber, J., D'Agati, V., Erdjument-Bromage, H., Saggi, S., . . . Barasch, J. (2017). Unique Transcriptional Programs Identify Subtypes of AKI. *J Am Soc Nephrol*, *28*(6), 1729-1740. https://doi.org/10.1681/ASN.2016090974

Yan, Y., Jones, C. A., Sigmund, C. D., Gross, K. W., & Catanzaro, D. F. (1997). Conserved enhancer elements in human and mouse renin genes have different transcriptional effects in As4.1 cells. *Circ Res*, *81*(4), 558-566. https://doi.org/10.1161/01.res.81.4.558

Yin, S., Zhang, Q., Yang, J., Lin, W., Li, Y., Chen, F., & Cao, W. (2017). TGFbeta-incurred epigenetic aberrations of miRNA and DNA methyltransferase suppress Klotho and potentiate renal fibrosis. *Biochim Biophys Acta Mol Cell Res*, *1864*(7), 1207-1216. https://doi.org/10.1016/j.bbamcr.2017.03.002

Yokoyama, N., Nonaka, T., Kimura, N., Sasabuchi, Y., Hori, D., Matsunaga, W., Fujimori, T., Miyoshi, K., Matsumoto, H., & Yamaguchi, A. (2020). Acute Kidney Injury Following Elective Open Aortic Repair with Suprarenal Clamping. *Ann Vasc Dis*, *13*(1), 45-51. https://doi.org/10.3400/avd.oa.19-00095

Zhang, Q. X., Zhao, D. B., Gu, R. Y., Zhao, X. H., Zhao, H. X., Valenzuela, R. K., Xi, M. M., Zhang, R., & Ma, J. (2022). Study of a functional SNP rs13423388 in a novel enhancer element of schizophrenia-associated ZNF804A. *Asian J Psychiatr*, *74*, 103191. https://doi.org/10.1016/j.ajp.2022.103191

Zhou, X., Fan, L. X., Peters, D. J., Trudel, M., Bradner, J. E., & Li, X. (2015). Therapeutic targeting of BET bromodomain protein, Brd4, delays cyst growth in ADPKD. *Hum Mol Genet*, *24*(14), 3982-3993. https://doi.org/10.1093/hmg/ddv136

Ziegler, C. G. K., Allon, S. J., Nyquist, S. K., Mbano, I. M., Miao, V. N., Tzouanas, C. N., Cao, Y., Yousif, A. S., Bals, J., Hauser, B. M., Feldman, J., Muus, C., Wadsworth, M. H., 2nd, Kazer, S. W., Hughes, T. K., Doran, B., Gatter, G. J., Vukovic, M., Taliaferro, F., . . . Network, H. C. A. L. B. (2020). SARS-CoV-2 Receptor ACE2 Is an Interferon-Stimulated Gene in Human Airway Epithelial Cells and Is Detected in Specific Cell Subsets across Tissues. *Cell*, *181*(5), 1016-1035 e1019. https://doi.org/10.1016/j.cell.2020.04.035